Aus der
Klinik für Orthopädie und Unfallchirurgie
Klinik der Universität München
Direktoren: Prof. Dr. Wolfgang Böcker und Prof. Dr. Boris Holzapfel

Characterization of Non-Virally Delivered BMP Overexpressing Human Mesenchymal Stem Cells

Dissertation
zum Erwerb des Doktorgrades der Medizin
an der Medizinischen Fakultät der
Ludwig-Maximilians-Universität zu München

vorgelegt von

Nina Bendeliani

aus Tiflis

Jahr
2025

Mit Genehmigung der Medizinischen Fakultät der Universität München

Berichterstatter:	Prof. Dr. Wolfgang Böcker
Mitberichterstatter:	Prof. Dr. Florian Haasters
Mitbetreuung durch die promovierte Mitarbeiterin:	Dr. rer. nat. Veronika Schönitzer
Dekan:	Prof. Dr. med. Thomas Gudermann

Tag der mündlichen Prüfung: 13.11.2025

Abstract

Bone Morphogenetic Proteins (BMPs) play a critical role in bone formation. The non-viral delivery of BMP genes can significantly increase the osteogenic potential of human mesenchymal stem cells (hMSCs). The development of non-viral transposon technology, particularly the Sleeping Beauty (SB) transposon system, offers an efficient nuclear integration of recombinant genes and could revolutionize future clinical trials.

In this study, we utilized the SB transposon system to generate transgenic hMSCs overexpressing BMP-6 and BMP-2/6 genes. We analyzed the transfection efficiency and overexpression of BMP genes at both the mRNA and protein levels using FACS, RT-PCR, Western blot, and ELISA. We also evaluated the biochemical properties of recombinant BMPs and their intrinsic capacity for transcriptional activity using a luciferase cell reporter assay.

Furthermore, our goal was to characterize and differentiate these transfected cells with various other BMP overexpressing hMSCs in distinct tissues, to emphasize our hypothesis that SB transposon-derived BMP overexpressing hMSCs harbor an enhanced osteogenic capacity *in vitro*. Additionally, we sought to determine the biological superiority of recombinant heterodimeric BMPs over homodimers. To achieve this, we conducted a comparative analysis of the osteogenic potential of heterodimeric BMP-2/6, BMP-2/7, and BMP-4/7 overexpressing hMSCs with homodimeric BMP-2, BMP-4, and BMP-6 in cell culture experiments.

Our *in vitro* findings revealed that the overexpression of SB-derived BMPs results in hMSCs exhibiting greater osteogenic potential compared to control hMSCs. Specifically, we found that the heterodimeric BMPs exhibited superior osteogenic potential and upregulation of osteogenic markers. Furthermore, results from Western blot indicated that heterodimeric BMPs showed superiority over homodimers by enhancing BMP signaling pathways. Additionally, some BMPs effectively influenced the adipogenic potential of hMSCs compared to the control.

This study offers an innovative approach for bone regeneration using non-viral delivery of BMP overexpressing hMSCs, which could potentially offer an effective solution for challenging conditions.

Zusammenfassung

Knochenmorphogenetische Proteine (BMPs) spielen eine entscheidende Rolle bei der Knochenbildung. Der nicht-virale Gentransfer von BMP-Genen kann das osteogene Potenzial humaner mesenchymaler Stammzellen (hMSCs) erheblich steigern. Die Entwicklung der nicht-viralen Transposontechnologie, insbesondere des Sleeping Beauty (SB) Transposonsystems, bietet eine effiziente nukleare Integration rekombinanter Gene und könnte zukünftige klinische Studien revolutionieren. In dieser Studie verwendeten wir das SB Transposon System, um transgene hMSCs zu generieren, die die Gene BMP-6 und BMP-2/6 überexprimieren.

Wir analysierten die Transfektionseffizienz und die Überexpression von BMP-Genen sowohl auf mRNA als auch auf Proteinebene mithilfe von Methoden wie FACS, RT-PCR, Western Blot und ELISA. Außerdem haben wir die biochemischen Eigenschaften von rekombinanten BMPs und deren intrinsische Fähigkeit zur Transkriptionsaktivität mittels eines Luciferase Zellreporter Assays bewertet. Unser Ziel war es, diese transfizierten Zellen mit verschiedenen BMP-überexprimierenden hMSCs in verschiedenen Geweben zu charakterisieren und zu differenzieren, um unsere Hypothese zu unterstützen, dass SB Transposon abgeleitete BMP-überexprimierende hMSCs *in vitro* eine erhöhte osteogene Kapazität aufweisen. Außerdem sollte die biologische Überlegenheit rekombinanter heterodimerer BMPs gegenüber Homodimeren bestimmt werden.

Um dieses Ziel zu erreichen, haben wir in Zellkulturexperimenten das osteogene Potenzial von hMSCs, die heterodimere BMP-2/6, BMP-2/7 und BMP-4/7 überexprimieren, mit hMSCs, die homodimere BMP-2, BMP-4 und BMP-6 überexprimieren verglichen. Unsere *in vitro* Ergebnisse zeigten, dass die Überexpression von SB-abgeleiteten BMPs dazu führt, dass hMSCs ein größeres osteogenes Potenzial besitzen als Kontroll-hMSCs. Wir stellten fest, dass insbesondere die heterodimeren BMPs ein höheres osteogenes Potenzial und eine Hochregulierung osteogener Marker aufweisen. Die Ergebnisse des Western Blot zeigten zudem, dass heterodimere BMPs Homodimeren überlegen waren, indem sie die BMP-Signalwege verstärkten. Darüber hinaus beeinflussten einige BMPs effektiv das adipogene Potenzial von hMSCs im Vergleich zur Kontrolle.

Diese Studie präsentiert einen neuartigen Ansatz zur Regeneration von Knochen durch nicht-virale Herstellung von BMP-überexprimierenden hMSCs, welche möglicherweise eine effektive Lösung für schwerwiegende Bedingungen bieten kann.

Contents

Chapter 1

1. Introduction

Fracture healing is a physiologic process that follows a standardized course. However, approximately 5% to 10% of fractures demonstrate impaired healing, leading to potential complications such as segmental bone loss, delayed union, or pseudoarthrosis, resulting in a significant increase in morbidity and mortality (Einhorn, 1996; Calori *et al.*, 2007; Annamalaia *et al.*, 2019). Osteoporotic fractures are frequently associated with a complicated healing course, such as immobility, thrombosis, pulmonary embolism, and pneumonia. This places a significant burden on the healthcare system. The aging population, increasing incidence, and consequent rise in costs of osteoporotic complications, necessitate the implementation of interventions to mitigate this trend (Burge *et al.*, 2007; Hernlund *et al.*, 2013; Böcker *et al.*, 2022; Bormann *et al.*, 2023).

The treatment of complicated non-union fractures currently relies on autologous bone grafts and alternative materials such as metals and ceramics. Historically, various artificial bone synthesis materials have been utilized for bone reconstruction. However, certain issues have arisen with their use, including the possible immune response triggered by metallic atoms, which can lead to pathological inflammation. These materials frequently lack the ability to vascularize and integrate the fracture. Furthermore, the high stiffness of the materials used in osteosynthesis may result in stress shielding of the bone, which can cause osteopenia, weakening, and structural failure of the implant (Konttinen *et al.*, 2s005; Schemitsch, 2017; Koons, Diba and Mikos, 2020).

Autografts derived from the patient's own body remain the gold standard for the treatment of bone defects, as they provide a powerful source of osteogenic stem cells and osteoinductive factors essential for bone regeneration (Salgado, Coutinho and Reis, 2004; Rupp *et al.*, 2021; Schmidt, 2021). Despite their efficacy, the shortage of available grafting materials and the accompanying local site morbidity remain the major challenges. Recent advances in regenerative medicine offer promising alternatives to address issues related to bone reconstruction (Kneser *et al.*, 2006; Henkel *et al.*, 2013; Campana *et al.*, 2014; Bohner and Miron, 2019).

Mesenchymal stem cells (MSCs) harbor immense therapeutic potential within the realm of orthopedic procedures, particularly in the treatment of osteoporotic fractures, which primarily affect elderly patients. In such patients, autografts may have lost their regenerative potential due to the disease itself, a decrease in mesenchymal stem cell titers, or the onset of cellular senescence (Caplan, 2007; Shekaran and García, 2011; Liu *et al.*, 2017). A promising therapeutic approach for such situations is the combination of osteoinductive factors with mesenchymal stem cells. However, without controlled release mechanisms, these factors are generally rapidly released and degraded in the environment. An improved solution could be genetically modified stem cells, capable of stably overexpressing these osteoinductive cytokines, which are typically quite unstable and easily degraded in the environment (Rose, Kucharski and Uludağ, 2012; Koons, Diba and Mikos, 2020).

Genetically modified stem cells are characterized by controlled action and response to the host tissue environment, leading to ultimate tissue regeneration and replacement. The Sleeping Beauty transposon system represents a viable option for the delivery of osteogenic genes into cells. Combined with the advantages of non-viral vectors, this system, with a lower immunogenicity and safety profile, ensures a sustained release of osteogenic factors, resulting in prolonged bioactivity and bioavailability and increased efficacy of osteoinduction (Skipper *et al.*, 2013; Kebriaei *et al.*, 2017; Hudecek and Ivics, 2018).

The overexpression of Bone Morphogenetic Proteins (BMPs) has already been shown to have osteoinductive potential in mesenchymal stem cells. BMP-2 and BMP-7 have been approved by the FDA for multiple applications to support bone formation (Burkus *et al.*, 2003; McKay and et al, 2007; Boerckel *et al.*, 2011; Bohner and Miron, 2019). MSCs overexpressing BMPs could lead to enhanced bone healing and complete bridging of the bone defect cavity. Together with the multipotential differentiation capacity of MSCs, BMP overexpressing MSCs are a promising source for bone tissue engineering applications and cell-based therapies (Luo *et al.*, 2005; Annamalaia *et al.*, 2019).

1.1. Bone composition

As the rigid body tissue that forms the vertebrate skeleton, bone plays a vital role in providing mobility, storing minerals, and producing blood cells. It is composed of an extracellular matrix and specialized cells that are responsible for its production and maintenance. The bone matrix consists of approximately 35% organic matter and 65% inorganic components (Kumar *et al.*, 2017). Osteoblasts produce an organic matrix and control the mineralization process within the matrix (Clarke, 2008). The organic matrix, or ossein, comprises mainly elastic type I collagen fibers, which provide bone with its tensile strength, and minor type V collagen fibers (Franz-Odendaal, Hall and Witten, 2006; Boskey, 2013). Additionally, the organic extracellular matrix includes an amorphous ground substance containing chondroitin and keratan sulfates and hyaluronic acid, as well as glycoproteins such as osteocalcin, osteopontin, and bone sialoprotein. The inorganic constituent of bone contributes to its hardness. The major inorganic component of human bone is hydroxyapatite ($Ca_{10}(PO_4)_6(OH)_2$), which gives bone its hardness and acts as a reservoir for 99% of the body's calcium and 85% of its phosphorus. In addition, bone harbors notable quantities of bicarbonate, citrate, magnesium, and sodium ions, which contribute to its overall structural integrity. This composition gives bone resistance to bending stresses, enabling its role in maintaining skeletal integrity and supporting physiological functions (Boskey, 2013; Leslie P.Gartner and James L. Hiatt, 2018; Annamalaia *et al.*, 2019).

The cells found in bone tissues originate from two cell lineages: mesenchymal and hematopoietic. Bone tissue contains three major cell types: bone-forming osteoblasts and osteocytes, and bone-resorbing osteoclasts (Buckwalter *et al.*, 1996). Osteoblasts are derived from immature mesenchymal stem cells. They have a remarkable capacity for sustained production of bone matrix. This continuous production of bone matrix persists until the osteoblasts become embedded in the newly formed matrix and undergo differentiation into osteocytes (Pittenger *et al.*, 1999; Alhadlaq and Mao, 2004; Franz-Odendaal, Hall and Witten, 2006). Osteoclasts are multinucleated phagocytic cells that resorb bone to maintain bone turnover by breaking down old bone tissue (Boyle, Simonet and Lacey, 2003; Kang *et al.*, 2004). Bone tissue is highly dynamic and has the unique ability to heal and undergo continuous remodeling through the balanced activity of osteoclasts and osteoblasts. Bone tissue can also mobilize stored minerals as needed for metabolic demands (Salgado, Coutinho and Reis, 2004; Henkel *et al.*, 2013).

1.1.1. Regeneration mechanisms of bone tissue

Bone is formed either by subsequent ossification of cartilage (endochondral ossification) or by desmal ossification (intramembranous ossification). Endochondral ossification takes place in long bones where undifferentiated MSCs form a cartilage framework that calcifies and is eventually replaced by bone. Flat bones such as the skull are formed by desmal ossification, in which MSCs directly differentiate into osteoblasts and produce osteoid (unmineralized bone matrix) that gradually calcifies (Olsen, Reginato and Wang, 2000; Downey and Siegel, 2006; Berendsen and Olsen, 2015; Salhotra *et al.*, 2020).

In the event of a fracture, the healing process is initiated and involves several stages. It begins with hematoma formation, followed by inflammation, a fibrovascular phase, bone formation, and finally bone remodeling (Hollinger and Wong, 1996; Marsell and Einhorn, 2011; Bahney *et al.*, 2019). The hematoma in the fracture gap provides a fibrin mesh and creates a scaffold for the increased presence of inflammatory cells (Fig. 1). The immune cells and MSCs are activated and recruited to the site of injury by the release of inflammatory cytokines and osteogenic substances (Dimitriou *et al.*, 2005; Einhorn and Gerstenfeld, 2015).

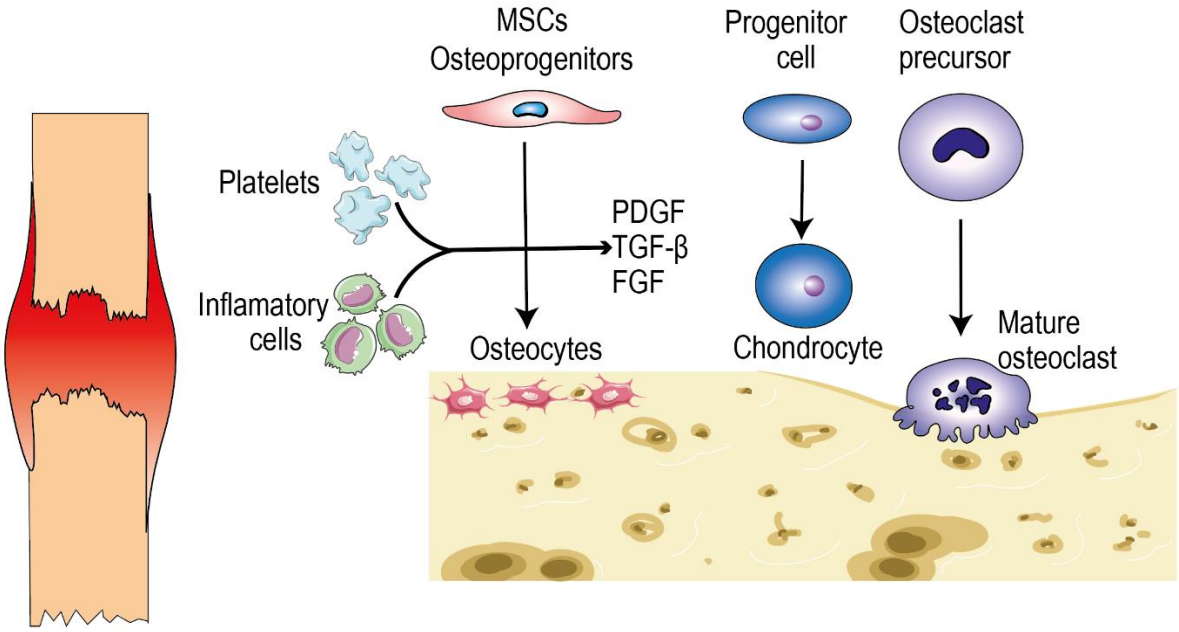

Figure 1 Schematic illustration of hematoma organization during fracture healing.

Fracture healing begins with hematoma formation, followed by differentiation of progenitor cells into osteoclasts, osteoblasts, and chondrocytes. Modified and adapted from (Kumar *et al.*, 2017; Tang *et al.*, 2018).

There are two major types of osteoinductive substances: the peptide molecules, also referred to as growth factors, and the immunomodulatory cytokines (Einhorn, 1996). Examples of growth factors include fibroblast growth factors (FGFs), insulin-like growth factors I and II (IGF I/II), transforming growth factor-β (TGF-β), platelet-derived growth factors (PDGF), and epidermal growth factor (EGF). Osteoinductive cytokines, on the other hand include interleukin-1, interleukin-6, and tumor necrosis factor-alpha (TNF-a) (Salgado, Coutinho and Reis, 2004; Shekaran and García, 2011; Henkel *et al.*, 2013).

During the fibrovascular phase, vascular endothelial growth factor (VEGF) and hypoxia inducible factor-1α (HIF-1α) are considered key regulators of vasculogenesis and angiogenesis. This process is essential to provide oxygen, nutrients, and cells for bone repair. Several other growth factors are involved in this phase, including BMPs, PDGF, and FGF. These factors may also regulate cell proliferation, differentiation, and extracellular matrix synthesis during fracture repair (Reddi, 1992; Luo, Sun and et al, 2005; Shekaran and García, 2011; Wang *et al.*, 2014; Huang *et al.*, 2020; Koons, Diba and Mikos, 2020).

The bone formation phase includes both intramembranous and endochondral ossification. Progenitor cells differentiate into chondroblasts between the fracture ends, resulting in the formation of a fibrocartilaginous bridging area, a mass of predominantly uncalcified tissue - called soft callus. This process occurs within the first 7-10 days. This mass consists mainly of type II procollagen and proteoglycans. Simultaneously, subperiosteal intramembranous ossification takes place adjacent to the fracture ends. Eventually, the soft callus is remodeled into a hard callus over the course of several weeks (Kraus and Kirker-Head, 2006; Marsell and Einhorn, 2011; Bahney *et al.*, 2019).

Subsequently, the final phase of bony callus formation, known as bone remodeling occurs, where the coordinated activity of osteoclasts and osteoblasts fully restores the structure and shape of the bone (Dimitriou *et al.*, 2005; Bahney *et al.*, 2019; Rather *et al.*, 2019).

1.1.2. Main principles of bone turnover

The process of bone turnover, also known as bone remodeling, is primarily controlled by the OPG/RANK/RANKL pathway. This pathway involves three cytokines, transmembrane receptor activator of NF-κB (RANK), RANK ligand (RANKL), and osteoprotegerin (OPG). RANKL proteins, both soluble and membrane-bound, are secreted by various cell types,

including osteoblasts. These proteins bind to the transmembrane RANK receptor located on the surface of osteoclasts and their progenitors. This stimulates osteoclast differentiation, activation, and survival (Theoleyre *et al.*, 2004; Yamaguchi, 2009; Marsell and Einhorn, 2011; Lacey *et al.*, 2012). OPG, which is also produced by osteoblasts, can inhibit osteoclastogenesis and survival by blocking the interaction of RANKL with RANK (Theoleyre *et al.*, 2004). The RANKL/OPG ratio is the main balancing factor for bone remodeling (Fig. 2). Several factors influence the RANKL/OPG ratio, including sex hormones, vitamin D, BMPs, parathyroid hormone (PTH), inflammatory cytokines such as interleukin-6 (IL-6), and glucocorticoids. BMPs and sex hormones have a positive effect on RANKL-mediated osteoclast differentiation (Wu, Chen and Li, 2016; Kumar *et al.*, 2017; Tang *et al.*, 2018).

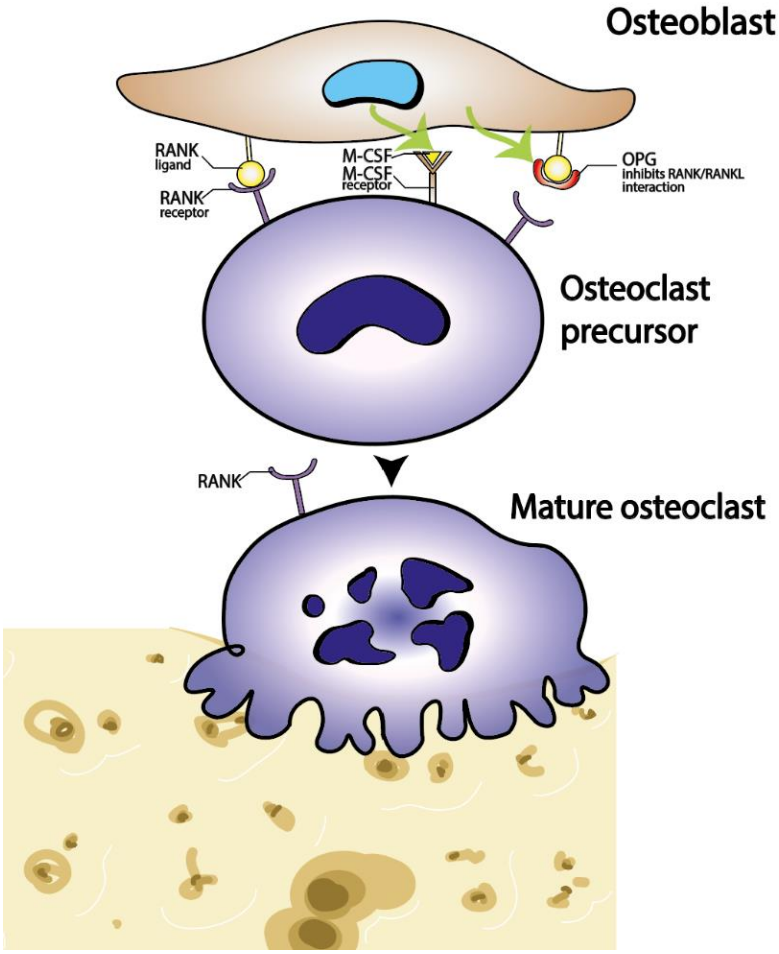

Figure 2 Schematic illustration of the bone remodeling mechanism.

Paracrine regulation of osteoclast differentiation, as a primary bone remodeling mechanism. Stimulation of osteoclastogenesis is mediated by the interaction of RANKL and M-CSF on the surface of osteoblasts with RANK and M-CSF-receptors on osteoclast precursors. Osteoblasts also produce osteoprotegerin (OPG), which blocks RANK/RANKL interaction and thus osteoclast maturation. Modified and adapted from (Kumar *et al.*, 2017; Tang *et al.*, 2018).

1.1.3. The role of mesenchymal stem cells (MSCs) in bone regeneration

MSCs, derived from the mesodermal germ layer, are powerful multipotent progenitor cells that play a critical role in bone formation and repair. These cells remain undifferentiated until stimulated to divide and differentiate into one or a few lineages. MSCs are primarily derived from the cambium layer of the periosteum or bone marrow and reside in the stem cell niche of bone, which provides an optimal microenvironment for their existence (Buckwalter *et al.*, 1996; Sell, 2013; Tang *et al.*, 2018).

Essential capacities that characterize MSCs are their ability to differentiate into distinct end-stage cell types. In addition, MSCs secrete a broad spectrum of bioactive factors that stimulate progenitor cell proliferation, induce angiogenesis, and create a regenerative microenvironment within injured tissues (Pittenger *et al.*, 1999; Tsutsumi *et al.*, 2001; Alhadlaq and Mao, 2004; Caplan, 2007).

When a bone fractures, the integrity of the matrix is disrupted, resulting in hemorrhage. In response to the acute inflammation of the injury, the migration of MSCs is induced. These cells differentiate into osteoprogenitors, then into pre-osteoblasts, mature osteoblasts, and finally into osteocytes (Yoo and Johnstone, 1998; Kraus and Kirker-Head, 2006; Caplan, 2007). This multi-step process is mainly orchestrated by the Runx-2 transcription factor, which plays a crucial role in the expression of osteoblast-specific genes (Long, 2012). Runx-2 binds to the promoters of osteogenic genes, such as osteocalcin (OCN), collagen alpha-1(I) (COL1A1), bone sialoprotein (BSP), and osteopontin (OPN). The transcription factors Runx-2 and Osterix can be upregulated in progenitor cells upon exposure to osteogenic growth factors, like BMPs (Ducy *et al.*, 1997; Zhou *et al.*, 2016; Bahney *et al.*, 2019). Mature osteoblasts produce a non-mineralized bone matrix, osteoid. The enzyme alkaline phosphatase (ALP) is critical for the ossification process. It promotes the deposition of collagen fibrils along with calcium and phosphate, thereby promoting the mineralization of the matrix (Birmingham *et al.*, 2012; Koons, Diba and Mikos, 2020). Once the osteoid is mineralized, osteoblasts become trapped in the bone lacunes as osteocytes or undergo apoptosis (Shekaran and García, 2011).

The diminished number of MSCs as a result of aging is the leading factor responsible for impaired cell migration, proliferation, and differentiation, resulting in abnormalities in callus formation at the fracture site (Caplan, 2007). Furthermore, osteoblasts exhibit decreased

responses to growth factors compared to younger individuals, which ultimately culminates in reduced bone regeneration rates - the principal pathological factor in low-turnover osteoporosis. Low-turnover osteoporosis, sometimes referred to as inactive osteoporosis, is characterized by normal osteoclast activity but inadequate bone formation by osteoblasts. The elderly population, or individuals with chronic illnesses (e.g., diabetes mellitus, chronic kidney disease), commonly experience low-turnover osteoporosis. In contrast, high-turnover osteoporosis is the consequence of accelerated bone resorption by osteoclasts which surpasses the osteoblasts' capacity to generate new bone and also results in a significant loss of bone mass (Bouillon, 1992; Boskey, A. L. West, 2005; Boskey, 2013; Kumar *et al.*, 2017; Annamalaia *et al.*, 2019; Hsu, Chen and Chen, 2020).

1.2.1. Bone Morphogenetic Proteins (BMPs) are members of the TGF- β superfamily

Bone Morphogenetic Proteins (BMPs) are a group of growth factors initially identified for their osteogenic properties. However, they are now known to have versatile roles in vertebrate tissues (Urist and McLean, 1965; Bragdon *et al.*, 2011; Wang *et al.*, 2014). BMPs are members of the transforming growth factor β (TGF-β) superfamily, a large group of regulatory polypeptides. Nowadays, more than 20 members of the BMP superfamily are known (Horbelt, Denkis and Knaus, 2012).

Some BMPs, including BMP-2, -4, -6, -7, and -9, are recognized for their osteogenic capacity (Wang *et al.*, 2014). Diverse studies have demonstrated the significant potential of recombinant human BMP-2 (rhBMP-2) and rhBMP-7 to promote endochondral bone formation. They are used in various therapeutic clinical trials such as bone defect reconstruction in non-union fractures, spinal fusion, open tibial fractures, osteoporotic fractures, and root canal surgery (as described below) (Friedlaender *et al.*, 2001; Burkus *et al.*, 2002; McKay and et al, 2007; Ghodadra and Singh, 2008; Kohan *et al.*, 2013). The off-label use of rhBMP-2 has been shown to improve healing and reduce morbidity in studies of cleft lip repair, compared to the traditional bone graft-only repair technique (Allareddy *et al.*, 2012).

The name bone morphogenetic protein is misleading because these proteins engage in broad biological processes beyond bone formation. In vertebrates, BMPs are ac-

tively involved in the genesis of almost all organs and tissues (Hogan, 1996). Disruptions in BMP signaling during embryogenesis can cause severe pathological changes that may be incompatible with life (Yamaguchi, Komori and Suda, 2000; Butler and Dodd, 2003; Du, Xiao and Yip, 2010; Sell, 2013). In the adult organism, BMPs are primarily expressed during the early phase of fracture healing (Salgado, Coutinho and Reis, 2004). Furthermore, BMPs influence the entire panoply of human health conditions such as cancer, osteogenic, cardiovascular, reproductive, renal and pulmonary diseases (Hogan, 1996; Shimasaki *et al.*, 2004; Horbelt, Denkis and Knaus, 2012). Mutations in BMP receptors lead to impaired bone formation (Zhao *et al.*, 2002). For example, the ACVR1 (ALK2) BMP receptor is involved in the pathology of a rare disease, fibrodysplasia ossificans progressiva (FOP), which is characterized by the formation of heterotopic ossifications (Gannon *et al.*, 1997; Chen, Zhao and Mundy, 2004). A mutation in BMPR1B is associated with brachydactyly type A2 with hypoplasia or aplasia of the distal and middle phalanges of the index finger and sometimes the little finger (Kjaer *et al.*, 2006). In addition to skeletal disorders, primary pulmonary hypertension develops on the basis of mutations in the BMPRII receptor (Miyazono, Kamiya and Morikawa, 2010).

The BMPs are divided into numerous subgroups based on their amino acid sequence similarities, such as BMP-2 and -4, BMP-5 to -8, and BMP-9 and -10 together. For instance, BMP-2 and BMP-4 share up to 80% homology in their amino acid-specific sequences, whereas BMP-6 and BMP-7 share 78% homology (Lavery *et al.*, 2008; Carreira *et al.*, 2014).

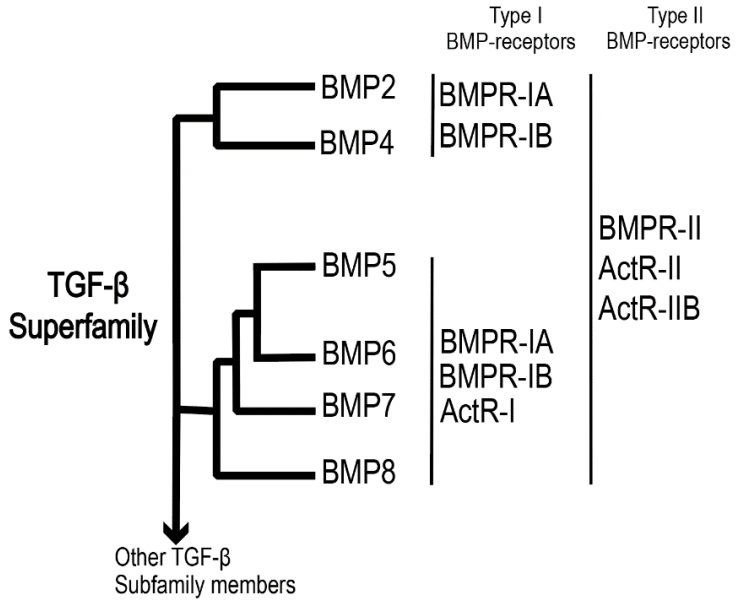

Figure 3 BMPs are members of the TGF-β superfamily.

Representation of BMPs as part of the TGF-β superfamily. They are grouped based on their sequence relationship and corresponding receptors listed on the right. Modified and adapted from (Mueller and Nickel 2012).

1.2.2. BMP cell signaling pathways

Cell signaling pathways are essential in regulating the function of numerous cellular processes, including cell differentiation and proliferation. BMPs exert their signals via two TGF-β receptors, type I and type II transmembrane receptors located on the cell surface (Kawabata, Imamura and Kohei, 1998; Valera *et al.*, 2010). These receptors possess serine/threonine kinase activity that induces the phosphorylation of downstream cytoplasmic transcription factors, thereby activating the BMP-canonical (SMAD) and non-canonical (MAPK/ERK) signaling pathways (Massagué, 1998; Chubinskaya *et al.*, 2000; Yamaguchi, Komori and Suda, 2000; Xiao *et al.*, 2002; Botchkarev, 2003; Kumar *et al.*, 2017).

Different homodimeric BMP ligands exhibit different affinities for each type of receptor. For instance, BMP-2 and BMP-4 have greater affinity for class I receptors and weaker affinity for type II receptors. While BMP-6 and BMP-7 exhibit greater affinity for type II receptors and weaker affinity for type I receptors (Fig. 3). BMP signaling involves three types of type I receptors (BMPR-IA (ALK-3), BMPR-IB (ALK-6) and ActR-I (ALK-2)) and three types of type II receptors (BMPR2, ACVR2A, and ACVR2B) (Botchkarev, 2003; Lavery *et al.*, 2008; Guo and Wu, 2012; Wang *et al.*, 2014).

After binding to surface receptors, BMPs induce the formation of a heterodimeric complex composed of type I and type II receptors. The type II receptor kinase then phosphorylates the GS domain of the type I receptor, which in turn phosphorylates SMAD1/5/8 and I-SMADs, also known as R-SMADs or SMAD6 and SMAD7 (Fig. 4). SMAD proteins are transcription factors and act as either transcriptional coactivators or corepressors to regulate the transcription of TGF-β/BMP-dependent genes (Zhu, Kavsak and Abdollah, 1999; Yamaguchi, Komori and Suda, 2000; Chen, Zhao and Mundy, 2004; Mouillesseaux *et al.*, 2016). SMAD1/5/8, also known as receptor-regulated SMADs, form a heteromeric complex with SMAD4. This complex is transported to the nucleus and initiates the transcription of early BMP-responsive genes (Jonk *et al.*, 1998; Derynck and Zhang, 2003; Massagué, Seoane and Wotton, 2005; Du, Xiao and Yip, 2010; Bruce and Sapkota, 2012; Horbelt, Denkis and Knaus, 2012). SMADs regulate osteogenic genes, including the distal-less homeobox 5 (Dlx5) gene. This gene activates the Runx2 transcription factor, which is a critical regulator of osteogenic genes (Lee *et al.*, 2003; Jang *et al.*, 2012). SMADs interact with a remarkable number of DNA-binding transcription factors. This pathway is also called canonical and plays a crucial role in BMP signaling.

I-SMADs negatively impact the phosphorylation of R-SMADs by type I receptors. Additionally, BMP signal transduction is regulated by other intracellular and extracellular molecules that bind to BMPs or BMP-pathway components, blocking signal transduction, and thereby decreasing bone formation. More than 15 BMP antagonists have been identified, such as chordin, sclerostin, noggin, and follistatin (Botchkarev, 2003; Winkler *et al.*, 2003; Song *et al.*, 2010; Bruce and Sapkota, 2012; Carreira *et al.*, 2014).

Besides the canonical BMP signaling, there is a non-canonical (non-SMAD) BMP signaling pathway mediated by mitogen-activated protein kinases (MAPKs). BMP-induced differentiation of osteoblasts requires MAPK activity, and both BMP and MAPK signaling pathways are essential for osteogenic gene expression, including OCN (Lai and Cheng, 2002; Xiao *et al.*, 2002; Miyazono, Kamiya and Morikawa, 2010; Rahman *et al.*, 2015; Miao *et al.*, 2019).

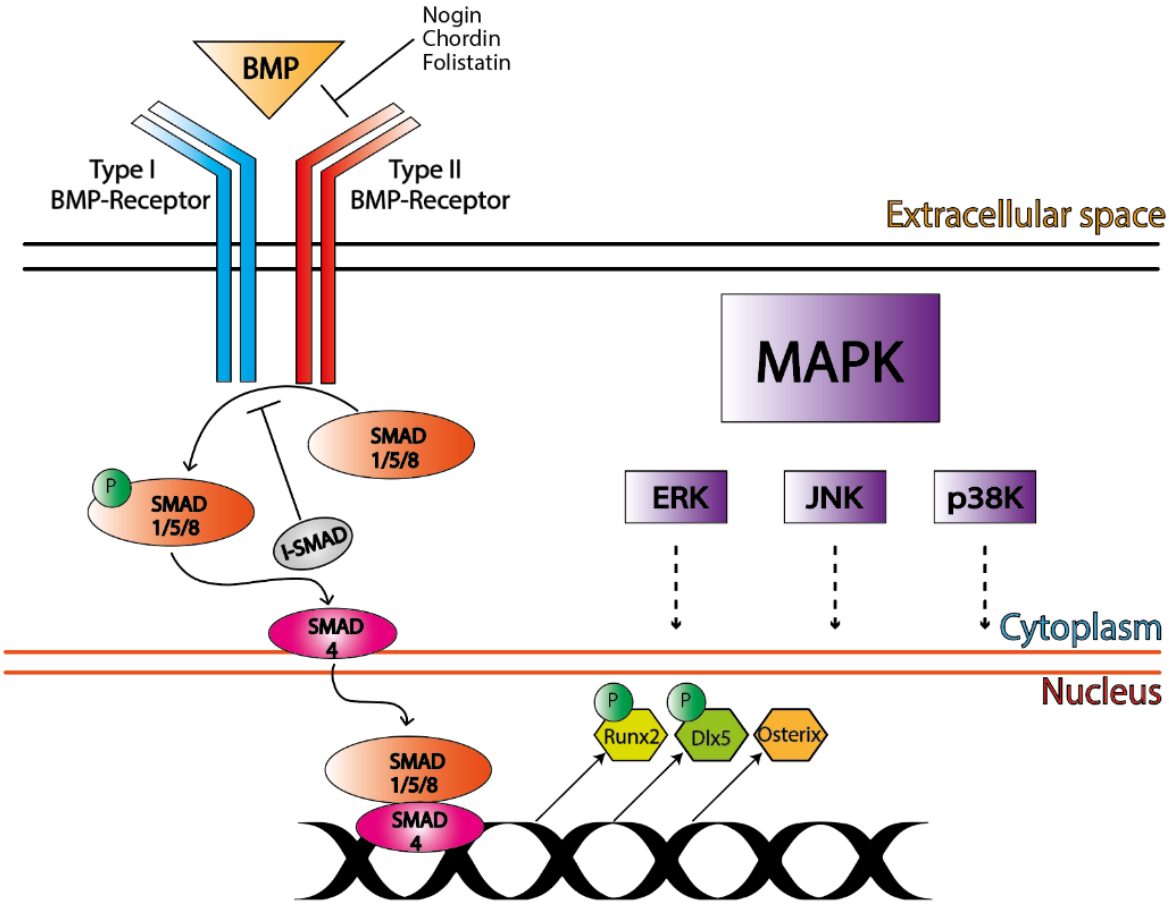

Figure 4 Schematic overview of the BMP signaling pathway.

The BMP intracellular signaling cascade involves both canonical (SMAD) and non-canonical (non-SMAD/MAPK) pathways. BMPs bind to type I and type II receptors on the cell surface, which can activate the SMAD and MAPK pathways, including ERK, JNK, and p38. DLX5 and other primary

osteoblast-related transcription factors, including Osterix and Runx2, are among the downstream target transcription factors of BMPs. SMAD6 and SMAD7 have the ability to repress signaling by inhibiting the association between R-SMAD and Co-SMAD, or R-SMAD phosphorylation. Modified and adapted from (Lavery *et al.*, 2008; Carreira *et al.*, 2014; Sanchez-Duffhues *et al.*, 2020).

MAPKs represent a family of protein kinases that utilize protein kinases, phospholipases, transcription factors, and cytoskeletal proteins as substrates (Johnson and Lapadat, 2002). The MAPK family comprises extracellular signal-regulated kinase (ERK), C-Jun N-terminal kinase (JNK), and p38 kinase (p38K). These signaling pathways induce a number of transcription factors in the nucleus and stimulate cell growth and differentiation (Favata *et al.*, 1998; Nawshad *et al.*, 2005; Valera *et al.*, 2010; Cai *et al.*, 2012; Mueller and Nickel, 2012). The ERK signaling pathway is involved in cell survival, proliferation, and apoptosis. Studies have also shown that BMPs can stimulate osteoclast differentiation and survival. Through dose-dependent stimulation of BMPR-IA and BMPR-II receptors on osteoclasts, the SMAD1/5/8 and ERK pathways are upregulated (Kaneko *et al.*, 2000; Fong *et al.*, 2013; Lee *et al.*, 2018). Upon phosphorylation by tyrosine kinase receptors or Ras, ERK intrinsically induces nuclear transcriptional activity of various genes. Mutations in Ras proto-oncogenes cause persistent activation of ERK1/2 genes. This promotes proliferation and growth of tumor cells (Johnson and Lapadat, 2002; Kraunz *et al.*, 2005). BMPs, especially BMP-6, have been shown to activate the ERK and p38K pathways, leading to increased melanogenesis in skin cells (Rothhammer *et al.*, 2005; Haubold *et al.*, 2010; Singh, Abbas and Tobin, 2012).

The JNK pathway has been implicated in the regulation of growth and programmed cell death. P38Ks regulate the production of inflammatory cytokines (Johnson and Lapadat, 2002). After exposure to UV radiation and external stress, the stress-dependent MAPKs JNK and p38 are upregulated (Sapkota *et al.*, 2007).

1.2.3. Bone Morphogenetic Protein constitution patterns and relevant differences in signal transduction

BMPs are synthesized as peptide precursors consisting of 400-500 amino acids that undergo posttranslational modification. Each BMP comprises a short signal sequence at the

N-terminus, a prodomain, and a mature osteoinductive domain at the carboxy-terminal. The mature domain of each BMP contains a region of seven cysteine amino acids that is highly conserved among the TGF-β family of proteins (Fig. 5) (Mueller and Nickel, 2012).

BMPs are synthesized as monomers and form disulfide bonds with other monomers at the C-terminus between cysteine amino acid sequences, resulting in the formation of homodimers or even heterodimers (Guo and Wu, 2012). These disulfide linkages provide significant stability to the mature proteins (dimers). After proteolytic cleavage at the RXXR maturation site, located between the prodomain and the mature region, an active BMP dimer is released (Hazama *et al.*, 1995; Valera *et al.*, 2010; Mueller and Nickel, 2012).

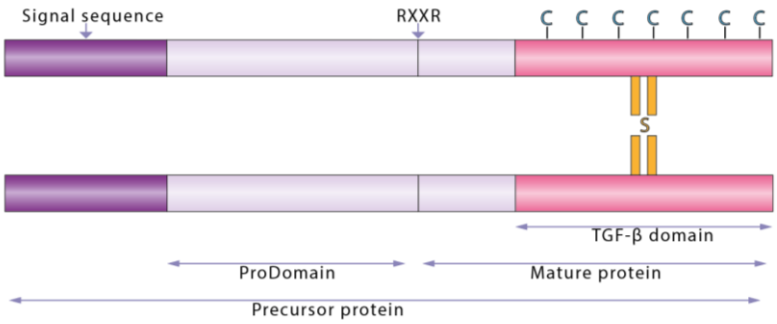

Figure 5 General BMP structure.

BMP has a dimeric protein structure linked by disulfide bonds. The protein consists of a signal sequence at the N-terminus, followed by a large prodomain and a mature part containing the characteristic cysteine-knot sequence at the C-terminus. Modified and adapted from (Vukicevic et al 2017and Mueller and Nickel 2012).

The co-expression of diverse BMPs in tissues results in the formation of heterodimers composed of two different BMP subunits. BMPs are classified into subfamilies based on their sequence homology, and class I BMP-2 and BMP-4 can form disulfide linkages with class II members, namely BMP-6 or BMP-7 (Khan *et al.*, 2012). While it is widely accepted that recombinant class I/II BMP heterodimers exhibit greater specific activity compared to homodimers, heterodimers composed of different BMP family members show increased potential for osteogenic differentiation compared to homodimers of either subunit (Aono and Hazama M., 1995; Hazama *et al.*, 1995; Kim *et al.*, 2019). For example, the heterodimer BMP-2/6 consists of one BMP-2 and one BMP-6 subunit, with the BMP-2 subunit having a higher affinity for the type I receptor, while BMP-6 has a higher affinity for type II receptors.

Consequently, heterodimeric BMP induces higher levels of BMP cell signaling pathway molecules and more effectively stimulates the differentiation of hMSCs (Valera *et al.*, 2010). Therefore, the biological activity of BMP-2/6 as a heterodimer is increased due to its higher affinity for both BMP receptors compared to the homodimeric counterparts. The diversity of BMP receptor affinity within heterodimeric subunits is suggested to be the reason for the higher efficacy of heterodimeric BMPs (Israel *et al.*, 1996; Guo and Wu, 2012; Miao *et al.*, 2019).

1.2.4. BMP-induced enhancement of bone extracellular matrix

The BMPs play a crucial role in promoting an environment that facilitates the effective formation and remodeling of the extracellular matrix (ECM). The production of the matrix is a critical aspect of bone regeneration, as it provides a specific tissue environment and serves as a reservoir for various essential elements such as growth factors, cytokines, and nutritional elements (Einhorn, 1996; Reddi, 1998; Salgado, Coutinho and Reis, 2004; Harris *et al.*, 2011; Rather *et al.*, 2019).

BMPs are known to attract MSCs to the fracture site in an autocrine or paracrine manner, thereby promoting the proliferation and differentiation of progenitor cells into osteoblasts responsible for bone formation. They modulate the expression of genes involved in the production of extracellular matrix proteins through a broad cascade of SMAD and MAPK cellular signaling. BMPs also enhance collagen production by osteoblasts, which is a major component of the ECM. Collagen serves as an early marker of osteogenesis and provides tensile strength and stability to bone. Additionally, BMPs stimulate the synthesis of extracellular matrix components such as fibronectin, proteoglycans, osteocalcin, and osteopontin, which help to shape the functional and structural characteristics of bone. BMPs also upregulate ALP, which facilitates the deposition of hydroxyapatite crystals (Salgado, Coutinho and Reis, 2004; Horbelt, Denkis and Knaus, 2012; Boskey, 2013; Bahney *et al.*, 2019). Overall, BMPs enhance ECM production and play a fundamental role in bone regeneration, remodeling, and maintenance.

1.3. Gene therapy in tissue engineering

Advances in cell biology have led to promising developments in bone tissue engineering. When conventional orthopedic surgery fails to restore function or replace bone, tissue engineering is proposed as an alternative. Gene therapy has proven to be a valuable approach to address unresolved issues in bone tissue engineering by integrating orthopedic surgical principles with basic science. This strategy involves the delivery of genetic material specifically into progenitor cells, such as MSCs, to correct genetic abnormalities or enhance beneficial growth factors and facilitate bone regeneration. Delivery of natural or synthetic target genes can enhance the efficiency of somatic cell differentiation, leading to the formation of osteogenic tissue that facilitates bone healing (Salgado, Coutinho and Reis, 2004).

Overexpression of biological factors, particularly BMPs, in genetically modified MSCs has shown favorable outcomes in several studies (Luo *et al.*, 2005; Loozen *et al.*, 2018). These MSCs can be administered to targeted anatomical sites, and by overexpressing the gene of interest, such as BMPs, at appropriate concentrations, they can promote differentiation, osteoid matrix production, and repair of bone tissue defects (Kim *et al.*, 2018).

Despite the promising potential of gene therapy in bone tissue engineering, several critical inquiries remain unanswered before human trials can be conducted. The safe and stable integration of transgenes needs to be established prior to clinical implementation, while economic factors must also be considered. However, in the near future, gene therapy may be effectively used to fill bone defects in a minimally invasive manner (Collon, Gallo and Lieberman, 2021).

1.3.1. Viral versus non-viral gene delivery systems

Gene transfer can be accomplished using either viral or non-viral delivery systems. Viral vectors have been widely utilized because of their ability to efficiently deliver genetic material into cells. About 70% of current gene therapy clinical trials are based on viral delivery systems (Ivics and Izsvák, 2011; Yin *et al.*, 2014; Ghosh *et al.*, 2020; Ahern *et al.*, 2021). The most common types of viral vectors include adeno-associated viruses (AAVs), adenoviruses (AVs), retroviruses (RVs), lentiviruses (LVs), and herpes simplex viruses (HSVs). Although viral vectors are generally deemed safe and effective in clinical trials, viruses that

integrate their vectors into the genome, such as retroviruses and lentiviruses, carry the risk of insertional mutagenesis and subsequent oncogenesis (Skipper *et al.*, 2013). Additionally, genes derived from viral vectors can undergo transcriptional silencing over time, making these systems less effective (Ellis, 2005). In contrast, non-integrating viruses, such as adenoviruses and herpes viruses, are considered non-oncogenic. Nonetheless, the lack of chromosomal integration results in genetic cargo being episomal and leads to a gradual loss of transfected material, particularly in mitotically active cells. Thus, multiple transfections are required to achieve efficient gene delivery, resulting in cell toxicity and immunogenic responses (Yin *et al.*, 2014; Kebriaei *et al.*, 2017; Ghosh *et al.*, 2020).

Several disadvantages of viral vector systems, such as carcinogenicity, immunogenicity, broad tropism, and limited delivery of genetic cargo, make non-viral vectors more desirable. Non-viral vectors are gaining popularity due to their safety and reduced immunogenicity (Ivics and Izsvák, 2011; Gantenbein *et al.*, 2020). They are also less expensive and easier to produce than viral vectors. In addition, certain non-viral vectors may have a greater capacity to deliver genetic material than viruses. However, due to the short half-life of nucleic acids in plasma and degradation by endonucleases, physical or carrier-mediated transfection is required for non-viral delivery (Yin *et al.*, 2014). Transfection can be achieved through carrier-free methods, including electroporation and microinjection, or with lipophilic carriers, such as liposomes and lipid nanoparticles, which provide protection against nucleic acid degradation and facilitate delivery of negatively charged nucleic acids into cells (Hamann, Nguyen and Pannier, 2019; Gantenbein *et al.*, 2020). Recent advances in lipid nanoparticle delivery systems have demonstrated their potential for gene transfer, as evidenced by their use in the COVID-19 mRNA vaccines (Pardi and et.al, 2015; Liang *et al.*, 2017; Polack *et al.*, 2020).

Most non-viral vectors function similarly to other non-integrating viral systems, providing only short-term, episomal transgene expression. Therefore, the lack of nuclear maintenance of the genetic cargo makes this therapy ineffective in some cases. The development of transposon technology, which allows for nuclear integration of transgenes, is equipped with non-viral features and could be a game changer in future clinical trials. Further details on transposons are discussed below.

However, some of these non-viral gene delivery methods are still limited by cytotoxicity of transfection reagents, electrotoxicity, and disruption of the cell plasma membrane during

electroporation, heat, pH changes, and oxidative damage from reactive oxygen species (Kneser *et al.*, 2002; Hamann, Nguyen and Pannier, 2019; Gantenbein *et al.*, 2020).

1.3.2. Transposable elements

Successful gene therapy in tissue engineering requires a robust gene delivery system that offers long-term, stable gene expression while being safe and less immunogenic. In addition, clinical trials require cost-effective gene delivery systems that are easy to manufacture. As a result, various gene delivery systems have been developed and discovered by scientists. Transposable elements have favorable properties that can potentially provide effective gene therapy in the future, such as lower immunogenicity, safety profile, and simplified production (Skipper *et al.*, 2013; Kebriaei *et al.*, 2017; Hudecek and Ivics, 2018).

Transposable elements, or transposons, are small primitive, functional DNA elements that can change their position throughout the genome and have played an enormous role in adapting and reshaping the genome throughout evolution. Barbara McClintock, a Nobel Prize-winning cytogeneticist, first discovered the transposable element in 1950 during her research on maize cytogenetics (McClintock, 1950; Skipper *et al.*, 2013).

Various criteria classify the many types of transposable elements, including their division into two classes of transposons (Wicker *et al.*, 2007). Class I transposons, also known as retrotransposons, replicate genetic material and insert it into the genome by reverse transcription of RNA intermediates (Finnegan, 2012; Bourque *et al.*, 2018). On the other hand, class II transposons, or DNA transposons, move genetic material using a “cut and paste” mechanism facilitated by the enzyme transposase (Bourque *et al.*, 2018). In vertebrates, the remnants of transposable elements have been deactivated during evolution and are found as introns or inactivated gene sequences in the genome (Plasterk, Izsvák and Ivics, 1999; Wicker *et al.*, 2007; Ivics, Li and Mátés, 2009). The Tc1/mariner superfamily, a class II transposon system, is the focus of this research.

An autonomous system of DNA transposons encodes a transposase protein. This system comprises a transposase gene that is flanked by inverted terminal repeats (ITR) at the 5’ and 3’ ends of the transposon. The ITRs are reversed complements of each other and have a typical length of up to 100 bp (Fig. 6) (Plasterk, Izsvák and Ivics, 1999).

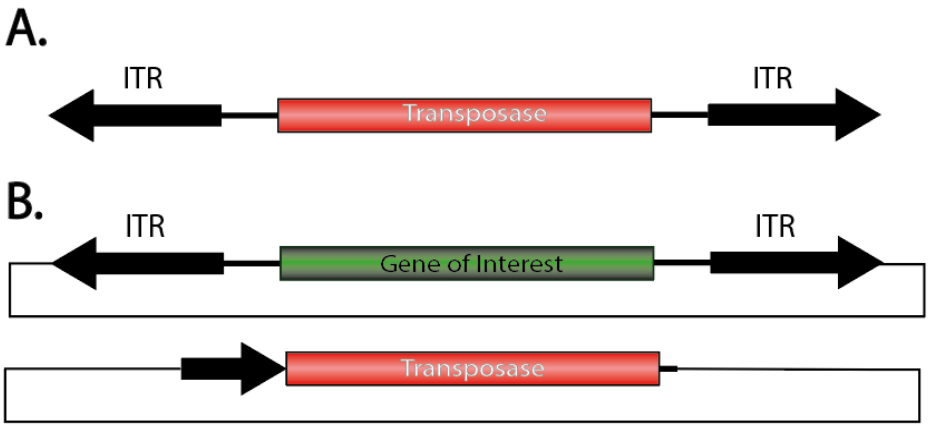

Figure 6 Type II Transposon system.

(A) The autonomous DNA transposon system consists of the transposase gene linked to the inverted terminal repeats (ITRs). **(B)** The transposon delivery system consists of two components that form a bicomponent structure. The gene of interest (GOI) is flanked by the ITRs and the transposase enzyme is delivered by a separate plasmid. Modified and adapted from (Mátés *et al.*, 2009; Ivics and Izsvák, 2011).

For transposition to occur, the transposase gene must undergo transcription and translation into an active transposase enzyme. Transposase enzymes recognize the 5´and 3´ends of a transposon and bind to its ITRs. They bring the DNA ends together and cut out the DNA transposon. The transposase then delivers it to the recipient DNA, cleaves it, and inserts the transposon into the recipient DNA. Finally, DNA polymerase synthesizes across the gaps and DNA ligase seals them. After the insertion of the transposon into the DNA, short, a few nucleotide footprints called direct repeats (DRs) are left in the DNA. The inserted transposon is bound to the DRs (Ivics and Izsvák, 2015; Holstein *et al.*, 2018).

Different gene delivery vectors display distinct tendencies to integrate into DNA. For example, retroviruses and lentiviruses integrate within a gene or in the upstream proximity of active genes (Hudecek *et al.*, 2017), whereas the PiggyBac transposon from the Tc1/Mariner transposon family tends to insert around the transcription start sites of active genes (Ivics, Li and Mátés, 2009; Chen *et al.*, 2015). Studies show that the Sleeping Beauty transposon from the Tc1/mariner transposon superfamily does not target specific transcriptional or non-transcriptional units for integration. Therefore, the probability of being integrated into non-transcriptional regions, such as the largest genomic regions, is higher than that of being integrated into transcriptional regions. Thus, Sleeping Beauty transposon may have a safer insertion distribution compared to other viral or non-viral integration vectors (Ivics, Li and

Mátés, 2009; Holstein *et al.*, 2018). Some transposons show their preferred integration sequences, such as PiggyBac, which targets TTAA sequences, and Sleeping Beauty, which prefers TA dinucleotides (Vigdal *et al.*, 2002; Grabundzija *et al.*, 2010).

Tc1/mariner transposons integrate a single copy of a gene of interest (GOI) into DNA, thus ensuring stable and long-term transgene expression in target cells (Plasterk, Izsvák and Ivics, 1999). Although there is still a risk that the transposons may integrate into an active genome and cause gene malfunction, according to the two-hit theory of tumor epidemiology, a single cell requires multiple hits in cancer genes to undergo carcinogenesis. Autonomous transposon systems with an integrated transposase gene can cause massive transposition in a genome, leading to genetic instability (Skipper *et al.*, 2013). However, the bicomponent structure of modern transposable elements and effective control of transposon expression can reduce these risks and make them a promising gene delivery system for future gene therapy applications (Ivics, Li and Mátés, 2009; Hudecek *et al.*, 2017).

1.3.3. The Sleeping Beauty transposon system

The Sleeping Beauty transposon system is a synthetic transposon designed for vertebrates, including humans, and belongs to the Tc1/mariner superfamily of DNA transposons. This transposable element was “reawakened” from a salmon genome and named after the popular fairy tale (Plasterk, Izsvák and Ivics, 1999; Ivics and Izsvák, 2011; Kebriaei *et al.*, 2017). The SB transposon system operates via a “cut and paste” method. The SB transposon is characterized by the ability to replace the coding region of a transposase gene with any DNA sequence. In the SB transposon system, the transposase gene has been separated from the transposon ITRs (Fig. 7). This modification enables the gene of interest (GOI) to be linked to the ITRs located within the transposon plasmid (Hudecek and Ivics, 2018).

The ITRs of the SB transposon may extend up to 250 bp in length, with the region responsible for transposase binding positioned within these sequences (Ivics and Izsvák, 2015). For the transposon system to operate, a separate plasmid carrying either the transposase gene or a transposase-encoding mRNA is required (Ivics and Izsvák, 2015; Hudecek *et al.*, 2017). Following translation, the transposase enzyme binds to the ITRs and “cuts and pastes” the transposon into the genome in a random manner (Fig. 7). It is observed that the SB transposons demonstrate a preference for integration into TA dinucleotide sequences,

which are duplicated on either end of the insertion site (Vigdal *et al.*, 2002; Skipper *et al.*, 2013). Random insertions of transfected DNA into the genome have the potential to cause oncogenesis. As mentioned above, the Sleeping Beauty transposon has no statistical preference for transcription units and therefore displays a significantly low preference for gene sequences, resulting in a lower risk of oncogenesis compared to integrating viral vectors (Liu and Visner, 2007; Hudecek *et al.*, 2017).

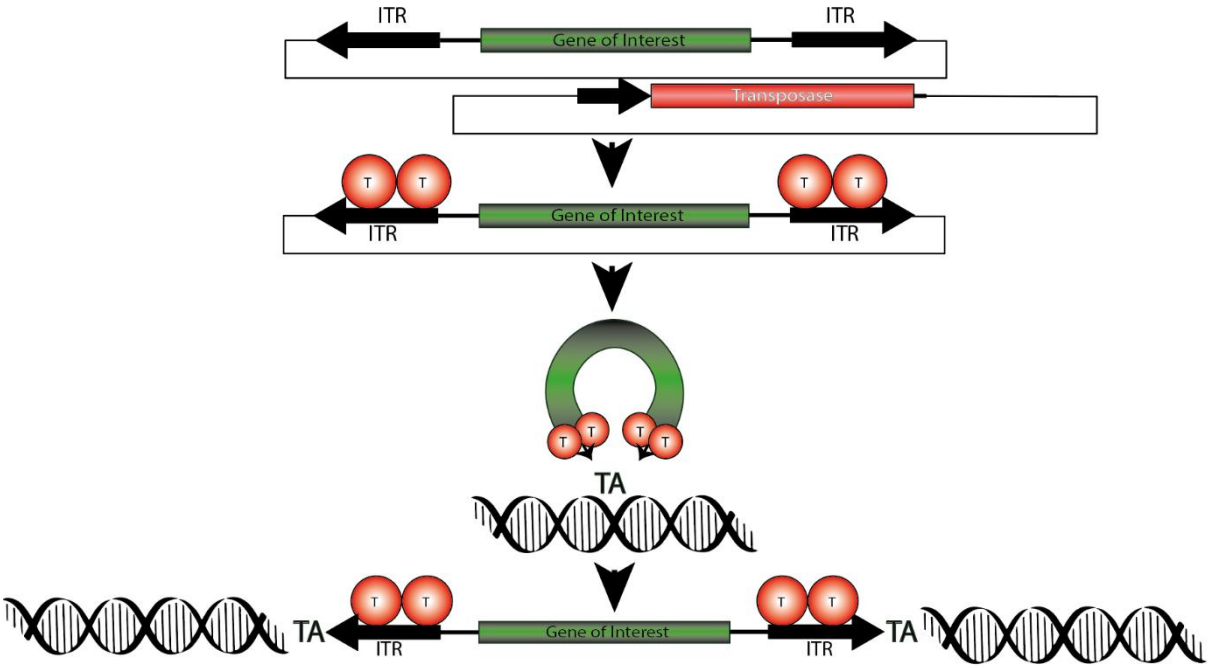

Figure 7 Sleeping Beauty transposon gene delivery system.

After delivery of the two-component Sleeping Beauty transposon system into the cell, the transposase is transcribed and translated into an active enzyme, which then binds to the ITRs, ultimately resulting in the excision of the gene of interest (GOI). Transposon excision is followed by random insertion into DNA, specifically into the duplicated TA dinucleotide sequence flanking the integrated transposon. Modified and adapted from (Mátés *et al.*, 2009; Ivics and Izsvák, 2011; Hudecek *et al.*, 2017).

The SB transposon system is typically delivered into target cells using a bicomponent system consisting of an artificial transposon containing a transgene flanked by ITRs and a linear plasmid carrying the transposase (Geurts *et al.*, 2003). Nucleofection is the primary method for the delivery of SB transposon vectors to primary human cells in *ex vivo* experiments. New nucleofection methods and transfection solutions have been developed to improve the delivery of the SB transposon system (Hudecek *et al.*, 2017; Holstein *et al.*, 2018; Hudecek

and Ivics, 2018). After successful transfection, cells express the genes encoded by the plasmid. If the plasmid contains a green fluorescent protein (GFP) gene, it can be utilized to assess the successful delivery of the plasmid into the cell and nucleus. The fluorescence intensity signal increases as the number of integrated transposon copies increases (Holstein *et al.*, 2018).

In summary, the SB transposon enables effective non-viral gene delivery with lower immunogenicity and no limitations in genetic cargo size (Geurts *et al.*, 2003; Hudecek *et al.*, 2017; Kebriaei *et al.*, 2017). Chromosomal integration allows for sustained and stable gene expression following transfection, even in rapidly dividing cell generations, with a minimal probability of transgene silencing. Additionally, it is considered a safer, non-viral approach (Narayanavari *et al.*, 2017). Thus, the SB transposon system was used in these experiments to generate stem cells that overexpress BMPs.

1.3.4. The differentiation properties of genetically modified BMP overexpressing hMSCs

The potential use of BMPs to stimulate osteogenesis and promote fracture healing has generated considerable interest in recent years. MSCs are multipotent cells that can differentiate into various cell types, including bone cells. Nonetheless, their numbers decrease almost exponentially with age, presenting a challenge for their therapeutic use (Caplan, 2007).

BMPs are crucial growth factors involved in bone formation. When combined with MSCs, BMPs can enhance their differentiation potential and improve fracture healing outcomes. However, due to the short half-life of the protein, the administration of recombinant homodimeric BMPs requires supraphysiologic doses. The high cost of recombinant BMPs makes BMP overexpressing transfected MSCs a more attractive option. Studies have demonstrated that MSCs that overexpress BMP-2, BMP-6, and BMP-7 exhibit greater osteogenic potency compared to control cell lines in both *in vitro* and *in vivo* animal models (Pelled *et al.*, 2016; Kim *et al.*, 2018; Hamann, Nguyen and Pannier, 2019). However, the osteogenic ability of MSCs is higher when overexpressing BMP heterodimers, such as BMP-2/6 and BMP-2/7, as opposed to homodimeric BMPs (Zhu *et al.*, 2006; Valera *et al.*, 2010; Loozen *et al.*, 2018). The BMPs may also have the ability to create a vascular trophic environment

and impact cellular differentiation into other cell lineages, including adipocytes (Yamaguchi, Komori and Suda, 2000; Kim *et al.*, 2018).

Sleeping Beauty-based gene therapy systems provide stable and prolonged gene expression, which makes them an ideal candidate for bone tissue engineering. SB-delivery can bypass the inflammatory response triggered by viral vectors and offer a safer approach for integrating transgenes into the genome (Liu and Visner, 2007; Hudecek *et al.*, 2017). By using the SB transposon transposase system, delivery of recombinant BMPs into hMSCs can lead to the secretion of BMPs above physiological levels. This approach holds the potential to effectively target specific sites and remodel tissue.

1.4. The current treatment methods of FDA approved rhBMPs

Recombinant human Bone Morphogenetic Protein 2 and 7 (rhBMP-2 and rhBMP-7) have been authorized for clinical use in the induction of bone in spinal fusion (Burkus *et al.*, 2003), open fractures of long bones, non-unions, and sinus augmentation (Luo *et al.*, 2005; McKay and et al, 2007; Kanakaris *et al.*, 2008). Interbody fusion is a major spinal surgery for the treatment of chronic back and leg pain. However, this operation is associated with a 35% chance of unsuccessful fusion and the formation of pseudoarthrosis. Another significant challenge is represented by the donor site (primarily the iliac crest) morbidity, which includes chronic pain at the harvest site and potential complications such as impaired wound healing and blood loss. Therefore, there must be a better way to overcome these challenges and enhance the success rate of fusion.

In 2002, the US FDA approved the use of rhBMP-2 for anterior lumbar interbody fusion (ALIF) at the single level (L4/L5 or L5/S1). A concentration of 1.5 mg/cc of rhBMP-2 was delivered in liquid form, applied to a type I collagen scaffold (INFUSE®, Medtronic), and then inserted into a Lumbar Tapered Titanium Cage (LT-CAGE) (McKay and et al, 2007). The cage is securely fixed to provide enhanced support during the bone formation process, which is facilitated by the osteoprogenitor cells being stimulated by rhBMP-2, eventually leading to their differentiation. The fusion success rate in the INFUSE group was 94.5% compared to 88.7% in the autograft group after 24 months post-surgery. Additionally, the INFUSE group had a shorter hospital stay and experienced less blood loss during surgery, which were significant advantages (Burkus *et al.*, 2003).

Govender and colleagues (2002) conducted a study to evaluate the safety and efficacy of rhBMP-2 in the treatment of open tibial fractures in 450 patients. The study showed that rhBMP-2 was superior to the standard treatment in the treatment of open tibial fractures. Patients treated with rhBMP-2 had a significantly higher rate of successful healing without hardware failure or the need for secondary intervention (Govender and et.al, 2002). Following the results of the BESTT study, rhBMP-2 (as INFUSE® bone graft) was approved by the EMEA in 2002 and by the FDA in 2004 for use in open tibial fractures with an intramedullary (IM) nail fixation as an alternative to bone grafts (Jones and et.al, 2006; Ghodadra and Singh, 2008). Cost analysis of open tibial fracture treatment with nail, or nail plus rhBMP-2 indicated significant cost savings per patient with rhBMP-2 and a reduced need for secondary interventions (Ghodadra and Singh, 2008).

In March 2007, rhBMP-2 was also approved as an alternative to autogenous bone grafting for sinus augmentation. It was demonstrated that INFUSE® was an effective autogenous bone graft alternative (McKay and et al, 2007).

In a multicenter, prospective, randomized trial of 33 patients requiring one- or two-level cervical fusion were compared across two groups: rhBMP-2 and autograft. After a two-year follow-up, significant improvements in neck disability and arm pain scores were observed in the group that received fusion with 0.4 mg/cc rhBMP-2/ACS placed in the CORNERSTONE SR® ring compared to the iliac crest bone autograft group (Baskin *et al.*, 2003).

In 2001, rhBMP-7 (0.9 mg/cc) was also approved for clinical use in treating non-unions. Patients treated with rhBMP-7 had a history of previously failed conventional fracture treatment. Studies indicated a non-significant difference between rhBMP-7 and autologous bone graft groups. However, the decreased operating time and lack of postoperative morbidity at the donor site make rhBMP-7 therapy the more preferred treatment option. The incidence of infection and osteomyelitis was significantly reduced in the group treated with rhBMP-7 compared to those who underwent autologous bone grafting (Friedlaender *et al.*, 2001; White *et al.*, 2007; Kanakaris *et al.*, 2008).

However, these benefits are accompanied by risks, particularly when supraphysiological dosing and off-label application for inappropriate indications in specific anatomical regions are employed. Complications, including osteolysis and heterotopic bone formation, are possible risks associated with off-label PLIF and TLIF procedures, where

epidural leakage of BMP can occur (Carragee, Hurwitz and Weiner, 2011; Fu *et al.*, 2012; James *et al.*, 2016).

The results of clinical trials have shown the safety and efficacy of rhBMPs in bone fusion procedures, as recommended by the FDA. The use of rhBMPs yields a greater fusion rate while reducing operation time and avoiding the side effects associated with autogenous bone grafting procedures (Baskin *et al.*, 2003; McKay and et al, 2007).

Chapter 2

2. Aim of the study

The presence of local growth factors, stem cells, and osteoprogenitors is critical to promote fracture healing. However, in elderly individuals with osteoporotic fractures or other bone diseases, reduced stem cell numbers, cellular senescence, or diminished differentiation potential often result in delayed fracture healing. To address this issue, the delivery of genetically modified stem cells with enhanced osteogenic potential to the site of the defect may be beneficial for certain patient groups with high mortality rates.

In this study, we aimed to create transgenic stem cells that stably overexpress BMPs using a non-viral Sleeping Beauty transposon system. Therefore, we sought to characterize and differentiate transgenic cells with various other BMP overexpressing hMSCs in osteogenic and adipogenic tissues and to demonstrate the enhanced osteogenic capacity of SB-transposon-derived BMP overexpressing hMSCs *in vitro*. Additionally, we aimed to evaluate the biological superiority of transgenic heterodimeric BMPs over homodimers.

For the experimental verification of this thesis, we have outlined the following tasks:

1. Generate homodimeric rhBMP-6 and heterodimeric rhBMP-2/6 sequences in the Sleeping Beauty transposon plasmid.
2. Transfect and establish transgenic, non-virally delivered hMSCs that stably overexpress rhBMPs.
3. Characterize BMP overexpressing cells and analyze of their cellular functionality.
4. Conduct *In vitro* differentiation of transgenic hMSCs overexpressing BMP-2, -4, -6, -7, -2/6, -2/7, and -4/7. Explore the impact of BMP overexpression in transgenic cells and BMP-mediated biochemical signaling. Investigate the influence of BMP overexpression on adjacent stem cells using conditioned medium and co-culture experiments to assess the impact of transgenic hMSCs on the differentiation potential of surrounding cells.

Chapter 3

3. Materials & Methods

3.1. Molecular biology Materials

Table 1 Devices

Devices	**Manufacturer**
4D-Nucleofector™ System	Lonza, Switzerland
Analytical Laboratory Balance / Scales 770	Kern, Balingen
Centrifuge 5415 D	Eppendorf, Germany
Centrifuge 5417R	Eppendorf, Germany
Chemiluminescence detector Typ ImageQuant LAS 4000 mini	GE Healthcare, Munich
Electric pH-meter	WTW Inolab, Weilheim
ELISA Mini Microplate Reader	Thermo Scientific, USA
FIREBOY safety Bunsen burner	Integra Bioscience
Gel imaging system	Vilber Lourmat, Germany
Gel-electrophoresis system	Peqlab, Erlangen
HERAcell 240 I cell culture Incubator	Thermo Scientific, USA
Incubator for microbiology	Memmert, Schwabach
Laboratory Platform Shaker with Incubator 1000	Heidolph, Schwabach
Laboratory Platform Shaker, Rotamax 120	Heidolph, Schwabach
Laboratory water bath	GFL, Burgwedel
Labscales	Sartorius, Gottingen
Magnetic stirrer	Axon, Kaiserslautern
Micropipette Pipetman Classic	Glison, Middleton
Micropscope Axiovert S100, Axiocam ICc3	Zeiss, Oberkochen
Microscope AxioObserver Z1, AxioCam MRm	Zeiss, Oberkochen
Mini Star Zentrifuge	neoLab, Heidelberg
Nanodrop	Thermo Scientific, USA
Neubauer Counting Chamber	Brand, Wertheim
Peltier Thermal Cycler 200	Bio-Rad, USA
Pipetboy	Hirschmann, Eberstadt
Stream Sterilizer	H+P Labortechnik
Thermomixer 5436	Eppendorf, Germany
Thermomixer comfort 1,5ml	Eppendorf, Germany
Trans-Blot cell	Bio-Rad, Munich
Trans-Blot Turbo Transfer System	Bio-Rad, Munich

UV Light - Table Model	Heraeus, Hanau
Vortex Mixer Genie 2	Scientific Industries
Zellculture microscope, Diavert	Leitz, Wetzlar
Zellculture Zentrifuge, Univ. 16R	Hettich, Tuttlingen
Zentrifuge, Jouan BR 4	Thermo Scientific, USA

Table 2 Chemicals

Chemicals and solutions	**Manufacturer**
Acetic acid	Merck, Darmstadt
Ampicillin	Roth, karlsruhe
Antibiotic-Antimycotic	Gibco, USA
APS	Roth, Karlsruhe
Bacto™ Agar is a solidifying agent	BD Diagnostics, USA
Bovine Serum Albumin (BSA)	Roth, Karlsruhe
Bromphenol bue	Merck, Darmstadt
Cellculture Media D-MEM high Glucose	Gibco, USA
Cellculture Media α-MEM high Glucose	Life Technologies, Darmstadt
cOmplete-ULTRA-Mini-Tablets, Protease-Inhibitor-Cocktail	Roche, Germany
DAPI	Sima Aldrich, Taufkirchen
DEPC	Thermo Scientific, USA
DMEM high glucose	Gibco, USA
DMEM without phenol red	Gibco, USA
DNA-Ladder 1 kb	New England Biolabs Inc.
Dubecco's Phosphat- buffered saline	PAA, Pasching
ECL-Solution Crescendo	Immobilon, USA
ECL-Solution Forte	Immobilon, USA
EDTA	Sima Aldrich, Taufkirchen
Ethanol	Merck, Darmstadt
Ethidium bromide	Sima Aldrich, Taufkirchen
Ethidium bromide solution	Sigma-Aldrich, Taufkirchen
Fetal Bovine Serum	Sima Aldrich, Taufkirchen
Formaldehyde	Merck, Darmstadt
Gel Loading Dye, Blue (6X)	New England BioLabs, Frankfurt
Glycerin	Roth, Karlsruhe
Glycerol	Sima Aldrich, Taufkirchen
Glycerol molecular biology grade	Promega
HCl	Merck, Darmstadt
HEPES	Roth, Karlsruhe
IPTG	Sigma-Aldrich
Kanamycin	Roth, Karlsruhe
KCl	Roth, Karlsruhe
Methanol	Emplura, Germany
NACl	Carl Roth, Germany
NaDOC	Sigma-Aldrich, Taufkirchen
NaF	Merck, Darmstadt

NEB Buffer	New England Biolabs, USA
PhosSTOP	Roche, Germany
Protein Marker V	peqGOLD
Prestained Protein Ladder, (10 to 180 kDa)	MBI Fermentas, St. Leon-Rot
S.O.C. Medium	Invitrogen, Darmstadt
SDS	Roth, Karlsruhe
Skim Milk Powder	Merck, Darmstadt
TEMED	Roth, Karlsruhe
Tris-Base	Sigma-Aldrich, Taufkirchen
Tris-HCl	Sigma-Aldrich, Taufkirchen
Triton X-100	Fluka, Steinheim
Tryptone	Becton Dickinson, USA
Tween 20	Sigma-Aldrich, Taufkirchen
Typsin-EDTA (10X)	PAA, Pasching
X-GAL	Roth, Karlsruhe
β-Mercaptoethanol	Sigma-Aldrich, Taufkirchen

Table 3 Cell culture materials

Cell culture materials	**Manufacturer**
Cell culture plates 6, 25, 48, 96 cm^2	Nunb, Wiesbaden
Cell scraper	Sarstedt, Germany
Falcon tube 15 ml	Sarstedt, Germany
Glass slide AA00000102E	Menzel, Braunschweig
Ibidi 8-Well µ-Slide	Ibidi, Germany
T-Flask 2, 5, 25, 75, 150, 275 cm^2	Nunc, Wiesbaden

Table 4 Kits and enzymes

Kits and enzymes	**Manufacturer**
BCA protein assay kit	Thermo Scientific, USA
BamHI-HF restriction enzyme	New England Biolabs, USA
BstAPI restriction enzyme	New England Biolabs, USA
BstEI restriction enzyme	New England Biolabs, USA
EcoRI restriction enzyme	New England Biolabs, USA
EcoRI-HF restriction enzyme	New England Biolabs, USA
HindIII restriction enzyme	New England Biolabs, USA
HotStar HiFidelity Polymerase Kit	Qiagen, Hilden
NcoI-HF restriction enzyme	New England Biolabs, USA
NEBNext Quick Ligation	New England Biolabs, USA
NheI restriction enzyme	New England Biolabs, USA
NucleoSpin Gel and PCR Clean-up	Macherey-Nagel, Duren
P2 Primary Cell 4D-Nucleofector X kit	Lonza, Switzerland
pCR 2.1 TOPO™ TA Cloning™ Kit	Thermo Scientific, USA

PstI restriction enzyme	New England Biolabs, USA
PureYield™ Plasmid Miniprep System	Promega, USA
Luciferase Assay System	Promega USA
QIAprep Spin Midiprep Kit	Qiagen, Hilden
Quick Ligase (Quick T4 DNA Ligase)	New England Biolabs, USA
Restriction Endonucleases	New England Biolabs, USA
RNAse free DNase	Qiagen, Hilden
SfiI restriction enzyme	New England Biolabs, USA
T4 Rapid Ligation Kit	Thermo Scientific, USA
XcmI restriction enzyme	New England Biolabs, USA
XhoI restriction enzyme	New England Biolabs, USA
XmnI restriction enzyme	New England Biolabs, USA

Table 5 Antibodies

Antibodies	**Working Concentration**	**Manufacturer**
Anti-Goat HRP-linked	1:10.000	Rockland, USA
Anti-Rabbit HRP-linked	1:10.000	Cell Signaling, USA
ERK (P44/42 MAP Kinase)	1:1000	Cell Signaling, USA
hBMP-2	1:1000	R&D Systems, USA
hBMP-6 (precursor specific)	1:1000	Cell Signaling, USA
P-38	1:1000	Cell Signaling, USA
Phospho-ERK (P44/43 MAP Kinase)	1:1000	Cell Signaling, USA
Phospho-P-38	1:1000	Cell Signaling, USA
Phpspho-SMAD1/5/9	1:1000	Cell Signaling, USA
SMAD1	1:1000	Cell Signaling, USA
ß-Actin	1:1000	Santa Cruz, USA

Table 6 Primers

Target gene	**Primer sequence**	**Annealing temp. °C**	**Nmbr. of cycles**	**Size (bp)**	**Reference**
Adipsin	F:5´-CAAGCAACAAAGTCCCGAGC-3´ R:5´-CCTGCGTTCAAGTCATCCTC-3´	56	30	261	(Shen, Glowacki and Zhou, 2011)
ALP	F:5´-TACAACACCAATGCCCAGGT-3´ R:5´-TTCCACCAGCAAGAAGAAGC-3´	55	30	696	(Potier *et al.*, 2007)
BMP-2	F:5'-CATCCCAGCCCTCTGAC-3' R:5'-CTTTCCCACCTGCTTGCA-3'	53	41	493	(Wozney *et al.*, 1989)
BMP2_P2A_6	F:5´-AAGCTTCCAGCCCCG-3´ R:5´-CCCGGGGTATCACGC-3´	53.3 56	35 35	15 15	Designed for cloning

BMP-6	F:5'-AGCGACACCACAAAGAGTTCA-3' R:5'- GCTGATGCTCCTGTAAGACTTGA-3'	60	41	159	(Wang *et al.*, 2017)
BSP	F:5´-CTATGGAGAGGACGCCACGCCTGG-3´ R:5´-CATAGCCATCGTAGCCTTGTCCT-3´	54	35	587	(Gronthos *et al.*, 2000)
Col1α1	F:5´-AGGGCTCCAACGAGATCGAGATCCG-3´ R:5´-TACAGGAAGCAGACAGGGCCAACGTCG-3´	54	40	223	(Twine *et al.*, 2016)
GAPDH	F:5'-GGAGCGAGATCCCTCCAAAAT-3' R:5'-GGCTGTTGTCATACTTCTCATGG-3'	60	30	197	(Su *et al.*, 2018)
hBMP6 _PspXI-for / HindIII_rev	F:5´- ACTCGAGCATGCCAACTTTGTAC-3´ R:5´- AAGCTTCTAGTGGCATCCACAAG-3´	60.6	35	23	Designed for cloning
OCN	F:5'-CCCTTTCTCCTGTCCGGATG-3' R:5'-GCTGAGCTCTAGGGGAGTCT-3'	56	37	242	(Murakami *et al.*, 2017)
PPAR-y	F:5'-ATTCTCCTATTGACCCAGAAAGCG-3' R:5'-AGCTTTATCTCCACAGACACGACATT-3'	55	35	419	(Shen, Glowacki and Zhou, 2011)
Runx2	F:5′-AGGGCATTCTCCGTGGCAGT-3′ R:5'-TCTTCACAAATCCTCCCC-a3'	55	35	230	(Fu *et al.*, 2016)

Table 7 Vectors

Gene & Vector	**Size**	**Manufacturer**
pENTR223.1-hBMP6 plasmid	4.3 kb	Harvard PlasmID, Harvard Medical School, Boston, MA
pUC 19	2.7 kb	Invitrogen, Darmstadt
pCR 2.1 TOPO TA	3.9 kb	Invitrogen, Darmstadt
pCMV(CAT)T7-SB100	4.7 kb	Gift from Zsuzsanna Izsvak Lab, Germany
pSBbi-GP	6.6 kb	Eric Kowarz, Plasmid #60511, Addgene, Cambridge

Table 8 Software

Software	**Usage**
Adobe Illustrator 2021	Figures
Bioedit 7.2	Molecular biology
Carl Zeiss Axio Vision SE64 Rel	Photo acquisition
Clone Manager 10	Cloning strategies
FlowJo FACS analysis 10	FACS-Analysis
GraphPad Prism 9	Statistics

ImageJ analysis Software 1.52e	Image evaluation
Zen 3.5 (blue edition)	Microscopy photos

3.2. Materials and methods used for cloning

The non-viral Sleeping Beauty transposon system was used to generate BMP-6 and BMP-2/6 overexpressing cells. The following subchapters provide details on the methodologies utilized for plasmid cloning, nucleofection for gene transfer, and transgene expression analysis.

The pENTR223.1-hBMP6 plasmid was originally obtained from the Harvard PlasmID at Harvard Medical School in Boston, MA. The hBMP2 gene (Wyeth Research, Cambridge, USA) was already cloned into the entry vector pENTR11 (Invitrogen), which was readily available at the ExperiMED laboratory. Briefly, the BMP genes were amplified, and the ends were modified using PCR before being inserted into the pCR2.1 TOPO plasmid. Subsequently, the homo- and heterodimeric sequences were constructed within the pSBbi-GP plasmid. These plasmids were delivered into hMSCs by nucleofection. The transgene expression was validated through various experiments, which are described below.

3.2.1. Generation of competent *E. coli* cells

Competent cells capable of taking up free DNA were prepared and utilized for plasmid cloning using the calcium chloride method. First, DH5α cells were streaked on an agar plate and incubated overnight at 37°C. The precultures were then inoculated into 5 ml of LB medium and shaken overnight at 37°C and 190 rpm.

Next, 750 µl of each preculture was diluted in 50 ml of LB medium and incubated until the absorbance at 600 nm (OD_{600}nm) reached 0.6 AU. The cells were harvested, transferred to sterile, cold falcon tubes and stored on ice. The bacterial cultures were then centrifuged at 2,000 x g for 7 minutes at 4°C, and the cell pellet was resuspended in 15 ml of ice-cold Tfb I Buffer (30 mM potassium acetate, 10 mM potassium chloride, 50 mM manganese chloride, 15% (v/v) glycerol, pH 5.8 with acetic acid, filter sterilized).

This was followed by a 10-minute incubation on ice and centrifugation for 5 minutes at 700x g.

To each of these pellets, 2 ml of ice-cold Tfb II (10 mM MOPS/NaOH, 75 mM calcium chloride, 10 mM potassium chloride, 15% (v/v) glycerol, pH 6.5 with NaOH, filter sterilized) was added and carefully swirled to resuspend the cells in ice water. The suspension was then divided into 200 µl aliquots in pre-cooled cryotubes and immediately shock-frozen in liquid nitrogen. Storage took place at -80°C.

For quality control, the new DH5α *E. coli* cells were transfected with 10 pg of the pUC-19 plasmid.

3.2.2. Maintenance and storage of DH5α *E. coli* cells

The bacterial culture plates with desired clones were carefully stored at 4°C and wrapped in parafilm bands to prevent drying. However, prolonged storage in the refrigerator can lead to a loss of viability, so glycerol stocks were prepared and stored at -80°C for long-term preservation. To prepare glycerol stocks, a single colony was cultivated in 3 ml of the appropriate LB selection medium overnight at 37°C and 190 rpm. Then, in sterile 2 ml screw-top freezer tubes, 0.5 ml of the culture was mixed with 0.5 ml of 80% sterile glycerol using a pipette. The mixture was then immediately shock frozen in liquid nitrogen and stored at -80°C for future use.

3.2.3. Transformation of a plasmid into DH5α competent cells

To propagate the plasmid in *E. coli* cells, 2 µg of plasmid DNA was added to 50 µl of DH5α *E. coli* competent cells and incubated on ice for 30 min. The mixture was then heat shocked at 42°C for 90 seconds and immediately placed back on the ice again. Next, 500 µl of S.O.C. medium was added and incubated at 37°C for 45 minutes. The transformed bacteria were selected by plating on agar containing ampicillin or kanamycin (100 µg/ml) to select bacteria containing the desired plasmid (antibiotic resistance gene carried on the plasmid) and eliminate non-transfected ones. The plates were incubated overnight at 37°C to allow the growth of clones.

3.2.4. Plasmid preparation and restriction digestion

To analyze the clones, several individual colonies were streaked as a pure line and incubated at 37°C for approximately 8 hours. A portion of this pure line was then cultivated in a nutrient solution containing 5 ml of LB medium (prepared by autoclaving a solution of 900 ml distilled water, 9 g tryptone, 4.5 g yeast extract, and 9 g NaCl, pH 7.3) and 5 µl of ampicillin concentrate (100 µg/ml). The solution was then incubated overnight at 37°C with shaking at 225 rpm.

The plasmid DNA was extracted from the bacterial solution using the Promega PureYield™ Plasmid Miniprep System, following the manufacturer's instructions. The DNA concentration was determined using a Nanodrop spectrophotometer at a wavelength of 260 nm (OD_{260}). To perform restriction enzyme digestion, 500 ng of the plasmid DNA was incubated with 2 U of the appropriate enzyme in the presence of 1x buffer (NEB, Schwalbach) at 37°C for 1 hour. The resulting DNA fragments were analyzed by gel electrophoresis. All enzymes used are listed in Table 4.

3.2.5. Gel electrophoresis

Gel electrophoresis is a technique used to separate and subsequently identify DNA fragments based on their length. A 0.5% agarose gel was used to analyze the digested plasmids, while a 2% agarose gel was used for plasmid excision and purification of DNA fragments from the gel. The detection and extraction of PCR products are described in chapter 3.2.6.

To facilitate visualization during electrophoresis, 4 µl of 6x blue dye (NEB, Schwalbach) was added to 20 µl of digested solution. In addition, to make the DNA visible under UV light, ethidium bromide (6 µl/100 ml, from a 10 mg/ml stock) was added to the liquid gel due to its fluorescent property. The bands were observed under UV light at 254 nm for analytical samples and 366 nm for preparative ones. A DNA ladder was included in each run to estimate the fragment length. 1x TAE buffer (1:10 dilution of TAE Buffer

48.5 g Tris, 11.4 ml acetic acid and 100 ml of 0.5 M EDTA pH 8) was used as the running buffer.

Electrophoresis was performed at 120 V for approximately 50 minutes. After electrophoresis, the desired clones were selected for use in subsequent cloning steps.

3.2.6. DNA extraction from gel

To generate the destination vector, one of the essential steps was to extract the DNA from a gel. Therefore, the digested plasmid DNA or PCR product was run on a 2% agarose gel containing ethidium bromide, and the target fragment was excised. The use of ethidium bromide facilitated the visualization of the DNA bands under 366 nm UV light. Next, the DNA was purified using the NucleoSpin Gel and PCR Clean-up kit, according to the manufacturer's protocol. The cleaned-up DNA was eluted into 15 µl of elution buffer (from the PCR Clean-up kit) and analyzed for quality using a Nanodrop spectrophotometer. The DNA was considered pure with an $A_{260/280}$ ratio of ~1.8 and was utilized for subsequent experiments.

3.2.7. Polymerase Chain Reaction (PCR)

The polymerase chain reaction (PCR) is a widely employed technique used to amplify a specific DNA sequence. This process involves repeated cycles of heating and cooling to meld the DNA and facilitate enzyme-driven replication. We used the HotStar HiFidelity PCR Kit (Qiagen). For our cloning strategies, the specific PCR primers were synthesized by Eurofins MWG Operon.

PCR mix for preparative analysis:

1. Template DNA	100-200 ng
2. 5x HotStar HiFidelity PCR Buffer (contains dNTPs and 7.5 mM $MgSO_4$)	10 µl
4. Primer for. (10 pM/µl)	5 µl
5. Primer rev. (10 pM/µl)	5 µl
6. HotStar HiFidelity	1 µl

DNA Polymerase (2.5 units/µl)

7. PCR water

Total: 50 µl

All PCR solutions were stored in 0.2 ml PCR tubes and kept on ice. A DNA-free negative control sample was included in the PCR to ensure quality control. In the negative sample, PCR water was utilized instead of template DNA. A standard PCR program was used with an individual annealing temperature for each primer pair to facilitate primer hybridization to the DNA strand. The elongation temperature was set at 72°C. The primer annealing temperature for cloning the BMP-6 gene was set at 60.6°C, while that for the BMP2-P2A-BMP6 construct primer was set at 53.3°C. Each program was run for a total of 35 cycles.

Standard PCR-program:

		X Cycles					
94°C 10 min	→	94°C 30 sec	X°C 30 sec	72°C 1 min	→	72°C 10 min	→ 8°C

The PCR products were stored long-term at -20°C or the products were directly mixed with 6x Blue Dye gel loading buffer for analysis by gel electrophoresis (as described in 3.2.6.).

3.2.8. cDNA synthesis

To synthesize complementary DNA (cDNA), we used the First Strand cDNA Synthesis Kit for RT-PCR (Roche), along with the thermocycler (Peqstar 2x, Peqlabs Germany). The RNA was denatured as described below. Next, 7 µl of cDNA synthesis mix was added to the denatured RNA and cDNA synthesis was performed by running the designated program on the thermocycler.

RNA denaturation mix:

1. RNA 1 µg
2. Random Hexamer Primer 2 µl

Denaturation for 10 minutes at 65°C ⟶

Storage at 8°C

3. RNAse free H_2O

Total: 13 µl

cDNA synthesis mix:

1. Reaction buffer 4 µl
2. RNAse inhibitor 0.5 µl
3. dNTPs (10 mM) 2 µl
4. Reverse transcriptase 0.5 µl

7 µl mix was added to denatured RNA and run with the following program:

10 min 25°C

60 min 50°C

5 min 85°C

⟶ Storage at 8°C

3.2.9. Semi-quantitative PCR

All cDNA samples were diluted 1:10 using DNAse-free water and kept chilled on ice. For semi-quantitative reverse transcription, we used the Fast Start Taq DNA Polymerase Kit (Roche). The primers and their annealing temperatures are listed in Table 6. These primers were prepared and diluted to a concentration of 10 pmol/µl and stored at -20°C for future use.

RT-PCR mix and program:

1. 10xPCR-Buffer 2 µl
2. dNTP Mix (10 mM) 0.4 µl
3. Primer forward 0.5 µl
4. Primer reverse 0.5 µl
5. H_2O 15.4 µl

Vortex the PCR tube and add

6. Taq polymerase 0.2 µl

	Total volume of	19 µl

7.	cDNA	1 µl
	Total volume of	20 µl

The optimal number of PCR cycles and annealing temperature for amplification of a specific mRNA were determined for each primer (Table 6). For normalization, the GAPDH gene was selected as a reference housekeeping gene. After reverse transcription, the PCR products were analyzed by gel electrophoresis on a 2% agarose gel containing EtBr. The photos were acquired. Quantification of PCR results was performed using ImageJ, an open-source image analysis software platform.

3.2.10. Cloning in TOPO TA plasmid

The next steps in the cloning of recombinant plasmids involved the utilization of the pCR 2.1 TOPO TA cloning kit (Invitrogen, Darmstadt). TOPO-Cloning, also known as DNA topoisomerase cloning, is a method of DNA cloning that does not require a ligase enzyme and is highly efficient. The selection process involved kanamycin and ampicillin resistance genes and the Lac operon, which facilitates blue/white screening. The 3' overhangs allow for efficient ligation with HotStar HiFidelity DNA Polymerase-amplified PCR products that also have 3' overhangs.

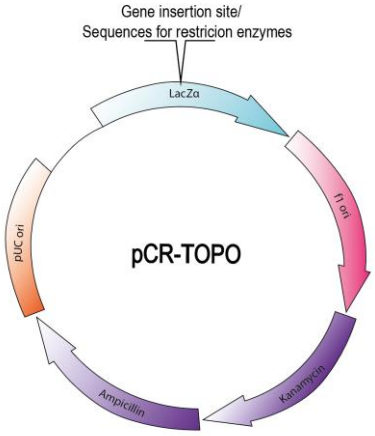

Figure 8 pCR 2.1 TOPO TA. Modified and adapted from www.Thermofisher.com.

The TOPO TA plasmid is covalently bound to topoisomerase I, which is an enzyme that can alter the amount of supercoiling in DNA molecules. Topoisomerase I breaks DNA strands by alternately breaking and resealing the sugar-phosphate backbone. In this case, topoisomerase I specifically recognizes the sequence 5´-(C/T)CCTT-3´ and covalently binds to the phosphate group attached to the 3´ thymidine, cleaves one DNA strand and relieves the supercoiling. The vector is simply mixed with the PCR product, and the linearized vector readily ligates adenine and thymine DNA sequences with compatible ends in a few minutes at room temperature (Fig. 9).

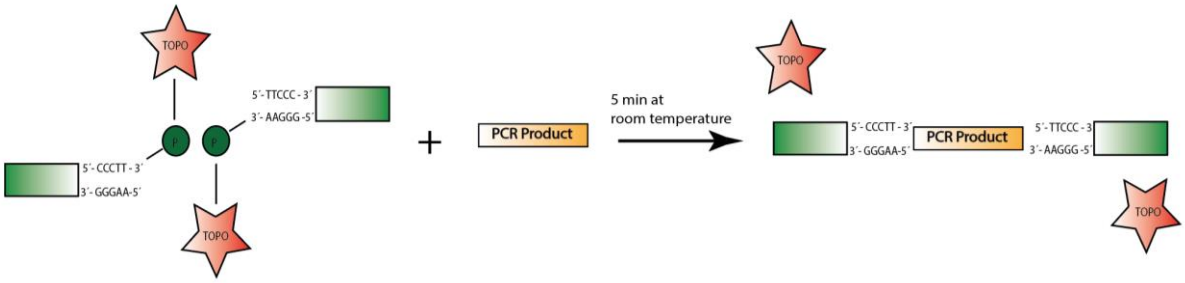

Figure 9 TOPO TA Cloning.

Following ligation, the topoisomerase is released. Modified and adapted from www.Thermofisher.com.

3.2.11. Blue-white screening of clones

To identify the clones containing the recombinant pCR-TOPO-hBMP6 plasmid, we employed a blue/white colony screening protocol from Gold Biotechnology. The TOPO-TA plasmid contains a lac operon that expresses the enzyme β-galactosidase (Fig. 11). In this screening method, 120 µl (20 mg/ml) 5-bromo-4-chloro-3-indolyl-β-D-galactopyranoside (X-gal) was added to an ampicillin-agar plate as a chromogenic substrate. Additionally, 40 µl of 100 mM isopropyl β-D-1-thiogalactopyranoside (IPTG) was added as an inducer to activate the β-galactosidase gene. In the absence of a new gene insertion, the LacZ gene remains uncut. However, in the presence of IPTG, the β-galactosidase enzyme is upregulated, and it hydrolyses X-gal to an insoluble blue pigment. Consequently, the colonies with an intact LacZ gene appear blue because they still have an intact Lac operon that produces β-galactosidase, which is required for lactose digestion. In contrast, the recombinant colonies appear white, allowing easy identification of the correct clones (Fig. 10).

Figure 10 Agar AXI-Plate for blue-white screening.

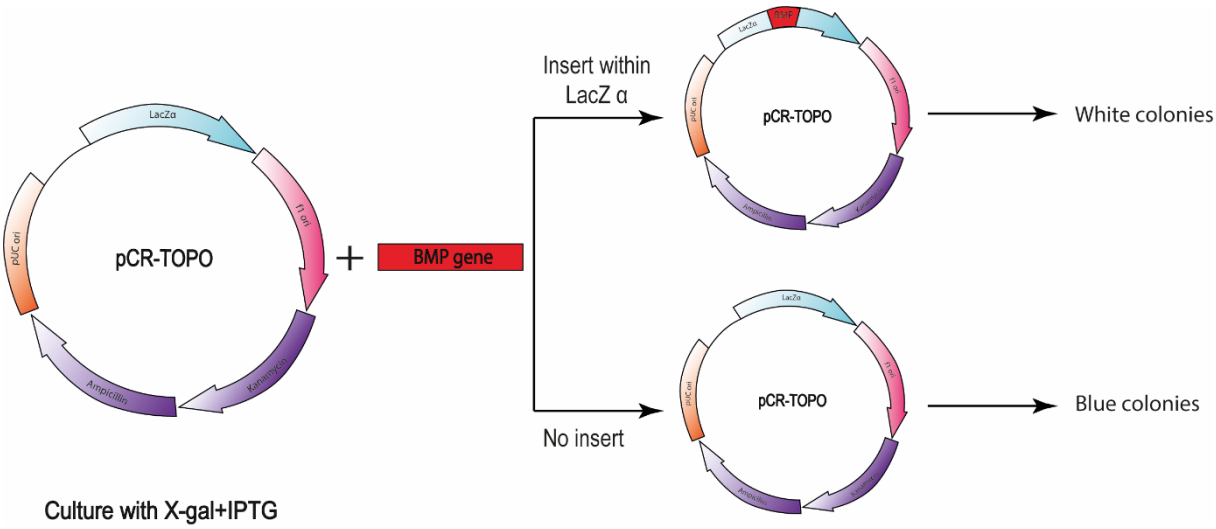

Figure 11 A schematic representation of a typical blue-white screening.

Modified and adapted from www.sigmaaldrich.com.

3.2.12. Ligation of plasmid DNA with T4 ligase

To enable easy ligation, the gene fragment and the vector were digested with the same restriction enzymes, resulting in complementary overhangs. To ligate the gene DNA with a linearized plasmid, the plasmid ends and gene ends were restricted with enzymes and then ligated using T4 DNA ligase. Therefore, 20 µl of volume containing 0.5 µg of vector DNA

combined with a 3-fold molar excess of insert DNA, 2 µl of 10 x T4 DNA ligase buffer, 1 µl of T4 DNA ligase and nuclease-free H_2O were incubated overnight at 4°C. The reaction was stopped by heat inactivation of the ligase at 65°C for 10 min.

The ligated destination plasmid construct was subsequently transfected into DH5α *E. coli* competent cells (3.2.3.).

3.2.13. DNA Sequencing

DNA sequencing was performed by Eurofins MWG Operon (Ebersberg, Germany). Therefore, 15 µl of the sample, with a concentration of 50-100 ng/µl was requested. Our own sequencing primers were designed (Table 6). Sequencing up to 1,100 bases was possible. The sequences were analyzed using the BioEdit program.

3.2.14. Large-scale plasmid DNA isolation (Midiprep)

The desired clone was cultivated overnight in 100 ml of LB medium with 100 µg/ml ampicillin and incubated on a shaker at 37°C. The propagated plasmid was then extracted and purified using the QIAprep Spin Midiprep System. The DNA concentration was measured using Nanodrop. The $A_{260/280}$ ratio of ~1.8 DNA was qualified as pure and used for the following experiments. The resulting recombinant plasmid DNA was stored at -20°C.

3.3. Cell culture

3.3.1. Human mesenchymal stem cells (hMSCs)

Our experiments were performed using the SCP1 cell line. This is a well-established, immortalized human bone marrow-derived mesenchymal stem line described by Böcker et al. 2008 (Böcker *et al.*, 2008). SCP1 stands for Single Cell Picked Clone 1 and represents hTERT-transduced cells successfully introduced via lentiviruses.

Normally, cells undergo cellular senescence as they replicate due to the gradual shortening of telomeres, which are tandem repeat sequences located at the ends of chromosomes (Kim *et al.*, 1994; Liu *et al.*, 2017). However, the introduction of the human telomerase enzyme can prevent telomere shortening and allow indefinite cellular division, leading to the development of an immortalized cell line. This phenomenon is also observed in some tumor cells (Bodnar *et al.*, 1998; Smith, Hocking and Isik, 2004). Therefore, the SCP1 cell line was extensively evaluated to exclude its potential for neoplastic transformation and no evidence of tumorigenesis was found (Böcker *et al.*, 2008).

Immortalized cells such as SCP1 are a valuable research resource due to their ability to grow and differentiate without limitations. This makes them particularly useful in experiments where limited proliferation can lead to incomplete results and variations in different phenotypes and genotypes.

3.3.2. Cultivation of hMSCs and cell culture media

To maintain sterility throughout the work with hMSCs, a laminar airflow cabinet was used and all instruments and supplies were sterile. Prior to work, all surfaces were thoroughly cleaned with 80% ethanol to minimize the risk of contamination.

The hMSC cell lines were cultured in a humidified incubator (Hera cell 240, ThermoFisher Scientific) at 37°C with 95% humidity and 5% CO_2. The standard culture medium used in our experiments consisted of DMEM (Gibco), 10% FBS (Sigma), and 1% penicillin and streptomycin (Biochrom), in order to prevent the contamination of the cell culture.

The cells were cultivated in a cell culture flask (Nunc) with the appropriate amount of cell culture media and incubated in a humidified incubator. The medium was changed one day later and subsequently every two to three days until the cells reached 70-80% confluence of the surface area, indicating that the cells were ready for passage. The propagation process was monitored daily by an optical microscope.

3.3.3. Passaging cells, quantifying cell numbers and expansion

To maintain and expand hMSCs during the log phase, the surface of the T-flask was covered up to 80% prior to cell passage. All supplies were sterilized and prepared as described above. The cell culture medium was warmed to 37°C and the trypsin solution was prepared. Therefore, in a 50 ml Falcon tube, 36 ml of sterile PBS (Gibco) was mixed with 4 ml of 10× trypsin (Trypsin-EDTA Gibco).

Using a sterile pipette, the medium was carefully removed from the adherent cells, and the cells were rinsed with PBS. The cell sheets were then covered with 1× trypsin solution as a cell dissociation reagent. The T-flask was incubated at 37°C in an incubator for 5 minutes. A double amount of warm cell culture medium was added, and the cell clumps were carefully broken up by repeated pipetting. The cell suspension was transferred into a falcon tube and centrifuged at 500 × g for 5 minutes to remove the trypsin reagent and wash the cells, ensuring their viability, minimizing the potential for enzymatic degradation, and to provide a clean environment for further culture experiments. The medium was removed from the well-formed pellet, and the pellet was resuspended in prewarmed growth medium. From a homogeneous solution of single cells, a small sample was removed for cell counting.

Cell counting was performed using trypan blue (Lonza) vital staining. The dye was well mixed with the cell suspension in a 1:1 ratio. A Neubauer counting chamber was then used to count the cells. After evaluation of all four chambers, the number of cells was divided by 2 (due to dilution with trypan blue) and multiplied by 10^4 to calculate the number of cells per milliliter.

For further cell expansion, cells were seeded into a new T-flask (Nunc). The number of cells seeded in the T-flask and the volume of cell culture media were determined after manufacturer's instructions. The seeded cells were incubated again at 37°C.

3.3.4. Freezing (cryoconservation) and storage of cells

Cryoconservation of hMSCs is critical to maintain healthy and viable cells. Prior to cryoconservation, the cells were in the logarithmic growth phase. The freezing medium was made with growth medium (DMEM+1% P/S+10% FBS) by adding 10% DMSO (DMSO, AppliChem) and 10% FBS and stored at 4°C.

After the cells were trypsinized, counted and centrifuged, an appropriate amount of freezing medium was added to the cell pellet. The ratio of cells to freezing medium was approximately 1 million cells per milliliter, and 1 ml of cell suspension was aliquoted into each cryogenic, pre-labeled vial. The vials were placed on dry ice and then transferred to liquid nitrogen for long-term storage.

3.3.5. Thawing hMSC samples

Thawing is a stressful process for the cells and must be done quickly to minimize potential damage. The presence of toxic DMSO in the freezing medium further highlights the importance of careful handling. The work with a liquid nitrogen tank was done according to our work safety policy with the appropriate personal protective equipment (PPE).

To begin the thawing process, the cryogenic vial was placed on dry ice and quickly transferred to a 37°C water bath where it was agitated with gentle shaking. After thawing, the vial was cleaned with 80% ethanol and opened in a hood. The contents were then transferred into a 15 ml Falcon tube (Sarstedt, Germany), supplemented with prewarmed cell culture media, and centrifuged at 500× g for 5 minutes. The supernatant was carefully removed, and the cell pellet was resuspended in media, the volume depending on the number of cells and the size of the T-flask used for cell seeding.

3.3.6. Nucleofection of hMSCs and early transfection events in cell microscopy

Nucleofection is an electroporation-based technique that allows the efficient transfer of genetic material (DNA/RNA) into the nucleus of cells by creating pores in the cell membrane and increasing its permeability using electrophoretic forces (Gantenbein *et al.*, 2020). The efficiency of transfection depends on the cell culture and methods used, and typically gene expression can be observed after 4 hours of the procedure. However, nucleofection has been known to cause high cell toxicity (Kneser *et al.*, 2002; Wu and Yuan, 2011; Hamann, Nguyen and Pannier, 2019). To overcome this issue, modern nucleofection methods and buffers have been developed and improved. Therefore, we have used the 4D-Nucleofector

X Unit system from Lonza along with the P2 Primary Cell 4D-Nucleofector X kit for the nucleofection process.

To perform nucleofection, cells were first resuspended in 20 µl nucleofection buffer containing supplemented nucleofector solution. The cell suspension was mixed with 0.6 µg DNA of the Sleeping Beauty plasmid and the transposase plasmid pCMV(CAT)T7-SB100 in a 3:1 ratio and transferred to a 16-well Nucleocuvette column (Lonza). The Nucleocuvettes were covered with a lid and transferred to the 4D nucleofector (program CM-138, Lonza) for nucleofection. After nucleofection, prewarmed media was added to the Nucleocuvettes and the cells were transferred to a T-flask and incubated overnight at 37°C. Simultaneously, the transfected cells were treated with 2 µg/µl of puromycin (Sigma Aldrich) for one week to eliminate non-transfected cells. After 24 hours, the media was changed, and the cells were observed daily for GFP expression under a fluorescent microscope (Axio Observer Z1 from Carl Zeiss).

3.3.7. Fluorescence-activated cell sorting (FACS)

After nucleofection and puromycin selection, the transfected cells were prepared for sorting of cell populations according to their GFP expression levels using fluorescence-activated cell sorting (FACS). In FACS, a laser beam is used to scatter light from a single cell at all angles, and the optics detect fluorescent signals and convert cellular structures into light signals. The forward scatter (FSC) describes the cell size, while the side scatter (SSC) indicates the fluorescence signal, cell granularity, and structural complexity. These signals are plotted on two-dimensional scatter plots. At least 10,000 cells were sorted per treatment, and SCP1 cells were used as a negative control for evaluating cellular background autofluorescence. After flow cytometric analysis, the cell droplets were separated into different samples according to their fluorescence intensity.

The FACS medium was prepared with DMEM without phenol red (Gibco), 10% FBS, 1% P/S, and 1% antibiotic-antimycotic solution (Gibco). 1 million cells were resuspended in 0.3 ml FACS solution and stored on ice and transported to the FACS facility. After sorting, the cells were seeded in a 225 ml T-flask with cell culture medium containing 1% antibiotic-antimycotic. FACS sorting was performed at the core facility of

the Dr. von Hauner Children's Hospital, Department of Pediatrics, University Hospital, Ludwig-Maximilians University, Munich, Germany.

3.4. RNA Isolation

3.4.1. Isolation of total RNA from cell culture

To determine transgene transcription at the mRNA level, RNA was isolated from cells using the RNeasy Mini kit (Qiagen) according to the manufacturer's instructions. For safety reasons, the work was done under a fume hood and with appropriate PPE.

Prior to RNA isolation, 300,000 cells per cell clone were seeded in a T25-flask and cultivated for three days. On the third day, the cells were washed with PBS. 350 µl of RLT buffer containing 1% β-mercaptoethanol (Sigma-Aldrich) was added to the T25-flask to ensure uniform distribution over the cell sheet. Cells were detached from the bottom of the flask using a cell scraper and the cell pellet was dissolved by pipetting. The solution was then transferred to a sterile 1.5 ml tube (Eppendorf, Germany) and stored on ice. RNA isolation was performed according to the manufacturer's protocol, including the optional DNase digestion step on the column.

After isolation, the RNA pellet was resuspended in 30 µl DEPC H_2O and the RNA concentration was measured in ng/µl and purity was determined spectrophotometrically using a Nanodrop (Nanodrop 2000 spectrophotometer, Thermo Scientific) at A_{260} and $A_{260/280}$. The isolated RNA was stored at -20°C until further use.

3.4.2. RNA isolation using QIAzol lysis reagent

This method was used for hMSCs that were stimulated for 21 days to differentiate into the osteogenic lineage. Due to the formation of calcium phosphate deposits, the cells are difficult to lyse. Therefore, from the positive control samples, the RNA was isolated using QIAzol lysis reagent (Qiagen, Germany) following the manufacturer's instructions. Briefly, the cell monolayer was covered with the QIAzol lysis reagent, and the cells were detached using a cell scraper. The samples were homogenized, transferred into tubes, and stored at room temperature for five minutes. Chloroform was added

and vortexed vigorously for 15 seconds. The samples were stored for three min at room temperature and centrifuged at 12,000 x g for 15 min at 4°C. Three color phases were separated in the samples. The upper, colorless phase containing RNA was transferred to a new tube, isopropanol was added, and the samples were resuspended. After incubation at room temperature for 10 min and centrifugation at 4°C for 10 min, the supernatant was removed and the colorless RNA pellet was resuspended with 75% ethanol. The tubes were centrifuged at 7,500 × g at 4°C for 5 min, the supernatant was removed from the pellet, and the pellets were air-dried. After drying the pellets from ethanol, the pellets were resuspended in 70 µl of RNase-free water and stored on ice.

3.5. Luciferase reporter assay

Luciferase is a class of oxidative enzymes that efficiently convert energy into light. One of the well-known luciferase enzymes is the luciferase firefly, which involves the following reaction:

$$\text{Luciferin} + O_2 + \text{ATP} \xrightarrow{Mg2+} \text{Oxyluciferin} + CO_2 + \text{AMP} + \text{PPi} + \text{light}$$

The luciferase protein does not undergo post-translational modification, resulting in rapid and reliable results. The luciferase reporter cells allow to evaluate where the recombinant BMPs activate the BMP response pathway at the gene level. Compared to other assays such as ELISA, the luciferase reporter assay can detect the total biologically active BMP isoforms in samples (Smith and Trempe, 2000; Logeart-Avramoglou *et al.*, 2005; Herrera and Inman, 2009).

In our experiment, we used HepG1BRA BMP-reporter cells, which were kindly provided by Prof. Daniel Rifkin from NYU. The HepG1BRA cells were stably transfected with a vector consisting of an Id-1-derived enhancer recognized as a BRE-promoter. BMP-Response Element (BRE) acts as a promoter and is activated by R-SMADs and SMAD4 complexes. In this construct, the Id-1-derived enhancer is fused to a luciferase gene. The activated BRE itself activates luciferase transcription and thus translation (Zilberberg *et al.*, 2007).

We seeded $1x10^4$ HepG2BRA cells in a 96-well plate (Nunc, Wiesbaden) and let the cells recover and grow overnight. Our standard cell culture medium (described above)

was used as the growth medium. The next day, the cells were washed with PBS and incubated for 16 hours with cell culture supernatants obtained from the cultures of SCP1-BMP2-GFP-h, SCP1-BMP4-GFP-h, SCP1-BMP6-GFP, SCP1-BMP7-GFP-h, SCP1-BMP2/6-GFP-h, SCP1-BMP2/7-GFP-h, SCP1-BMP-4/7-GFP-h, and SCP1-GFP-h cells. The supernatants were collected for our experiments, as for the luciferase cell reporter assay and ELISA, by seeding 300,000 cells per cell line in T25-flasks. After 3 days, the cell supernatants were collected, centrifuged at 4°C at 10,000× g for 5 min, and stored at -20°C for a short time for the future experiments. For this assay, we chose black plates with transparent bottoms (Corning Costar plate).

After 16 hours, the cells were washed with PBS and lysed with 20 µl of 1x reporter lysis buffer (Luciferase Assay System, Promega USA). The 96-well plate was sealed with foil to protect the samples and stored at -20°C for one hour. The microplate detection system (Safire 2, Tecan Switzerland) was prepared for the experiment. Before the measurements, 100 µl of luciferase assay reagent (containing luciferin as luciferase substrate) was added to each sample and rapidly mixed by pipetting. Luciferase catalyzed the reaction, and the emitted light was measured. At least 6 measurements of each sample were done. All experiments were performed at least twice, with three independent wells per condition.

3.6. Protein analysis techniques

3.6.1. ELISA for BMP-2 and BMP-6

Enzyme-linked Immunosorbent assay (ELISA) is a widely used biochemical technique for the detection and quantification of specific proteins within a sample. We used Quantikine ELISA hBMP2-Immoassay and DuoSet ELISA hBMP-6 (R&D Systems, USA) for our samples. The procedures were performed according to the manufacturer´s instructions. Briefly, the supernatants were prepared and stored at -20°C as described above in chapter 3.5. The samples were the supernatants of SCP1-BMP2-GFPh, SCP1-BMP2/6-GFPh, SCP1-GFPh, and rhBMP-2 which served as the positive control for the BMP-2 ELISA. Similarly, SCP1-BMP6-GFP, SCP1-BMP2/6-GFPh, SCP1-GFPh, and rhBMP6 served as the positive control for the BMP-6 ELISA. The samples were thawed

on ice, diluted 1:10 and 1:100, and used immediately. All reagents were brought to room temperature, microplate strips were prepared, and all standards, samples, and negative and positive controls (rhBMP-2, rhBMP-6) were applied in duplicate.

After completing all protocol steps, the optical density of each well was measured at 450 nm, and wavelength correction was acquired at 550 nm using a microplate reader (Multiscan FC, Thermo Scientific). The concentration of BMP in the samples was determined based on the standard curve. During the procedure, an antibody binding to the bone morphogenetic protein epitopes converted a substrate into a colored product, which allowed us to quantify the amount of BMPs in the samples.

3.6.2. Preparation of cell lysates from cell culture

1×10^6 cells per cell line were seeded in T75-flasks and cultivated until reaching confluence. T-flasks were then washed with ice-cold PBS, and cell lysates were prepared using RIPA-Buffer.

RIPA-Lysis-Buffer:

Stock solution	Working concentration	Amount
10% SDS	0.1% SDS	2.5 ml
Powder NaDOC	1% NaDOC	2.5 g
100% Triton X-100	1% Triton X-100	2.5 ml
1 M Tris-base pH 8.2	50 mM Tris pH 8.2	12.5 ml
5 M NaCl	150 mM NaCl	7.5 ml
0,5 M EDTA pH 8.0	10 mM EDTA	5 ml
1 M NaF	20 mM NaF	5 ml
Filled up to 250 ml with H_2O and stored at 4°C for max. 6 months.		

Because SDS and NaF are toxic, the procedures were done under a fume hood with appropriate PPE. RIPA buffer was prepared by dissolving one tablet of protease and phosphatase inhibitors (Roche, Germany) and stored on ice. After washing the cells, 500 µl of RIPA-Buffer was added to the T75 flask. The cells were scraped with a cell scraper, transferred to pre-cooled Eppendorf tubes, and incubated on ice for 30

minutes. The lysates were homogenized by sonication for 5 seconds and incubated again on ice for 30 minutes. After centrifugation at 10,000 × g at 4°C in a pre-cooled centrifuge, the supernatants were carefully transferred to new tubes and stored on ice.

3.6.3. BCA-Assay

The total protein concentration of the samples was determined using the bicinchoninic acid assay. This assay measures protein concentration based on changes in sample color detected at 562 nm. The concentration of the samples is determined using a standard curve. For our experiment, Micro BCA Protein assay kit (Thermo Scientific, USA) was used for each sample, following the manufacturer's protocol.

Briefly, a total volume of 120 µl of working reagents was used for each sample. As per the protocol, an assay standard of 2 mg/ml BSA was diluted in RIPA-lysis buffer. The supernatant samples were diluted 1:10. 120 µl of each standard and sample was pipetted in triplicate into a 96-well ELISA plate (96-well plates, Nunc). Then, 120 µl of the prepared working solution was added, mixed on a shaker for 30 seconds at room temperature, covered with sealing tape, and incubated at 37°C for one hour. After the plate was cooled, the protein concentration was determined based on the standard curve at 562 nm in an ELISA microplate reader (ELISA Microplate Reader (Multiskan FC, Thermo Scientific, USA). This allowed for an accurate determination of the total protein concentration in each sample.

3.6.4. Sodium dodecyl sulfate-polyacrylamide gel electrophoresis (SDS-PAGE)

SDS-PAGE is a method used to separate proteins according to their molecular weight on a polyacrylamide gel. In this technique, proteins are denatured and negatively charged with SDS. During electrophoresis, the negatively charged proteins move toward the positively charged anode, thus getting separated according to their size. A

protein ladder is used to measure the molecular weight of each protein. For our experiments, we prepared a resolving gel with a reagent concentration of 12% and a thickness of 1.5 mm.

Resolving gel for SDS-PAGE:

Reagents	**Vol**	**Resolving gel 1.5 mm (10 ml)**
H_2O	ml	2.05
30% Acrylamide mix	ml	4
1 M Tris (pH8,8)	ml	3.75
10% SDS	µl	100
10% APS	µl	100
TMED	µl	4

Stacking gel for SDS-PAGE:

Reagents	**Vol**	**Stacking gel (1 gel 2.5 ml)**
H_2O	ml	1.72
30% Acrylamide mix	µl	415
1 M Tris (pH 6.8)	µl	315
10% SDS	µl	125
10% APS	µl	25
TMED	µl	2.5

The resolving gel was poured first between the glass plates, to polymerize and solidify. Deionized H_2O was carefully added to ensure the level surface of polyacrylamide gel once it was polymerized. Afterward, the stacking gel was carefully poured on top of the solidified resolving gel. An appropriate comb was inserted to create sample wells. The gel cassettes were prepared in a casual manner. After the gels were solidified, they were inserted into the clamping frame of the electrode assembly and placed in a mini tank. The tank was filled with 1 x running buffer.

10x Running Buffer		
Tris-base	25 mM Tris pH 8.3	30.28 g
Glycine	0.192 M Glycine	144.13 g
SDS	0.1% SDS	10 g

H_2O	Up to 1,000 ml

The protein concentration was previously measured using a BCA assay, as described earlier. A total of 35 µg of the protein sample was mixed with 4x Laemmli loading buffer containing β-mercaptoethanol (β-ME). β-ME is a reducing agent used to reduce disulfide bonds and homogenize protein samples to obtain well-defined bands. However, it is important to note that β-ME may disrupt the disulfide bonds of BMP proteins, alter protein structure, and make it difficult for some antibodies to recognize the original protein epitopes. Therefore, whether β-ME was added, depended on the manufacturer's instructions for a specific antibody.

4x Laemmli Buffer + β-Mercaptoethanol		
Tris-HCl	50 mM	2 ml from 1 M Tris-HCl pH 6.8
Glycerol	10%	4 ml from 99%
SDS	2.5%	1 g
Bromophenol blue	0.0005%	20 mg
β-Mercaptoethanol	7.5%	3 ml
H_2O		Up to 10 ml

The samples were boiled at 100°C for 5 minutes, centrifuged, and stored on ice. The samples and protein ladder were loaded in the desired order, and SDS-PAGE was then conducted at a constant voltage of 100 V for approximately 1.5 hours.

3.6.5. Western blot

Protein immunoblotting, also known as Western blot, is a reliable method for confirming the presence of specific proteins in a sample. It involves several steps, including SDS-PAGE. After proteins are separated by molecular weight, they are transferred from the gel to a membrane by a process called electroblotting. Blotting was performed using the Trans-Blot Turbo Transfer System (Bio-RAD). Blotting buffer was prepared and stored at 4°C.

10x Blotting Buffer:

Reagent	Working concentration
Tris-base 250 mM	25 mM
Glycine 1.92 M	125 mM
H_2O	up to 1 l pH 8.3

1x Blotting Buffer:

Reagent	Working concentration
10x blotting buffer	10%
Methanol 1.92 M	20%
H_2O	up to 2 l and stored at 4°C

The PVDF membrane was cut to the required size, soaked in methanol for 10 min, and washed briefly with distilled H_2O. Gels, PVDF membranes, and filter papers were equilibrated in 1 x blotting buffer. The gel sandwich was assembled. Therefore, the gel was placed on a filter paper soaked in transfer buffer, followed by the membrane on top of the gel, and then another paper on top of the membrane. The sandwich was placed in a transfer cassette. The blotting program was run at 25 V, 1.0 A for 30 min. The blotted membranes were labeled, washed with TBST twice, and placed in blocking solution in 5% BSA for 1 hour at room temperature. Depending on the manufacturer's instructions for specific antibodies, some membranes were blocked in 5% skim milk.

10x TBS:

Reagent	Working concentration
0.65 M Tris-Base	79 g
1.5 M NaCl	87.7 g
H_2O	up to 1 l and pH 7.4

Wash Buffer (TBS-Tween20):

Reagent	Working concentration
1 M Tris pH 7.4	65 mM
NaCl	150 mM
Tween 20	0.05%
H_2O	up to 2 l

Blocking Solution:

5% skim milk 5 g in 100 ml TBST

5% BSA 5 g in 100 ml TBST

Following the blocking step, the membranes were briefly rinsed with wash buffer, covered with a primary antibody (Table 5) diluted 1:1,000 in blocking solution, and stored on a shaker overnight at 4°C.

The next day, the membrane was washed three times and covered with secondary antibody (depending on the primary antibody) diluted 1:10,000 and stored at room temperature for one hour. After three additional washes each for five min, the protein side of the membrane was covered with ECL-solution forte (Immobilon, USA). The secondary antibody was oxidized with a chemiluminescent substrate, and the resulting chemiluminescence was detected using a Chemiluminescence detector (ImageQuant LAS 4000 mini, GE Healthcare, Munich).

As an internal control for protein loading, the housekeeping protein β-actin was detected on the same membrane. Therefore, the membrane was washed and stripped to remove all immunohistochemical precipitates. The membrane was incubated in a stripping buffer and heated at 50°C for 10 min.

Stripping Buffer:

Reagent	**concentration**
2-Mercaptoethanol	3.57 ml
SDS 10%	100 ml
TRIS 1 M pH 6.8	31.3 ml
H_2O	Up to 500 ml

Afterward, the membrane was washed with TBST and stored in blocking solution for one hour. The primary antibody was added at a dilution of 1:1,000, and the membranes were stored at 4°C overnight. As a reference protein to normalize our protein of interest, we used β-actin. The membranes were then treated with ECL-solution crescendo (Immobilon, USA) and chemiluminescence was measured using a chemiluminescence detector.

3.7. Cell culture experimental techniques

This chapter describes methods for cell culture experiments, as well as osteogenic and adipogenic differentiation techniques that have been applied to BMP overexpressing hMSCs. Experiments were performed on the cell lines, which included SCP1-BMP-2-GFPh, SCP1-BMP-4-GFPh, SCP1-BMP-6-GFP, SCP1-BMP-2/6-GFPh, SCP1-BMP-2/7-GFPh, SCP1-BMP-4/7-GFPh, and SCP1-BMP-GFPh. The differentiation of the cells into adipogenic and osteogenic lineages was performed in co-cultures with hMSCs up to passage 6 from a single donor (male, 67 years old). Therefore, in addition to analyzing the BMP overexpressing hMSCs, we also observed their paracrine influence on the surrounding cells, as this may occur *in vivo* tissues.

3.7.1. Fixation of human mesenchymal stem cells and DAPI staining of nuclei

For GFP expression analysis, 1,000 transfected cells per well were seeded in an Ibidi 8-Well µ-Slide (Ibidi, Germany) and covered with 300 µl of cell culture medium. After two days, the cells were washed with 300 µl of PBS and fixed with 4% PFA for 10 minutes at room temperature. After washing, PBS was gently aspirated, and 300 µl of a working solution of a 4',6-diamidino-2-phenylindole (DAPI) dye was added. DAPI is a nuclear dye that binds to double-stranded DNA in fixed cells, producing blue fluorescence that can be detected using a blue filter. The working concentration for the dye was 1 µg/ml.

The slides were stored in the dark at room temperature for 15 min. The cells were then washed with PBS and fresh PBS was added to the slides to prevent drying. The images were acquired using a fluorescent microscope (Axio Observer Z1 from Carl Zeiss, Germany).

3.7.2. Osteogenic differentiation

To initiate osteogenic differentiation, 20,000 cells were seeded in 24-well plates, with a 1:1 ratio of BMP overexpressing SCP1 to primary hMSCs. All transfected cell lines

were seeded in triplets, for both positive (stimulated) and negative (unstimulated) controls. During the first two days, the cells were cultured in a standard cell culture medium (DMEM+10%FBS+1%P/S). The cells had reached 80% confluence by 48 hours, and osteogenic differentiation was initiated by replacing the standard culture medium with an induction medium. The negative controls received the standard cell culture medium throughout the experiment. The medium was changed every third day, and the hMSCs followed the standard osteogenic differentiation protocol, which typically lasted 21 days.

Osteogenic induction media:

Reagent	**Concentration in stock solution**	**Concentration in OD-medium**
DMEM high glucose (Sigma)		
FBS (Sigma)	100%	10%
Pen/Strep (Gibco)	10,000 IU/ml	40 IU/ml
Dexamethasone (Sigma)	50 µM	100 nM
β-glycerophosphate (Sigma)	1.66 M	10 mM
L-ascorbic acid (Sigma)	12.5 mM	50 µM

3.7.3. Alizarin red S staining

Following 21 days of culture, the stimulated cells exhibited microscopic changes indicative of osteogenic differentiation. To confirm the findings, Alizarin red S staining (ARS) was utilized, which is an effective method for detecting calcium deposits. The Alizarin red S quantification assay is a sensitive technique that allows for the quantification of extracted dye from the cell monolayer.

To perform the ARS staining, the wells for the positive and negative controls were washed twice with PBS and fixed in 4% PFA for 15 minutes at room temperature. Afterward, the layers of cells were washed with dH_2O and incubated with 500 µl 40 mM ARS for 20 min. To prepare 40 mM ARS, 685 mg of the ARS dye (Sigma) was resuspended in 40 ml dH_2O, and the pH was adjusted to 4.1. The solution was then filled to

a total volume of 50 ml and filtered to remove any dye precipitates and clear the solution. Following several washes, the cell layer was covered with water to prevent the cells from drying out and visualized under a microscope.

3.7.4. Quantification of Alizarin Red S staining

After acquisition of images from the stained wells, a quantitative analysis of the ARS staining was performed. Therefore, the optical density of the stained samples was measured and quantified using the pre-established ARS standard curve, which serves as a reference curve. The concentration of calcium deposits in the samples was determined by comparing the OD values of the samples to the standard curve.

To create a standard curve, 40 mM ARS staining stock solution was diluted with acetic acid to obtain a 2 mM ARS solution. The 2 mM ARS solution was further diluted according to the steps as demonstrated in Figure 12. Each absorbance value was assigned a specific concentration of ARS. The absorbance of the standard represents the blank of the measurement. The absorbance and concentration were plotted against each other in a point diagram.

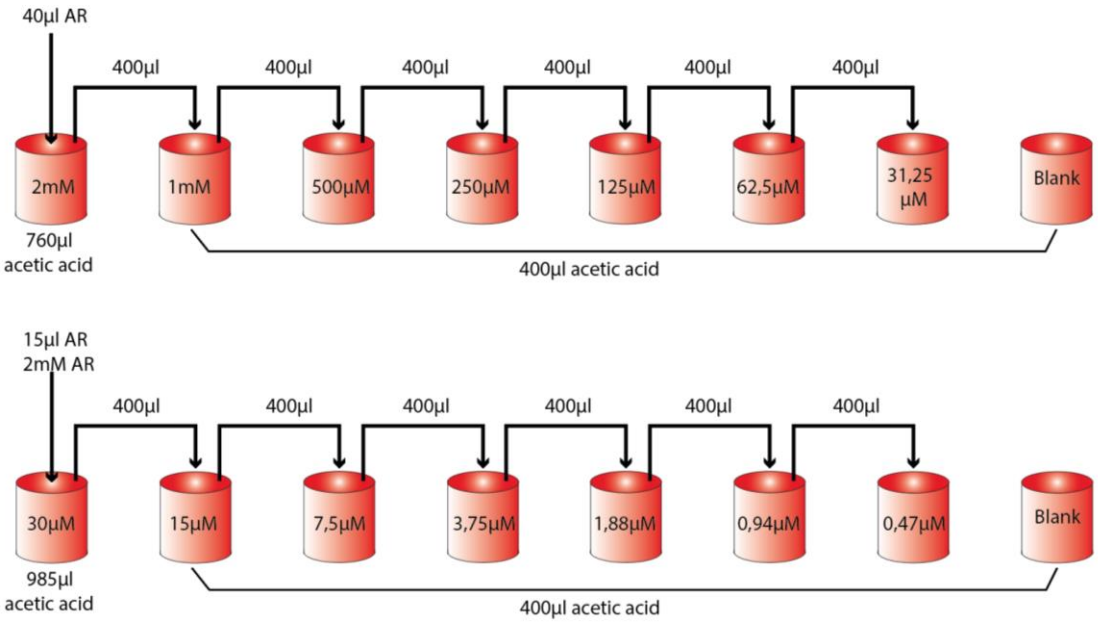

Figure 12 Alizarin red S staining dilution steps for standard.

To determine the OD of stained samples, the bound ARS dye was dissolved with 300 µl of 10% acetic acid in dH_2O for 30 minutes at RT. The cells were scraped from the bottom of the wells and the suspension was transferred into a 1.5 ml tube and vortexed vigorously. The tubes were heated to 85°C for 10 minutes and sealed with parafilm to prevent evaporation. The samples were then stored on ice for five minutes and centrifuged at 14,000× rpm for 15 minutes at RT. 200 µl of the supernatant was transferred into new Eppendorf tubes to which 75 µl of 3% ammonium hydroxide was added to neutralize the pH between 4.1 and 4.5. Due to the high concentration of ARS, all samples were diluted 1:10 and 1:20. Subsequently, 50 µl of all samples and standards were applied in triplicate to a 96-well plate. The optical density was measured at 405 nm using a microplate reader (ELISA Mini Microplate Reader, Thermo Scientific, Schwerte).

3.7.5. Adipogenic differentiation

To investigate the adipogenic differentiation potential of the cells, the same seeding conditions as for osteogenic differentiation were used, with 20,000 cells per 24-well and a 1:1 ratio of transfected BMP overexpressing SCP1 and primary hMSCs. Triplicate wells were used for both stimulated and unstimulated controls. Once the cells reached confluence, adipogenic differentiation was induced by replacing the standard culture medium with an adipogenic induction medium. After five days, the induction medium was changed to maintenance medium for two days before stimulation for another five days. The stimulated cells were treated in this manner for 14 days. The control cells were also treated with standard cell culture medium for 14 days and the medium was changed every third day throughout the experiment.

Adipogenic induction medium:

Reagent	**Concentration in stock solution**	**Concentration in AD-medium**
DMEM high glucose (Sigma)		
FBS (Sigma)	100%	10%
Pen/Strep (Gibco)	10,000 IU/ml	40 IU/ml
Dexamethasone (Sigma)	50 µM	1 µM

Indomethacin (R&D Systems)	50 mM	0.2 mM
Insulin (Sigma)	10 mg/ml	0.1 mg/ml
IBMX (Sigma)	500 mM	1 mM

Adipogenic maintenance medium:

Reagent	**Concentration in stock solution**	**Concentration in AD-medium**
DMEM high glucose (Sigma)		
FBS (Sigma)	100%	10%
Pen/Strep (Gibco)	10,000 IU/ml	40 IU/ml
Insulin (Sigma)	10 mg/ml	0.1 mg/ml

3.7.6. Bodipy staining and fluorescence microscopy

After 14 days of stimulation, microscopic morphological changes were observed in the stimulated cells. To visualize lipid droplets, cells in the 24-well plate were washed and fixed with 4% PFA, following the same protocol as described in chapter 3.7.1. Bodipy 493/503 (Invitrogen, USA) staining was used to visualize lipid droplets. Bodipy is a fluorescent dye that reacts with peroxidized polyunsaturated fatty acids in lipids. Its fluorescent property in the green range of the spectrum allows its application in fluorescence microscopy (Drummen *et al.*, 2002; Spangenburg *et al.*, 2011).

The staining procedure was performed according to the manufacturer's instructions. Briefly, fixed cells were washed three times with PBS and incubated with 5 mM Bodipy diluted in dH_2O for 15 minutes at room temperature. The cell layers were then washed three times with dH_2O and covered with PBS to prevent drying. The fluorescence signal (485/520 nm) emitted by Bodipy-stained lipid droplets was measured. The relative area occupied by lipid droplets and their fluorescence intensity were quantified using ImageJ.

3.8. Statistics

In this thesis, the data were analyzed and visualized using GraphPad Prism9 (USA). All results are presented as mean ± standard deviation (SD) for normally distributed data. To compare more than two groups, ANOVA was used. Specifically, one-way analysis of variance (ANOVA) was used to determine the significance of the mean of each data point compared to controls. For non-normal distributions Kruskal-Wallis test was applied. To identify which sample groups showed statistically significant differences from the control group, we performed post hoc statistical analysis using Dunnett's multiple comparison test. The results were considered statistically significant (marked with an asterisk *) with the probability of error below 5% (* $p<=0.05$).

3.9. Software

For sequence alignment, sequence editing, and molecular biological data analysis the Bioedit 7.2 program was used. DNA sequences were designed and analyzed with Clone Manager 10. The images were evaluated with the NIH ImageJ analysis software 1.52e. The FACS material was demonstrated in FlowJo FACS analysis 10. The fluorescence microscope images were processed using ZEN 3.5 software (Carl Zeiss) and then arranged in figures with Adobe Illustrator (version 26.0). The reference management software Mendeley 1.19.8. was used to manage the references.

Chapter 4

4.1. Results

In this thesis, BMP-6 and BMP-2/6 expressing plasmids were created in the Sleeping Beauty transposon vector to deliver BMP-6 and BMP-2/6 overexpressing hMSCs. Cells transfected with an empty vector containing only the *eGFP* gene were used as a negative control. Furthermore, our aim was to characterize these cells with other BMP-2, -4, -7, -2/7, and -4/7 overexpressing hMSCs and to differentiate them into bone and fat tissues. We also aimed to investigate the *in vitro* osteogenic capacity exhibited by hMSCs overexpressing BMPs derived from the SB-transposon system and to compare the biological superiority of transgenic heterodimeric BMPs with homodimers.

4.1.1. Cloning of pSBbi-GP-hBMP6

The *hBMP-6* gene was inserted into a pre-constructed pENTR223.1 plasmid, creating a “Gateway Entry Clone”. This technology facilitated the propagation and cloning of the *hBMP-6* gene and allowed the simultaneous transfer of this *hBMP-6* fragment into destination vectors while maintaining the reading frame.

To insert the *hBMP-6* gene (1,587 bp) from pENTR223.1 into the destination pSBbi-GP plasmid, the gene was amplified by PCR, and 5' HindIII and 3' PspXI overhangs were inserted at the ends of the gene. The resulting PCR product was ligated to the 3'-T-overhangs of the pCR2.1-TOPO plasmid and screened by blue-white selection.

As described above, the Sleeping Beauty gene delivery system comprises two plasmids: one carrying the gene of interest (GOI), and the other delivering the transposase enzyme (Ivics and Izsvák, 2015). The pSBbi-GP SB-plasmid is known for its robust, constitutive expression, with vector ITR sequences linked to the multiple cloning sites (MCS). The eGFP gene is separated by the P2A self-cleaving peptide from the puromycin selection marker (Eric Kowarz, Löscher and Marschalek, 2015).

The pSBbi-GP plasmid was digested with HindIII and PspXI restriction enzymes. Similarly, *hBMP-6* was excised from pCR2.1-TOPO using HindIII and PspXI restriction enzymes. Therefore, *hBMP-6* exhibited the same digested sites as the pSBbi-GP vector for cloning purposes and was ligated into the linearized plasmid using T4 ligase (Fig. 13). The resulting pSBbi-GP-hBMP6 plasmid was transfected into DH5α *E. coli* competent cells and plated on agar plates. The correct clones were identified by restriction digestion using BamHI, XcmI, XhoI, and XmnI restriction enzymes. The desired clone was verified by sequencing.

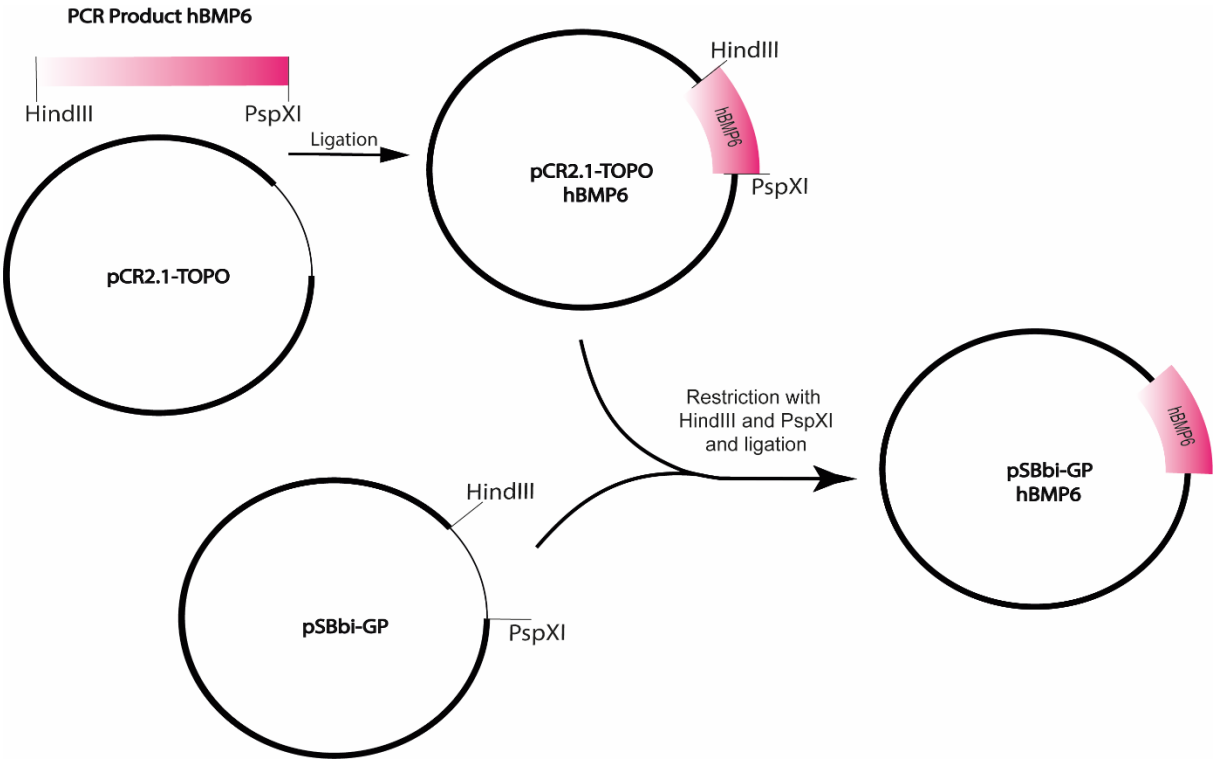

Figure 13 Schematic representation of the cloning of the *hBMP-6* gene into the pSBbi-GP-plasmid.

4.1.2. pSBbi-GP-hBMP2-P2A-hBMP6 heterodimer construct

In order to create the heterodimeric pSBbi-GP-hBMP2-P2A-hBMP6 construct, the following steps were performed. First, the BMP2-P2A-BMP6 oligo was generated and 5` SmaI and 3´ HindIII overhangs were inserted during PCR. The product was then ligated with the pCR2.1-TOPO plasmid (Fig. 14).

The pSBbi-GP-hBMP2 plasmid was previously designed in our laboratory by the working group of Dr. V. Schönitzer and was used in the cloning steps. The pSBbi-GP-hBMP2 and pCR2.1-TOPO-P2A plasmids were propagated in DH5α *E. coli* competent cells. The clones were selected and tested with restriction digest using BamHI-HF and SphI-HF enzymes. After DNA sequencing, high-quality DNA from selected clones was extracted on a large scale using the midi-prep system.

Next, the pSBbi-GP-hBMP2 plasmid and pCR2.1-TOPO-P2A sequence were digested with SmaI and HindIII restriction enzymes. The resulting DNA fragments were purified from the gel and then ligated. The generated pSBbi-GP-hBMP2-P2A plasmid was identified by restriction digestions using HindIII, XcmI, BamHI-HF, and SphI-HF enzymes. Midi-Prep was performed. The cleaned-up plasmid was ready for the next cloning steps.

To create the heterodimeric pSBbi-GP-hBMP2-P2A-hBMP6 plasmid, the pSBbi-GP-hBMP2-P2A and pSBbi-GP-hBMP6 plasmids were cleaved with HindIII and XcmI enzymes. The linearized pSBbi-GP-hBMP2-P2A plasmid and the BMP6-fragment were ligated (Fig. 14). The resulting clones were then analyzed using BamHI-HF, SacI, XcmI, EcoRI-HF, and NcoI-HF enzymes to identify the correct one, which was then sent for DNA sequencing to confirm its accuracy.

Once the correct heterodimeric plasmid was verified, high-quality plasmid DNA was extracted on a larger scale using the midi-prep system and subsequently cleaned up for use in further experiments.

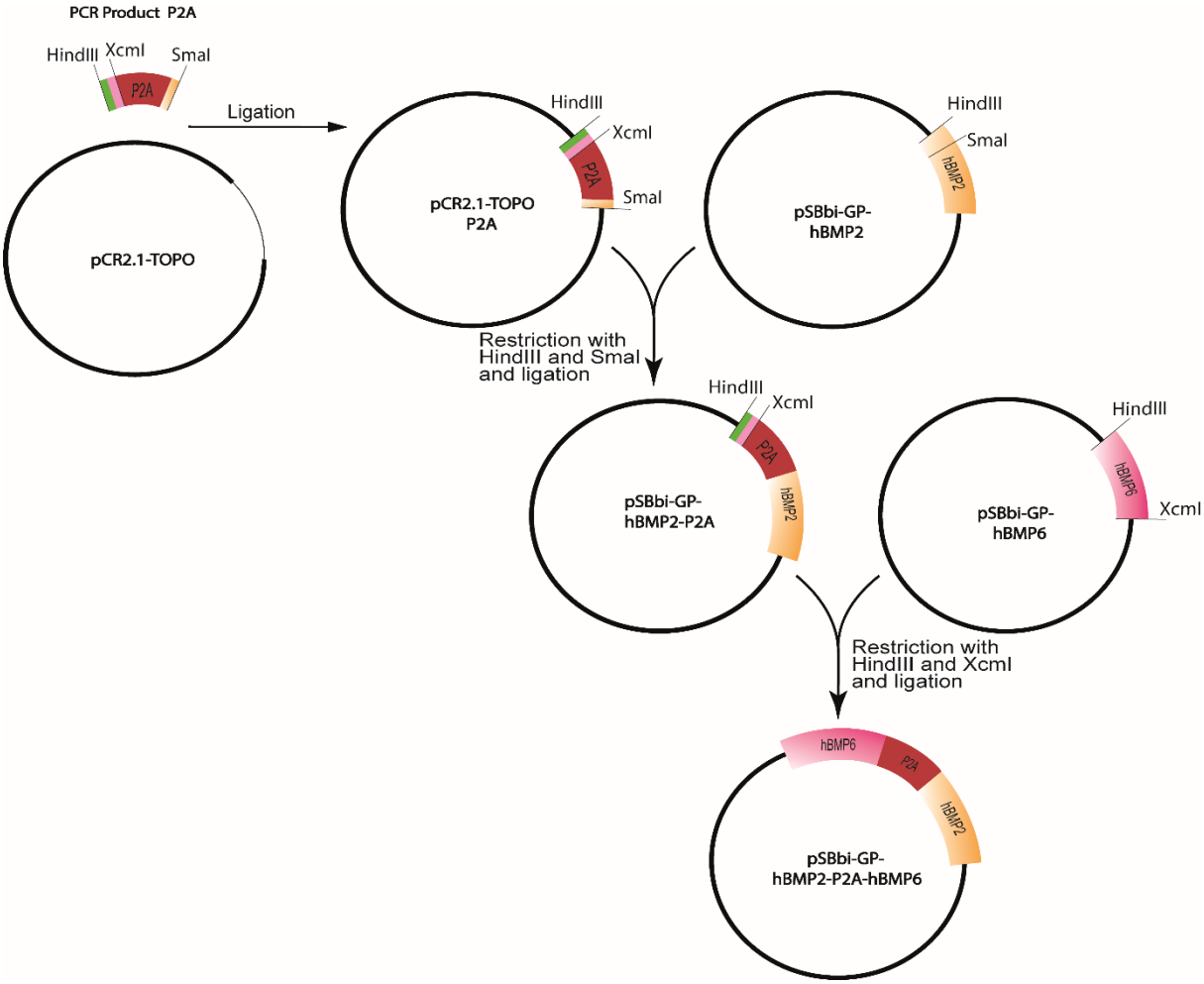

Figure 14 Cloning strategy of the pSBbi-GP-hBMP2-P2A-hBMP6 heterodimer plasmid.

4.1.3. eGFP-Expression and FACS

The pSBbi-GP plasmid is a robust vector belonging to the Sleeping Beauty transposon system family (Eric Kowarz, Löscher and Marschalek, 2015). This vector contains an integrated eGFP gene, allowing for successful transfection detection by early fluorescence microscopy. Initial fluorescence microscopy of nucleofected cell populations revealed inhomogeneous eGFP expression, indicating that some cells did not integrate the vector. To select hMSCs with integrated vectors, cells were treated with puromycin (as described in the methods) and underwent two weeks of selection. Afterward, FACS was used to sort cells based on eGFP expression.

Cells were sorted into two subpopulations, designated as eGFP high- and low-expressing subpopulations, except for BMP-6 overexpressing hMSCs. The BMP-6 overexpressing lineage appeared to have only one cell population with nearly the same eGFP expression pattern (Fig. 15). Also here, the intensity of eGFP expression was referred to as an indicator of successful transfection (Chalfie *et al.*, 1994). A higher intensity of eGFP fluorescence was assumed to be desirable, and it was hypothesized that cells with higher eGFP expression might produce more BMPs. Fluorescence microscopy of each new cell line after sorting showed relatively homogeneous eGFP expression, suggesting successful integration of the vector.

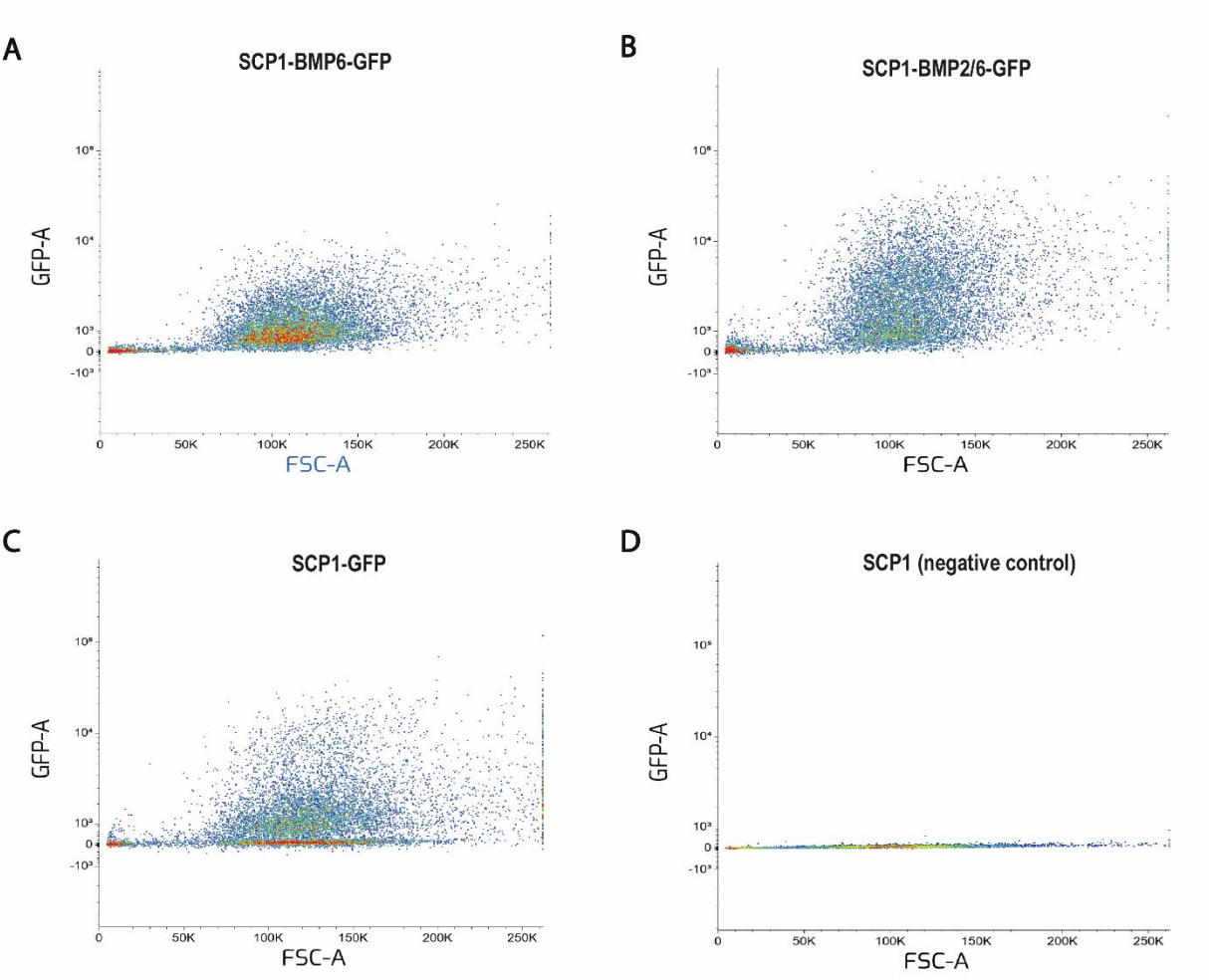

Figure 15 Fluorescence-activated cell sorting of transgenic SCP1 cells.

The flow cytometry analysis of transgenic SCP1-BMP6-GFP, SCP1-BMP2/6-GFP, SCP1-GFP, and negative control hMSCs cells, reveals distinct populations of cells expressing varying levels of eGFP. In the SCP1-BMP2/6-GFP and SCP1-GFP groups, cells were located higher on the GFP-axis, indicating a stronger GFP signal. Whereas in the SCP1-BMP6 group, the cells were located lower on the GFP-axis but still above the negative control baseline, indicating weaker eGFP signals. The analysis gates were set with reference to the negative control hMSCs, resulting in a purity of all eGFP overexpressing cells.

To visualize the differences in eGFP overexpression following FACS sorting, fluorescence images of the sorted transgenic cells were taken (AxioObserver Z1, Zeiss). However, the weak eGFP signal in the eGFP-low subpopulations made it challenging to orient and identify cells during fluorescence microscopy. To address this issue, the cells were fixed with 4% paraformaldehyde (PFA) and stained with DAPI to visualize their nuclei. The blue fluorescence emitted by DAPI in the ultraviolet range of the light spectrum facilitated the identification of cells. To ensure direct comparison, all images were taken with identical brightness and contrast adjustments.

As mentioned earlier, this project also included cell culture experiments with additional BMP overexpressing SCP1 cells, which were generated by Dr. V. Schönitzer's team. Consequently, these experiments aimed to compare homo- and heterodimeric BMP overexpressing cells based on different cellular characteristics. The eGFP fluorescence of all these cell lines was also compared along with other upcoming features, as shown below.

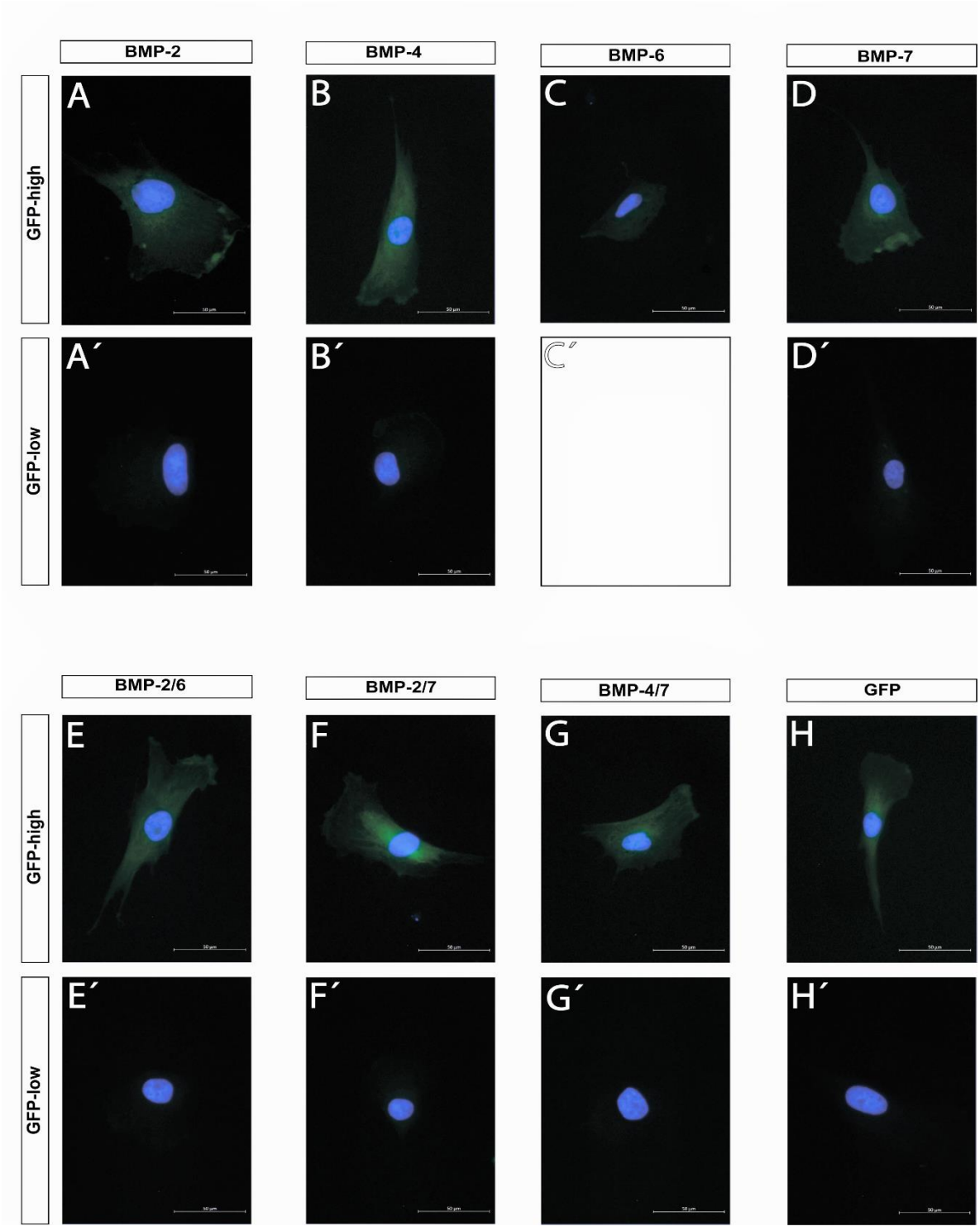

Figure 16 Visualization of differences in eGFP-overexpression levels of transgenic hMSC cell lines after fluorescence-activated cell sorting.

(A-H) GFP-high cells exhibited stronger green fluorescence. **(A´-H´)** GFP-low cells with weak, almost invisible green fluorescence**. C´** BMP-6 overexpressing transgenic cell line did not show variable GFP expressing subpopulations during FACS. Therefore, SB-generated BMP-6 overexpressing hMSCs yielded only the same GFP expression pattern. Cell nuclei were stained with DAPI for orientation during image acquisition. Calibration bars correspond to 50 µm.

4.1.4. SB-transposon derived homo- and heterodimeric hMSCs effectively overexpress BMPs at the mRNA levels

To confirm the successful overexpression of BMPs, we conducted an analysis of BMP transcription at the mRNA level in homo- and heterodimer cells. It was interesting to demonstrate changes in gene expression levels, especially compared to the control cell line (SCP1-GFPh). mRNA was extracted from the SCP1-BMP6-GFP, SCP1-BMP2/6-GFPh, and SCP1-GFPh cells, as well as the SCP1-BMP2-GFPh cells (generated by Dr. V. Schönitzer's team) to serve as a reference for BMP-2 mRNA.

Semi-quantitative RT-PCR was utilized to demonstrate the transfection efficiency of transgenic hMSCs at the mRNA level. BMP-6 RT-PCR showed that the SCP1-BMP2/6-GFPh cells produced a greater quantity of BMP-6 mRNA than the SCP1-BMP6-GFP cells (Fig. 17). No BMP-6 mRNA was detected in the SCP1-GFP cell line. All samples were normalized to the housekeeping gene GAPDH. Therefore, the expression of BMP-2 mRNA was found to be higher in homodimer cells compared to heterodimers (Fig. 18). An increased expression of endogenous BMP-2 mRNA was observed in control SCP1 hMSCs. Also here, the results were normalized using GAPDH as a reference.

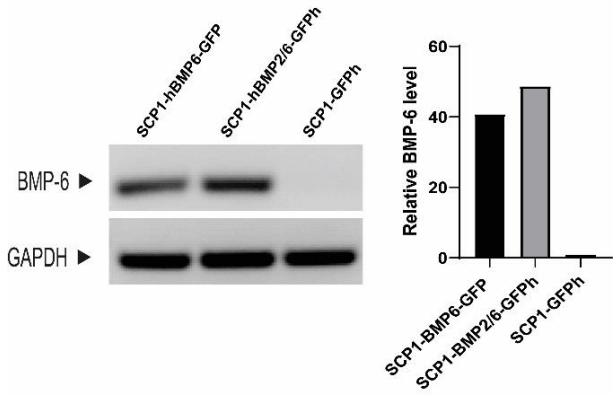

Figure 17 Semi-quantitative RT-PCR for BMP-6.

The semi-quantitative RT-PCR for BMP-6 showed relatively low expression of the BMP-6 mRNA in SCP1-BMP-6-GFP cells when compared to SCP1-BMP2/6-GFPh. The results were normalized with GAPDH.

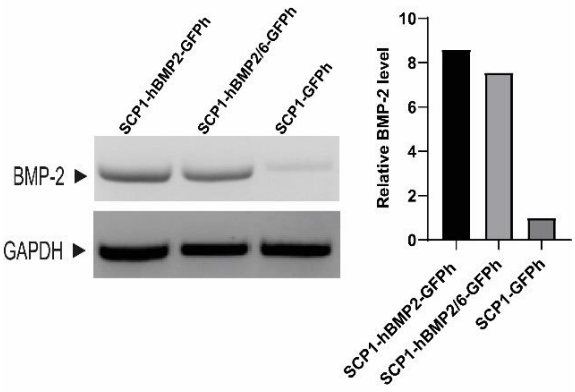

Figure 18 Semi-quantitative RT-PCR for BMP-2.

The BMP-2 mRNA is expressed at a higher level in homo- rather than in heterodimer cells. An elevated endogenous BMP-2 mRNA expression was observed in the control SCP1-GFPh. The results were normalized with GAPDH.

4.2. Western blot analysis of BMP-2 and BMP-6 in transfected cells

To demonstrate the successful translation of BMP-2 and BMP-6 proteins in transfected cells, Western blot (WB) and ELISA analyses were performed, using the SCP1-GFPh cell line as a control. For the WB cell lysates were prepared and run on SDS-PAGE under non-reduced conditions (Mueller and Nickel, 2012). We tested different amounts of optimal protein loading (not demonstrated here) for our experiments and ultimately chose 35 µg of protein lysate.

In Western blot analysis, the BMP-6 antibody detected immunoreactive bands corresponding to the hBMP-6 precursor at the expected molecular weight of 55-65 kDa (Fig. 19). As a loading control, the housekeeping protein ß-actin (43 kDa) was detected in all cell lines, ensuring equal protein loading across samples. We found that BMP-6 precursor was present in both SCP1-BMP6-GFP and SCP1-BMP2/6-GFPh overexpressing cells, while no BMP-6 was detected in the control SCP1-GFPh cells.

Western blot for BMP-2 revealed increased BMP-2 (18 kDa) levels in the SCP1-BMP2-GFPh cells compared to the SCP1-BMP2/6-GFPh cells, consistent with the RT-PCR results. WB also showed increased basal BMP-2 production in the control cell line. Overall, our results confirm the successful overexpression of BMP-2 and BMP-6 in both homo- and heterodimeric cell types.

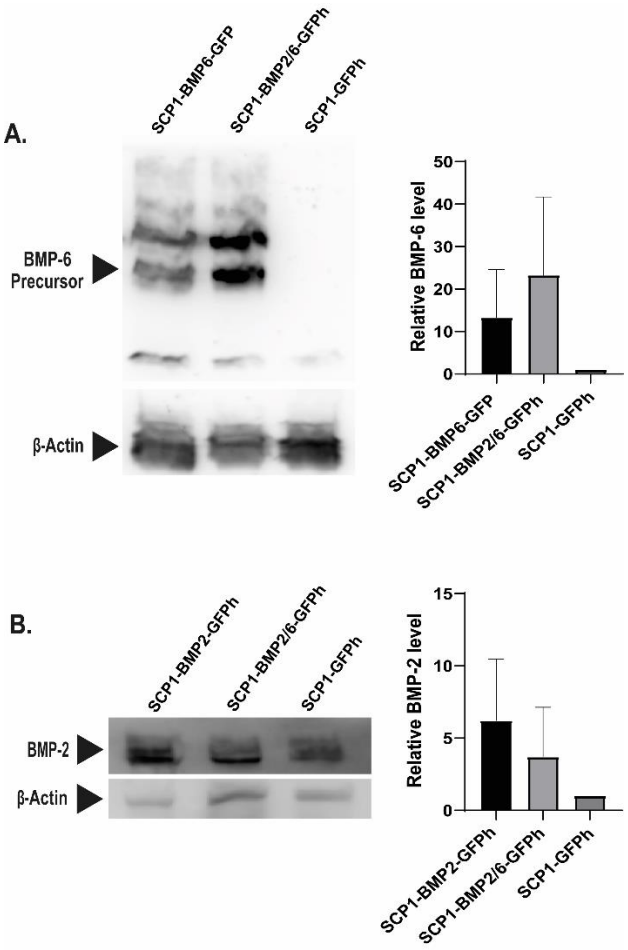

Figure 19 Western blot of BMP-6 and BMP-2.

A. The cell lysates of SCP1-BMP6-GFP, SCP1-BMP2/6-GFPh, and SCP1-GFPh were analyzed for BMP-6 expression (55-65 kDa). The results were normalized to ß-actin protein (43 kDa) intensity and reported as relative protein expression compared to SCP1-GFPh. Band intensities were measured using the NIH ImageJ software. BMP-6 expression was higher in the SCP1-BMP6-GFP and SCP1-BMP2/6-GFPh cells compared to the SCP1-GFPh cells (mean ± SD; n=2 independent experiments).
B. The cell lysates of SCP1-BMP2-GFPh, SCP1-BMP2/6-GFPh, and SCP1-GFPh were analyzed for BMP-2 expression (18 kDa). BMP-2 results are normalized to ß-actin (43 kDa) protein intensity and reported as relative protein expression compared to the control cell line (SCP1-GFPh) (mean ± SD; n=2 independent experiments). BMP-2 expression was increased in SCP1-BMP2-GFPh cells when compared to SCP1-GFPh cells. The experiment also showed increased basal BMP-2 production in the control cell line.

4.3. BMP-6 and BMP-2 ELISA

To validate the RT-PCR and Western blot results and to quantify the concentration of recombinant BMP proteins, we performed an enzyme-linked immunosorbent assay (ELISA)

using supernatants prepared as previously described. The results were measured in ng/ml and normalized to a cell count of 1 million to determine the effective BMP production per cell population.

The findings showed that SCP1-BMP2-GFPh cells produced 215 ng, while SCP1-BMP2/6-GFPh cells produced 31 ng BMP-2 per million cells. Whereas SCP1-BMP6-GFP produced only 3.6 ng BMP-6, while SCP1-BMP2/6-GFPh produced 300 ng BMP-6 per million cells. The endogenous BMP-2 and BMP-6 levels of the control supernatants were below the detection limit of the assay. These results are consistent with those obtained by RT-PCR and WB for BMP-6 and BMP-2.

To exclude the possibility of cross-reactivity between BMP proteins during immunodetection, especially in heterodimeric hMSC lines, 250 pg/ml rhBMP-2 in the BMP-6 ELISA and 500 pg/ml of rhBMP-6 in the BMP-2 ELISA were run as controls. Although the ELISAs did not detect any cross-reactivity of BMPs at these concentrations, it still needs to be precisely clarified whether higher concentrations of BMP-2 or BMP-6 could affect the assays.

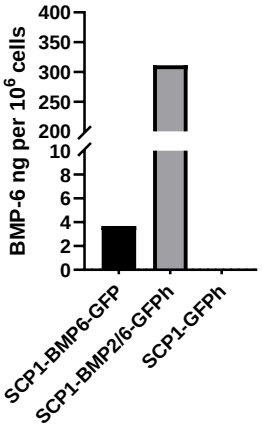

Figure 20 BMP-6 ELISA.

This assay evaluates the supernatants from the SCP1-BMP6-GFP, SCP1-BMP2/6-GFPh, and SCP1-GFPh cells. SCP1-BMP2/6-GFPh cells produced 300 ng BMP-6, while SCP1-BMP6-GFP cells produced only 3.6 ng BMP-6 per million cells. The SCP1-BMP2/6-GFPh cells produced almost 100 times more BMP-6 per million cells than the SCP1-BMP6-GFP cells. No endogenous BMP-6 protein production was detected in SCP1-GFPh cells.

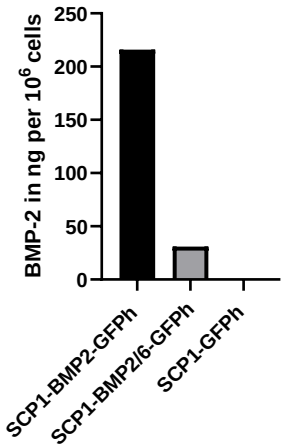

Figure 21 BMP-2 ELISA.

This assay evaluates the supernatants from the SCP1-BMP2-GFPh, SCP1-BMP2/6-GFPh, and SCP1-GFPh cells. SCP1-BMP2-GFPh cells produced 215 ng, while SCP1-BMP2/6-GFPh cells produced 31 ng of BMP-2 per million cells. SCP1-BMP2-GFPh homodimer cells express more BMP-2 protein than the heterodimer cell line. ELISA could not detect endogenous BMP-2 protein production in SCP1-GFPh cells.

4.4. BMPs are biologically active and induce luciferase luminescence activity in BMP-responsive reporter cells

The luciferase cell reporter assay is an effective method for determining the bioactivity of recombinant BMPs following transcription, translation, and post-translational processing (Zilberberg *et al.*, 2007). Specifically, the assay measures the stimulation of the BRE (Id-1 promoter) by recombinant BMPs, thereby providing information regarding the biological activity of BMPs on the gene level. Compared to other assays that measure total BMP levels, such as Western blot or ELISA, the luciferase cell reporter assay provides primarily information about the transcriptional activity of BMPs.

The background luciferase level in the control sample (SCP1-GFPh) corresponds to 1, and the results are expressed in relative luciferase units (RLU). As demonstrated in Figure 22 the supernatants of SCP1-BMP2/6-GFPh could induce nearly 4 times stronger luciferase activity compared to the supernatants of SCP1-BMP-6-GFP. Therefore, this assay confirms that recombinant BMPs are biologically active in transgenic cell supernatants and can induce luciferase activity.

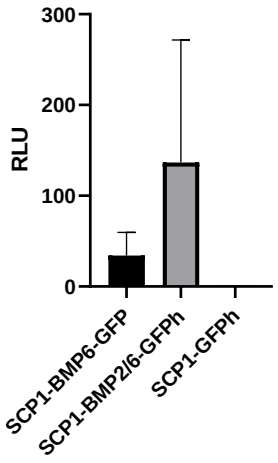

Figure 22 Luciferase Assay.

The data demonstrate that BMPs stimulate luciferase production in HepG2BRE cells over a range of concentrations in an isoform-specific manner. The background luciferase level in the control sample (SCP1-GFPh) is equivalent to 1. The results are presented with ± SEM. Each representative experiment was performed in triplicate. At least two separate experiments were conducted (n=2).

4.5. BMP overexpression in hMSCs enhances BMP cell signaling pathways compared to control in Western blot analysis

In this thesis, we investigated BMP cell signaling pathways in all BMP overexpressing cell lines using Western blot analysis. The cells subjected to analysis included SCP1-BMP2-GFPh, SCP1-BMP4-GFPh, SCP1-BMP6-GFP, SCP1-BMP7-GFPh, SCP1-BMP2/6-GFPh, SCP1-BMP2/7-GFPh, SCP1-BMP4/7-GFPh, and SCP1-GFPh. A total of 35 µg of protein was loaded on the gel for each sample.

The BMP signal is primarily mediated by two canonical SMAD and non-canonical MAP-kinase pathways (Mueller and Nickel, 2012). BMP overexpressing transfected cells were analyzed for autocrine upregulation of these canonical and non-canonical pathways.

BMP overexpression results in autoactivation of BMP receptors, which in turn leads to the recruitment and phosphorylation of SMAD1/5/8 (receptor-regulated SMADs, R-SMADs). R-SMADs form a complex with SMAD4, which then activates BMP target genes in the nucleus. Additionally, BMPs phosphorylate non-canonical signaling pathways, such as MAP-kinases, leading to their activation (Jonk *et al.*, 1998; Zhu, Kavsak and Abdollah, 1999; Von Bubnoff and Cho, 2001; Miyazono, Kamiya and Morikawa, 2010; Huang *et al.*, 2020).

To detect the effect of BMPs on the phosphorylation of these pathways, we used antibodies against phosphorylated (active) and total forms of SMADs (SMAD1/5/8(9)), ERK, and p-38 proteins in Western blot analysis and calculated the ratio. The expected size of the blotted proteins was 58-60 kDa for p-SMAD1/5/9 and SMAD1, 42 kDa for p-EKR and ERK, and 43 kDa for p-p-38 and p-38.

As expected, BMP overexpressing cells generally activated BMP cell signaling pathways compared to control SCP1-GFPh. All BMP overexpressing cells phosphorylated higher levels of SMAD1/5/9 than SCP1-GFPh. BMP-2, BMP-4, BMP-2/6, and BMP-2/7 overexpressing cells exhibited the highest levels of SMAD1/5/9 activation. Furthermore, BMP-4, BMP-7, and BMP-4/7 showed an increase in p-ERK levels, indicating their influence on this specific pathway. The highest levels of p-38 activation were observed in SCP1-BMP-2/6-GFPh cells, while the lowest levels of p-38 activation were observed in cells that overexpressed SCP1-BMP2-GFPh and SCP1-BMP7-GFPh.

The results suggest that the BMP overexpressing cells have generally upregulated biological properties that may be responsible for the observed enhanced activation of SMAD-dependent and SMAD-independent signaling pathways. The WB experimental reports confirmed the influence of BMP overexpression on BMP signaling pathways in our cells.

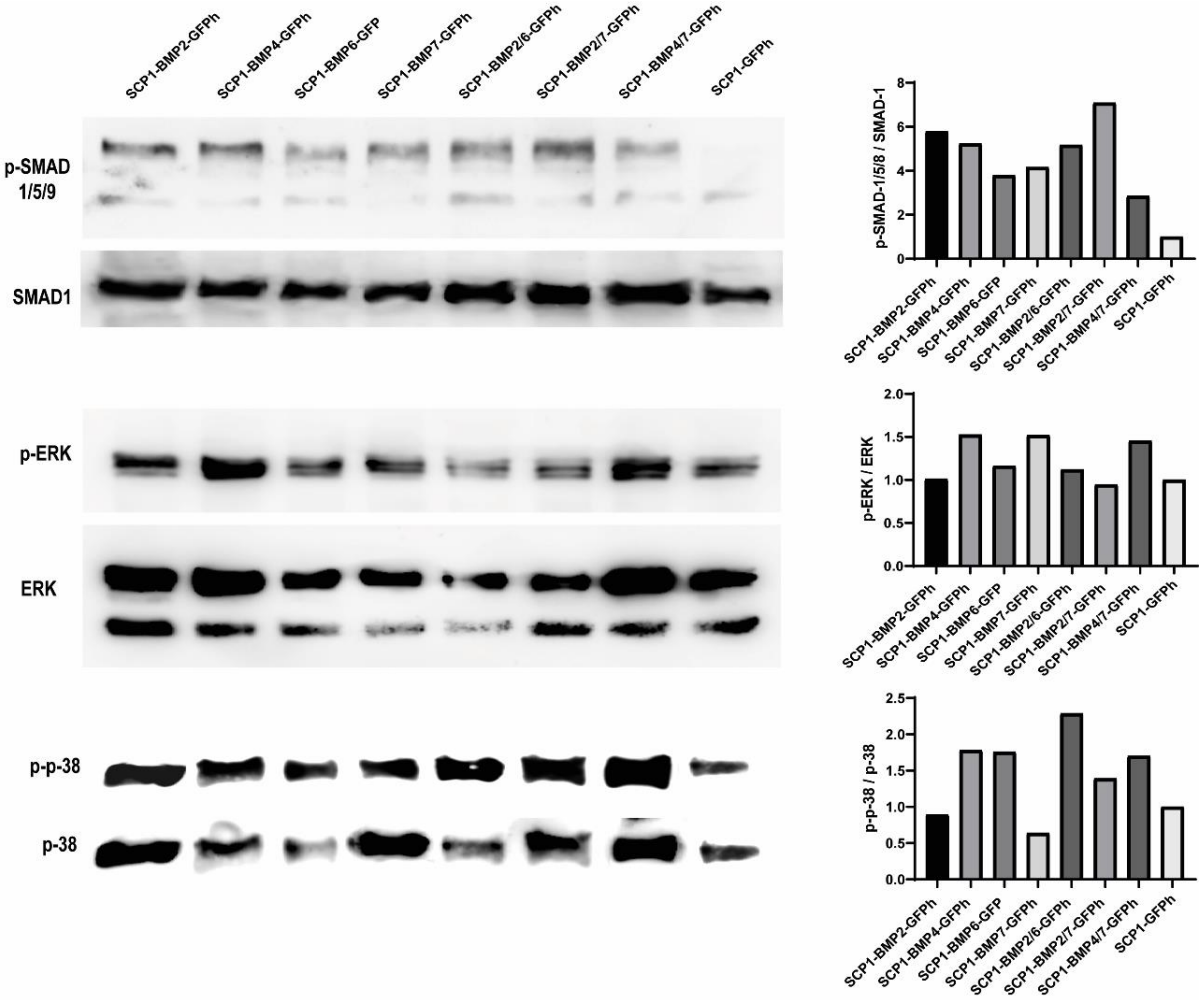

Figure 23 BMP-mediated activation of canonical (SMAD) and non-canonical BMP signaling pathways.

The cell lysates of SCP1-BMP2-GFPh, SCP1-BMP4-GFPh, SCP1-BMP6-GFP, SCP1-BMP7-GFPh, SCP1-BMP2/6-GFPh, SCP1-BMP2/7-GFPh, SCP1-BMP-4/7-GFPh, and SCP1-GFPh were immunoblotted using antibodies for phosphorylated (active) and total forms of cell signaling proteins. As anticipated, cell lines overexpressing BMP exhibited overall activation of BMP signaling compared to control SCP1-GFPh cells. SMAD1/5/9 phosphorylation levels were notably higher in BMP-overexpressing cells, with BMP-2, BMP-4, BMP-2/6, and BMP-2/7 cells showing the highest levels of activation. Additionally, BMP-4, BMP-7, and BMP-4/7 cells exhibited increased ERK activation, suggesting their influence on this pathway. In contrast, SCP1-BMP2-GFPh and SCP1-BMP-7-GFPh cells showed the lowest p-38 activation, while cells overexpressing BMP-2/6 displayed the highest levels of phosphorylated p-38.

4.6. hMSCs overexpressing BMP heterodimer showed greater osteogenic differentiation potency in Alizarin Red S staining

The transfected cells were stimulated in osteogenic medium for 21 days. At the end, osteogenesis was confirmed by Alizarin Red S staining (ARS), which visualizes calcium-rich deposits produced by differentiated cells (Fig. 24). The negative controls, which were not stimulated showed no evidence of osteogenesis. The ARS concentrations were quantified using the protocol as described previously (s. 3.7.4.).

The results of this experiment demonstrated increased osteogenic potential in all BMP-overexpressing cell lines compared to control cells. In particular, BMP-4/7 showed significantly enhanced osteogenic differentiation compared to the control. In general, cells overexpressing heterodimeric BMPs reached higher ARS concentrations than the homodimers.

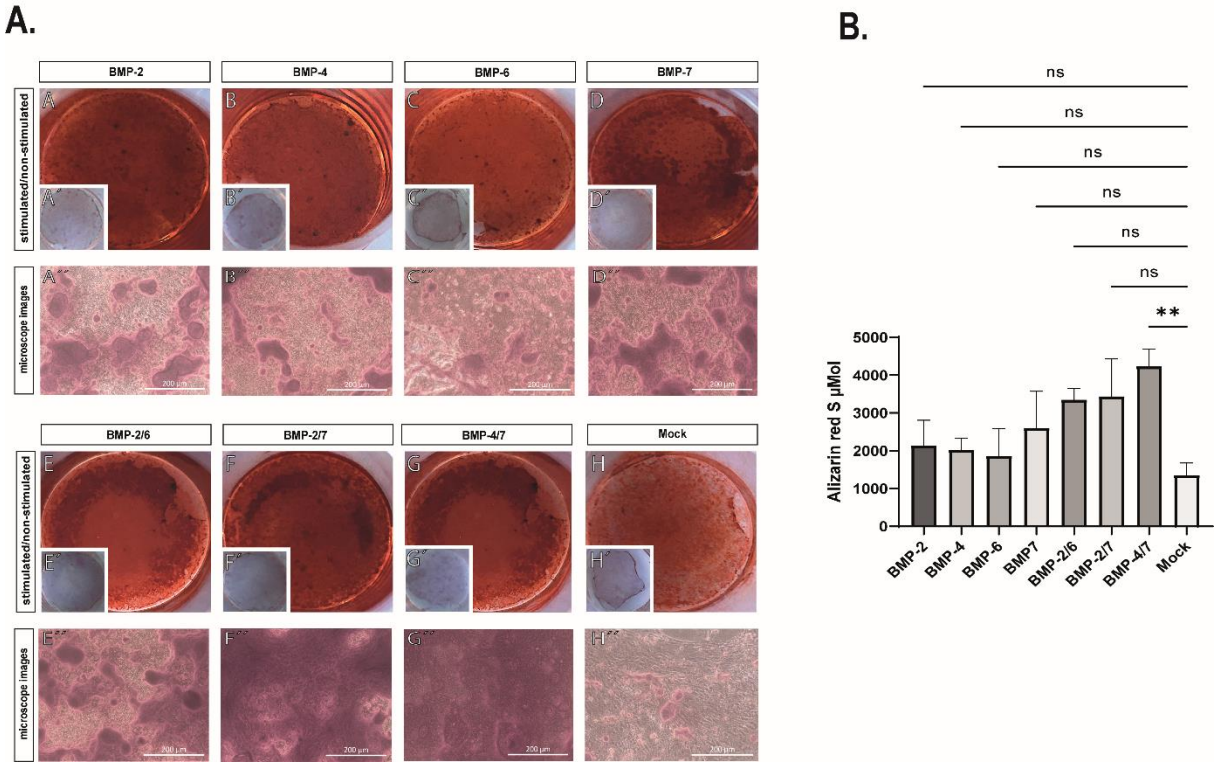

Figure 24 Representation of Alizarin Red S staining (ARS) and the subsequent quantification of osteogenic differentiation.

A. (A-H) Representative qualitative Alizarin red S staining images for calcium deposition on day 21. **(A´-H´)** Unstimulated negative controls demonstrated the absence of calcium depositions. Microscopic analysis of osteogenic differentiation. (A´´-H´´) Microscopic images of ARS-stained cells. Calibration bars correspond to 200 µm.

B. Transfected SCP1 were cultured in osteogenic medium for 21 days. Alizarin red S staining was performed to detect mineral deposition. For quantitative analysis, the absorbance was measured at 405 nm following destaining with 10% acetic acid. The highest concentration of ARS was achieved by the heterodimeric recombinant BMPs, followed by BMP-7. All BMP overexpressing cells demon-

strated a higher degree of osteoinduction than the control cell line (SCP1-GFPh). BMP-4/7 overexpressing cells exhibited the highest and statistically significant accumulation of calcium-rich deposits compared to the control. The negative controls (unstimulated) did not show calcium depositions and were negative on staining (no graphical demonstration). The experimental values are expressed as mean &SEM. (r=3, n=3). Significance levels: ** equals p≤0.01, ns: not significant.

4.7. Upregulation of early and late osteogenic markers

To investigate the transcription factors involved in osteogenesis, we analyzed osteogenic differentiation markers. The osteogenic differentiation of hMSCs is characterized by a slow mineralization phase lasting 7 days, followed by a rapid mineralization phase lasting approximately 10 days, leading to the development of mature osteoblasts (Gregory *et al.*, 2004). In the presence of dexamethasone, ascorbic acid, and β-glycerophosphate, hMSCs undergo a gradual differentiation process. Initially, they differentiate into osteoprogenitor cells, and subsequently into pre-osteoblasts and osteocytes (Id Boufker *et al.*, 2010), which are enclosed by the calcified bone matrix and are no longer capable of undergoing division. Dexamethasone promotes cell proliferation and differentiation, while ascorbic acid has been shown to increase alkaline phosphatase activity and support osteocalcin production (Langenbach and Handschel, 2013).

For RNA isolation, the transfected hMSC clones (SCP1-BMP2-GFPh, SCP1-BMP4-GFPh, SCP1-BMP6-GFP, SCP1-BMP2/6-GFPh, SCP1-BMP2/7-GFPh, SCP1-BMP4/7-GFPh, and SCP1-GFPh) and donor hMSCs were seeded in a 1:1 ratio. Upon reaching confluence, osteogenic differentiation was initiated using osteogenic differentiation media (as described in chapter 3.7.2). At days 3 and 21, RNA was isolated from both stimulated and negative control samples to determine the upregulation of early osteogenic markers.

To evaluate the expression levels of osteogenic markers during differentiation, we measured the relative mRNA levels of Runx2, OCN, ALP, BSP, and Col1α1 using GAPDH as a loading control (Fig. 25). In our experiment, BMP overexpressing cells generally exhibited higher expression levels of osteogenic markers compared to control cells, with a tendency for heterodimer cells to show greater overexpression than homodimer ones. Unstimulated negative control cells did not exhibit any results, indicating that there was no transcriptional upregulation of osteogenic markers (data not represented).

The expression level of Runx2 showed an increase from day 3 to day 21 in all BMP overexpressing cells, with the highest levels observed in BMP-2, -7, -2/7, and -4/7 overexpressing cells. However, BMP-6 overexpressing cells exhibited the least increase in Runx2 expression.

As an early marker of osteogenesis, ALP exhibited a notable upregulation even at day 3 in all BMP-overexpressing cells, compared to the control. Furthermore, ALP levels increased markedly at day 21 in all BMP overexpressing cells with BMP-7, -2/6, -2/7, and -4/7 demonstrating the highest levels.

Compared to day 3, an increase in BSP and OCN expression was evident at day 21 across all BMP overexpressing cells, with BMP-7, -2/7, -2/6, and -4/7 showing the highest levels. In contrast, control cells showed the lowest levels of these mRNA upregulation.

The expression of Col1α1 was considerably low and even undetectable in BMP-2, -4, and -6 overexpressing and control cells during the initial stages of differentiation (D3). However, it exhibited a striking upregulation in the late phase of differentiation (day 21) across all cell lines, including the control. The highest levels were observed in BMP-2/7 and BMP-4/7 overexpressing cells.

In conclusion, the overexpression of BMPs has been demonstrated to enhance the transcription of Runx2, OCN, ALP, BSP, and Col1α1, with heterodimer combinations such as BMP-2/7 and BMP-4/7 were found to induce the highest expression levels, particularly during the later stages of osteogenic differentiation.

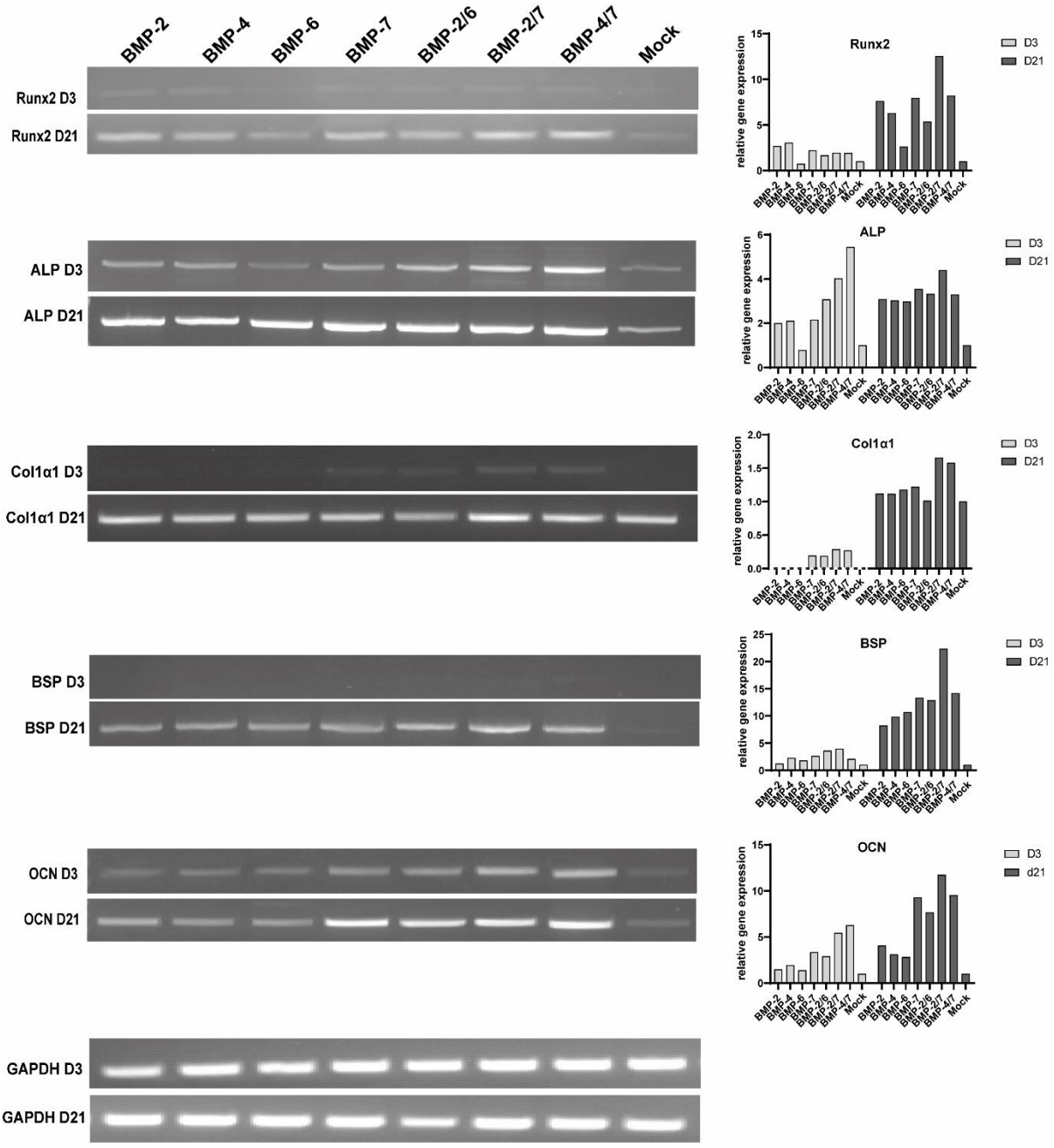

Figure 25 RT-PCR for osteogenic markers.

The relative expression levels of osteogenic differentiation-related genes (Runx2, OCN, ALP, BSP, and Col1α1) were determined by semiquantitative PCR. All stimulated and unstimulated cell lines (negative controls not shown in the figure) were tested at days 3 and 21 throughout the osteogenic differentiation process. BMP overexpression was found to be positively correlated with the enhanced transcription of these osteogenic markers. In particular, the heterodimer combinations of BMP-2/7 and BMP-4/7 were found to induce the highest expression levels, especially during the late stage of osteogenic differentiation. The control cells had a diminished response to osteogenic induction compared to other BMP overexpressing cells. The data was normalized to the loading control, GAPDH. The Col1α1 levels were undetectable in BMP-2, -4, and -6 overexpressing and control cells at day 3. Consequently, the Col1α1 values at day 3 were not normalized to the control but only to GAPDH, and therefore the graph is depicted with a dashed x-axis.

Marker	Timepoint	BMP-2	BMP-4	BMP-6	BMP-7	BMP-2/6	BMP-2/7	BMP-4/7	Mock
Runx4	D3	+	+	+	+	+	+	+	+
	D21	++	++	+	++	++	++++	++	+
ALP	D3	++	++	+	++	++	++++	++++	+
	D21	++	++	++	++	++	++++	++	+
Col1α1	D3	-	-	-	+	+	+	+	-
	D21	++	++	++	++	++	++++	++++	++
BSP	D3	+	+	+	+	+	+	+	+
	D21	++	++	++	+++	+++	++++	+++	+
OCN	D3	+	+	+	+	+	++	++	+
	D21	++	+	+	+++	++	+++	+++	+

Table 9 relative expression levels of the osteogenic markers.

This table demonstrates the relative expression levels of the osteogenic markers at both day 3 and day 21, illustrating the trends observed in our experiments. "-" indicates no significant expression. "+" indicates low expression. "++" moderate expression. "+++" high expression. "++++" very high expression.

4.8. BMP overexpressing and control cells showed comparable adipogenic differentiation, with significant enhancement in BMP-6 and BMP-2/6 overexpressing cells

The adipogenic differentiation of the stimulated cells was evidenced by the formation of lipid vacuoles and the upregulation of adipogenic markers. The formation of lipid droplets was demonstrated by Bodipy 493/503 staining, as the differentiated cells had taken it up (Fig. 26). Bodipy was detected using a fluorescence microscope (Zeiss). The unstimulated cells (negative control) showed no Bodipy staining. The signal intensity of the images was adjusted to eliminate background noise. Therefore, the brightness and contrast settings were modified to remove the influence of non-specific background signals and artifacts that did not represent the actual lipid droplets, thereby improving the clarity and accuracy of the observed results. Lipid droplets were analyzed in the open-source image analysis software platform ImageJ. Lipid droplet area was measured according to the protocol described by Adomshick et al. 2020 (Adomshick, Pu and Veiga-Lopez, 2020).

The results indicate that BMP-2, BMP-6, BMP-2/6, and BMP-4/7 overexpressing hMSCs stimulated in an adipogenic medium, exhibited significantly stronger BODIPY 493/503 staining of lipid droplets than control cells. However, the control cells showed higher adipogenic potential compared to BMP-7 and BMP-4/7 overexpressing cells.

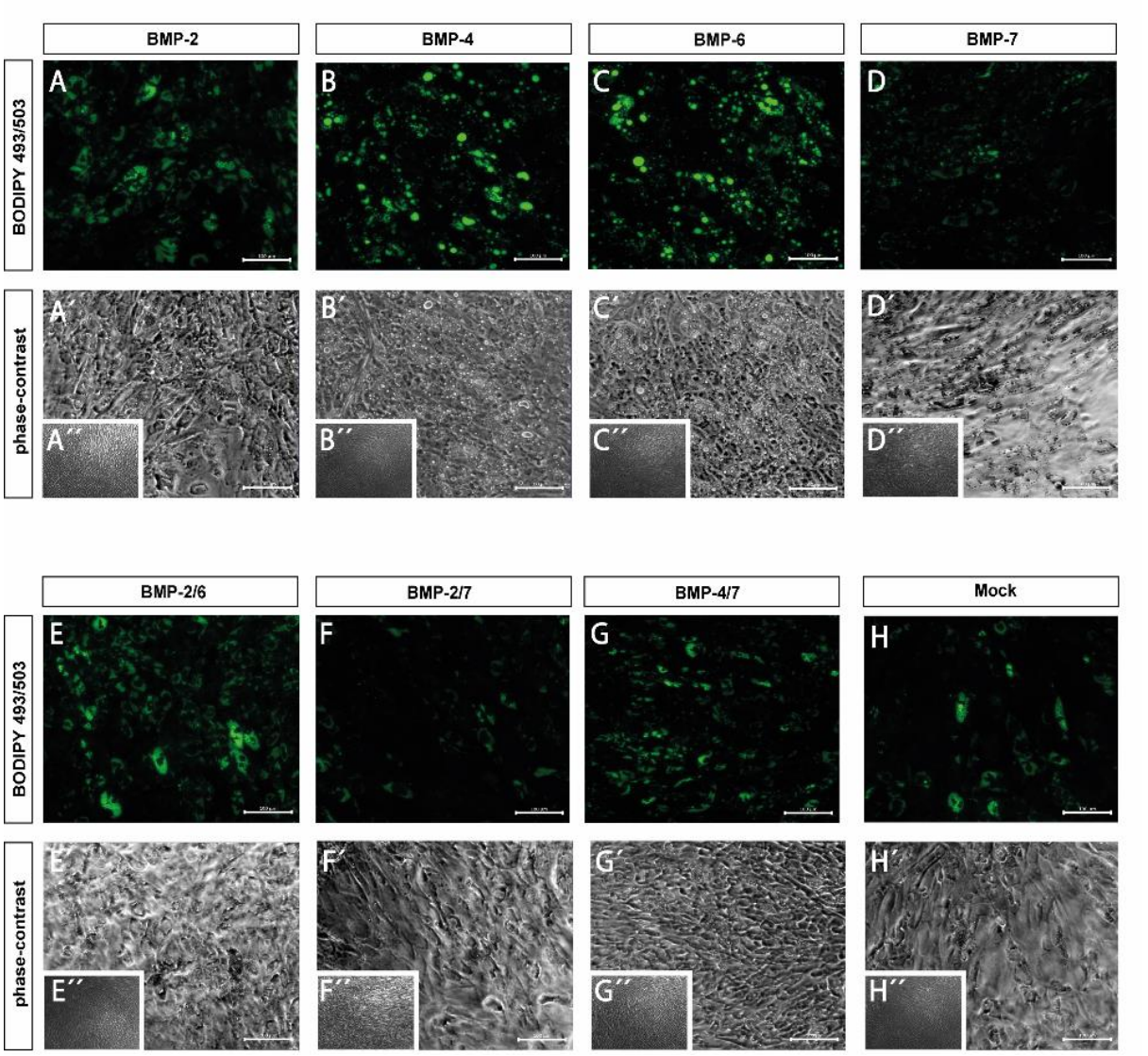

Figure 26 Representation of adipogenic differentiation in the presence of BMP overexpressing and control cell lines.

Fluorescence microscopy was performed on stimulated and unstimulated cells (negative controls) on day 14. (**A-H)** BODIPY 493/503 staining of adipogenic differentiated cells. (**A´-H´)** Images show the same differentiated cells on day 14, but under phase-contrast microscopy. **(A´´-H´´)** Unstimulated negative controls showed no lipid droplet formation and BODIPY uptake. Calibration bars correspond to 100 µm.

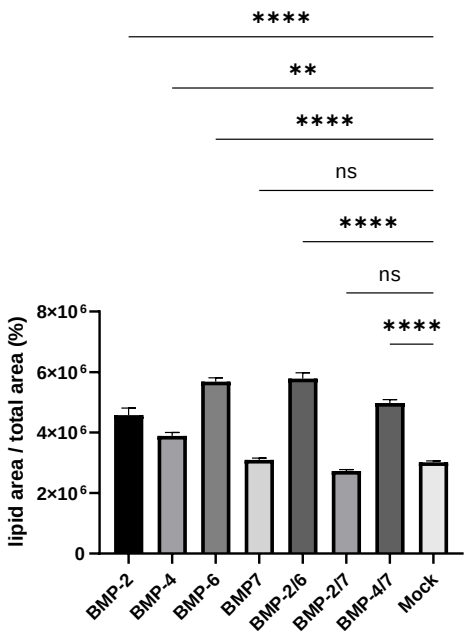

Figure 27 Quantitative measurements of lipid area.

Quantification of stained cells revealed statistically significant differences in Bodipy stained lipid droplet area between BMP-2, BMP-6, BMP-2/6, and BMP-4/7 overexpressing cells compared to control cells (r=3, n=3). Data represent the mean & SEM. Significance levels: *equals p≤0.05, ** equals p≤0.01, *** equals p≤0.001, *** equals p≤0.0001, ns: not significant.

4.9. BMP-6 and BMP-2/6 overexpressing hMSCs showed the strongest upregulation of adipogenic markers among the BMP overexpressing hMSC lines

For RNA isolation, the transfected hMSC clones (SCP1-BMP2-GFPh, SCP1-BMP4-GFPh, SCP1-BMP6-GFP, SCP1-BMP2/6-GFPh, SCP1-BMP2/7-GFPh, SCP1-BMP4/7-GFPh, and SCP1-GFPh) and donor hMSCs were seeded at a 1:1 ratio. Once the cells had reached confluence, the adipogenic stimulation was initiated (as described in chapter 3.7.5.). The adipogenic differentiation markers, PPAR-γ and adipsin, were assessed by semi-quantitative PCR to provide detailed quantitative measurements. Therefore, the stimulated and negative control cells were checked on days 3 and 14 (negative control data not represented).

The results of the semi-quantitative PCR showed that the BMP-6 and BMP-2/6 overexpressing cells exhibited the strongest upregulation of PPAR-γ. It is noteworthy that no expression of PPAR-γ was observed on day 3 in any of the samples. Adipsin had the

strongest signal stimulated by BMP-4, BMP-6, and BMP-2/6 overexpressing cells on day 21. Both markers were also remarkably upregulated in control cells. Interestingly, cells overexpressing BMP-7 displayed the least pronounced upregulation of adipogenic markers, even when compared to control cells.

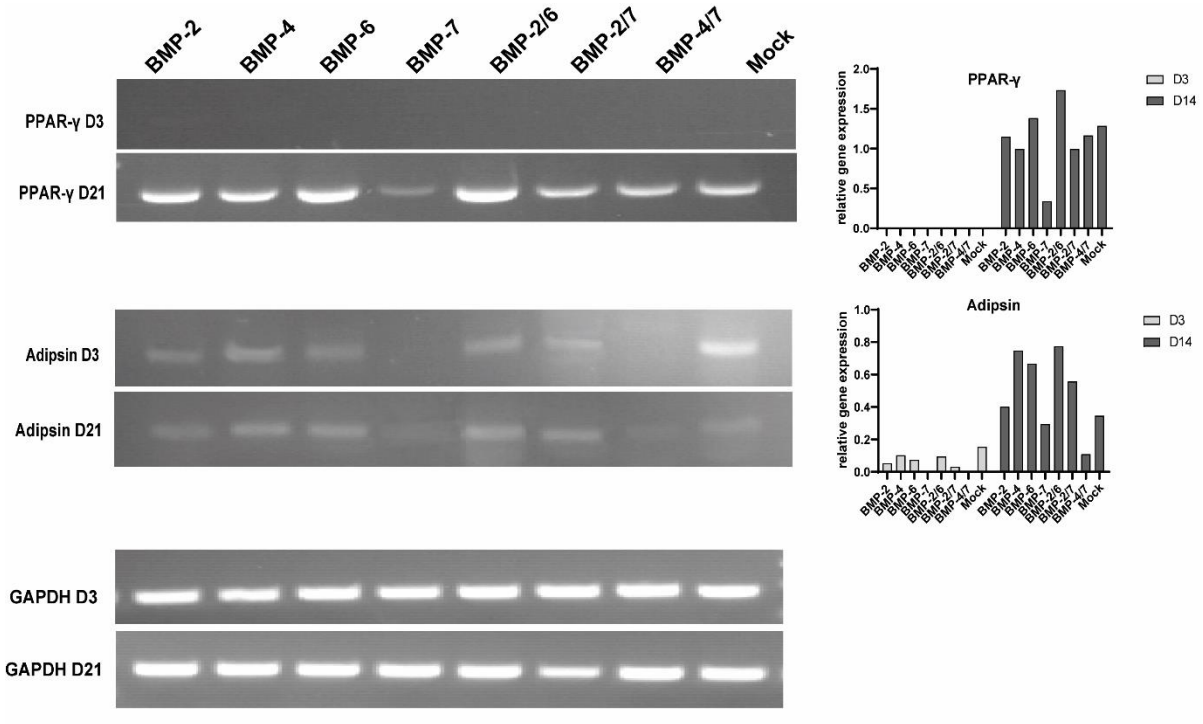

Figure 28 RT-PCR for adipogenic markers.

Adipogenic differentiation was further confirmed by semi-quantitative RT-PCR analysis of the adipogenic markers (PPAR-γ and adipsin). At the beginning of the induction (D3), PPAR-γ was undetectable, compared to adipsin (D3). The cells overexpressing BMP-6 and BMP-2/6 demonstrated the highest upregulation of PPAR-γ, whereas the cells overexpressing BMP-4, BMP-6, and BMP-2/6 stimulated adipsin. Expression of both markers was notably upregulated in control cells. Interestingly, BMP-7 overexpressing cells showed the least upregulation of adipogenic markers, even compared to control cells. The results of negative controls (unstimulated) are not represented.

Marker	Timepoint	BMP-2	BMP-4	BMP-6	BMP-7	BMP-2/6	BMP-2/7	BMP-4/7	Mock
PPAR-γ	D3	-	-	-	-	-	-	-	-
	D14	++	++	+++	+	+++	++	++	++
Adipsin	D3	+	+	+	-	+	+	-	+
	D14	++	+++	+++	+	+++	++	+	++

Table 10 relative expression levels of the adipogenic markers.

This table demonstrates the relative expression levels of the adipogenic markers at both day 3 and day 14, illustrating the trends observed in our experiments. "-" indicates no significant expression. "+" indicates low expression. "++" moderate expression. "+++" high expression. "++++" very high expression.

Chapter 5

5. Discussion

The proper amount of hMSCs and their preserved osteogenic capacity play a crucial role in bone regeneration and thus in fracture healing. The generation of non-virally delivered homo- and heterodimeric BMP overexpressing hMSCs and the understanding of their upregulated biological capacities in *in vitro* experiments could be crucial to develop an effective future treatment plan for impaired bone regeneration-related diseases. The aim of this study was to generate non-virally delivered bone morphogenetic protein (BMP) 6 and 2/6 and characterize them along with BMP-2, BMP-4, BMP-7, BMP-2/7 and BMP-4/7 overexpressing hMSCs. Therefore, these cells were generated and investigated in *in vitro* experiments to uncover their novel upregulated characteristics and related osteogenic potential.

The discussion chapter provides support for our hypothesis that heterodimeric BMP overexpressing hMSCs, delivered by a Sleeping Beauty transposon system, possess enhanced osteogenic capacity and biological superiority over homodimers *in vitro*, and may effectively address bone regeneration problems in the future. In addition, this chapter highlights the overall key findings in single discussion topics from the results, interprets the data, relates correlations to and contrasts with the existing literature, acknowledges study limitations, and provides recommendations for implementation and future research. In order to emphasize the significance of this work, the discussion chapter is structured around our overarching theoretical framework, around which this study revolved.

5.1. Heterodimeric BMP overexpressing hMSCs, a game-changer in the bone regeneration field

Bone morphogenetic proteins are osteogenic cytokines that effectively induce bone formation in a dose-dependent manner (Urist and McLean, 1965; Wang *et al.*, 1990). BMPs influence endochondral ossification by stimulating MSCs. BMP-2, BMP-4, BMP-

6, and BMP-7 have been proven to effectively induce bone formation in *in vitro* and animal models (Peng *et al.*, 2002; Hue H. Luu and et al., 2007; Samee *et al.*, 2008; Zhou *et al.*, 2016). While recombinant homodimeric BMPs produced by transfected mammalian cells have been demonstrated to stimulate new bone formation, heterodimeric BMPs appear to be even more potent (Aono and Hazama M., 1995; Zhao *et al.*, 2005; Zhu *et al.*, 2006; Isaacs *et al.*, 2010; Valera *et al.*, 2010).

In our experiments, we generally observed a higher rate of extracellular matrix (ECM) mineralization during the osteogenic differentiation of transgenic hMSCs overexpressing BMP heterodimers. The cells were fixed with formalin and stained using Alizarin Red S (ARS) dye, which forms a bright red complex with calcium deposits and allows for the visual detection of mineralization. This was followed by the extraction of the dye and subsequent quantitative analysis of the alizarin red S-calcium complex via colorimetric assay (Gregory *et al.*, 2004). hMSCs overexpressing heterodimers showed calcium deposition levels that were almost two times higher than those observed with homodimers. Compared to the control, heterodimeric BMPs induced mineralization levels that were approximately three to four times higher. This difference provides further support for the idea that hMSCs overexpressing heterodimer BMPs exhibit a greater functional response than homodimers, as described in previous studies (Zhu *et al.*, 2004; Isaacs *et al.*, 2010; Miao *et al.*, 2019).

Our analysis revealed that the transgenic cells did not always produce high levels of heterodimeric BMPs compared to homodimers, e.g., SCP1-BMP2-GFPh produced almost seven times more BMP-2 than SCP1-BMP2/6-GFPh, whereas SCP1-BMP6-GFP produced almost 100 times less BMP-6 than SCP1-BMP2/6-GFPh. Despite the lower concentration of certain BMPs in heterodimers (discussed below), *in vitro* osteogenic differentiation remained higher for heterodimers compared to homodimers. This leads to the conclusion that the heterodimeric BMPs have stronger biological activity than the homodimers, which matches those observed in earlier studies (Aono and Hazama M., 1995; Israel et al., 1996; Zhu et al., 2004; Zhao et al., 2005; Guo and Wu, 2012).

Nowadays, rhBMP-2 at 1.5 mg/cc (INFUSE®, Medtronic) and rhBMP-7 at 0.9 mg/cc (OP-1; Stryker Corporation) have been approved by the U.S. FDA for anterior lumbar interbody fusion (ALIF), open tibial fractures with intramedullary nail fixation, and sinus augmentation. Large studies confirm the effectiveness of rhBMP-2 compared to bone autografts in bone formation and fusion surgeries (Friedlaender *et al.*, 2001; Baskin *et*

al., 2003; Burkus *et al.*, 2003; McKay and et al, 2007; Ghodadra and Singh, 2008; Kanakaris *et al.*, 2008; Simmonds, Mark C. and et al., 2013). However, it is important to acknowledge that despite the effectiveness of therapy through the external delivery of these proteins, there remains a large group of patients with reduced numbers of circulating hMSCs and decreased osteogenic potential of the cells due to disease or cellular senescence (Caplan, 2007). Besides this, due to the short half-life of BMPs *in situ*, excess amounts of rhBMPs are required to maintain the therapeutic effect for as long as bone formation needs, which contributes to the high cost of treatment (Ghodadra and Singh, 2008; Sun *et al.*, 2012).

Thus, rhBMP therapy is FDA-approved, well-established, and safe for various surgical procedures. However, there are diverse unsolved bone defect pathologies and uninvestigated fields for BMPs. The enhanced osteogenic potency of BMP overexpressing hMSCs offers a potential solution to critical challenges and may become a novel strategy in the complex field of bone regeneration. Furthermore, BMP heterodimers with greater osteogenic potential than homodimers, combined with an effective and robust SB-transposon gene delivery system, may become a game-changer for BMPs in this field. This could reduce the high costs associated with commercialized rhBMPs, while simultaneously increasing the profit from multipotent hMSCs.

5.2. Bone formation features induced by heterodimers through non-viral gene delivery of BMP-2/6, BMP-2/7, and BMP-4/7

As highlighted in the Introduction chapter, genetically modified stem cells may offer a superior alternative to the protein application of osteoinductive factors. The stable long-term overexpression of osteoinductive cytokines, combined with the powerful regenerative potential of MSCs, can overcome problems such as the short half-life of proteins or local cellular senescence (Dimitriou *et al.*, 2005; Luo *et al.*, 2005).

However, to evaluate the osteoinductive capacity, the initial focus was to identify the osteogenic differentiation potential of hMSCs in cell culture experiments and the upregulation of osteogenic markers at the gene level (Chen *et al.*, 1998; Luo, Sun and et al, 2005; Zhuang *et al.*, 2015). In our assays, osteogenesis was stimulated in all seven BMP overexpressing cell lines, as well as in control cells. To identify the osteogenic influence of BMPs at the gene

level, the mRNAs of early and late osteogenic marker mRNAs were evaluated by RT-PCR analysis.

Bone homeostasis is regulated by the integrated action of osteoblasts, osteocytes, and osteoclasts. The maturation of hMSCs into osteoblasts is a crucial step in bone growth, homeostasis, regeneration, and osseointegration of bone implants (Buckwalter *et al.*, 1996; Sun *et al.*, 2012). Various key factors regulate the differentiation of hMSCs into osteoblasts, including Runt-related transcription factor 2 (RUNX2), which acts as a transcriptional regulator and is crucial for osteoblast differentiation (Botchkarev, 2003; Yang *et al.*, 2003; Phimphilai *et al.*, 2006). BMPs transmit their osteogenic responses through Dlx5, leading to the upregulation of OSX and RUNX2 transcription factors (Long, 2012; Hegarty, Sullivan and O'Keeffe, 2017; Rather *et al.*, 2019). Dlx5 is a crucial signaling molecule that links BMPs to downstream osteogenic factors and together with RUNX2, stimulates osteogenic markers (Lee *et al.*, 2003; Jang *et al.*, 2012). Our data showed that Runx2 was upregulated in BMP overexpressing hMSCs on day 21 after osteogenic stimulation compared to the control, with the most pronounced increase in the heterodimeric BMP-2/7 overexpressing hMSCs.

Upon stimulation by BMPs, precursor cells differentiate into osteoblasts, which produce several other early and late bone-related marker proteins, including type I collagen (COL I), osteocalcin (OCN), alkaline phosphatase (ALP), osteopontin (OPN), and bone sialoprotein (BSP) (Dimitriou *et al.*, 2005; Cho, Cho and Kim, 2009; Id Boufker *et al.*, 2010; Carreira *et al.*, 2014). ALP and OCN specifically serve as markers for bone turnover and osteoblast activity. As a membrane-bound enzyme, ALP is essential for preparing the bone matrix for mineralization (Birmingham *et al.*, 2012), and cells overexpressing ALP are primed for mineralization (Hazama *et al.*, 1995; Yoo and Johnstone, 1998; Chen, Deng and Li, 2012).

In our experiment, ALP mRNA levels were generally upregulated in BMP overexpressing cells compared to the control, with the highest levels observed in cells overexpressing BMP-7, -2/6, -2/7, and -4/7. ALP is typically considered as an early marker and its expression was also notably high at day 3 in our experiments, particularly in cells overexpressing BMP heterodimers. Among all the BMP overexpressing hMSCs, ALP levels remained consistently higher than in the control cells. This result aligns with the ARS staining findings, which indicate higher mineralization in these cells.

Type I collagen is a significant component of the non-mineralized bone matrix, essential for bone formation. According to the literature, RUNX2 does not directly influence Col expression (Hamidouche *et al.*, 2008; Langenbach and Handschel, 2013). As previously described, following stimulation with BMP heterodimer, Col1 exhibits a reciprocal increase (Sun *et al.*, 2012). In our study, the levels of Col1α1 mRNA reached the highest amounts on day 21 with the highest expression occurring in response to BMP-2/7 and BMP-4/7 stimulation. Although Col1α1 expression was also increased in control cells, this increase did not surpass the mRNA amounts expressed due to homodimer stimulation.

Non-collagenous bone extracellular matrix (ECM) proteins, OPN, OCN, and BSP, are widely used as standard markers for assessing osteogenic differentiation (Chen, Deng and Li, 2012; Granéli *et al.*, 2014). The study conducted by Xiao et al. (2002) revealed that MAPK (non-SMAD BMP pathway) could play an important role in ECM production and BMP-induced osteogenesis (Xiao *et al.*, 2002). In RT-PCR analysis, BSP and OCN mRNA expression reached their highest levels in BMP-7, -2/7, -2/6, and -4/7 overexpressing cells. In contrast, control cells did not show any noticeable increase in these markers when compared to BMP overexpressing cells.

To this end, our experiments showed that transgenic hMSCs overexpressing BMPs generally exhibited a tendency to upregulate osteogenic marker mRNAs when compared to control cells. However, some hMSCs overexpressing heterodimeric BMPs reached the highest values. Overall, our findings suggest that transgenic hMSCs overexpressing BMP heterodimers could be a promising approach to enhance bone regeneration.

5.3. Non-viral gene delivery with Sleeping Beauty transposon transposase system

This report demonstrates how non-viral delivery of BMP genes can efficiently stimulate osteogenesis in human mesenchymal stem cells (hMSCs) *in vitro.* We investigated the characteristics that enable us to surpass the viral gene delivery barriers that hinder specific stages of transgenic therapy in bone tissue engineering. Our results show that the SB-transposon system efficiently cuts and pastes BMP genes into the genome. Thanks to a robust plasmid system, this system enables low-cost and simplified propagation in high quantities

and quality. The integration efficiency of the gene of interest (GOI) was evaluated by assessing the expression of the transposon-inserted eGFP gene immediately after transfection (Ivics, Li and Mátés, 2009; Ivics and Izsvák, 2015; Narayanavari *et al.*, 2017).

The importance of the size of the GOI, different electroporation methods, and electroporation buffers in gene delivery is well studied, yet there is a need for better understanding. Doubtlessly, the negatively charged DNA on its own presents a challenge in penetrating cell membranes. It requires the use of gene delivery techniques, such as viral delivery vectors, lipid nanoparticles, or vector electroporation (Yin *et al.*, 2014; Gantenbein *et al.*, 2020). A non-viral gene delivery method, such as electroporation of plasmids, despite its high efficiency, exhibits high electro- and cytotoxicity, which can lead to cell death and, thus, low efficiency of gene delivery (Kneser *et al.*, 2002; Hamann, Nguyen and Pannier, 2019; Gantenbein *et al.*, 2020). This study shows that SCP1 hMSCs were effectively transfected using the SB-transposon transposase system and the 4D-Nucleofector from Lonza.

Our research demonstrates that the SB-transposon system can generate high levels of BMP-6 and BMP-2/6 while maintaining high cell viability. Successful overexpression of BMP mRNA was confirmed by RT-PCR analysis. In particular, SCP1-BMP2/6-GFPh cells generated higher amounts of BMP-6 mRNA than SCP1-BMP6-GFP homodimeric cells, while the overexpression of BMP-2 mRNA was greater in SCP1-BMP2-GFPh cells compared to heterodimeric SCP1-BMP2/6-GFPh cells. Western blot and ELISA, two immunoassay techniques, were used to detect and quantify the translation of BMP proteins produced by our cells. The results aligned with those of RT-PCR, SCP1-BMP2/6-GFPh cells delivering the highest amounts of BMP-6 and SCP1-BMP2-GFPh cells delivering the highest amount of BMP-2. The amount of BMPs produced by the cells during 3 days in the cell culture media was quantified by ELISA. Therefore, SCP1-BMP6-GFP cells produced 3.7 ng of BMP-6 per 10^6 cells, whereas SCP1-BMP2/6-GFPh cells produced 31 ng of BMP-2 per 10^6 cells and 311 ng of BMP-6 per 10^6 cells after a single transfection. The efficiency of BMP production, especially in GFP-high hMSCs, surpasses levels previously described in the literature. For example, in previous research by Loozen, non-virally delivered BMP overexpressing cells could only accumulate up to 16 ng of BMP-2 and BMP-6 per 10^6 cells in cell culture supernatant following 2-3 days of cultivation in cell culture medium (Loozen *et al.*, 2018).

As shown by RT-PCR and Western blot and measured using ELISA, the SCP1-BMP2/6-GFPh has yielded nearly 10 times more BMP-6 compared to BMP-2. This discrepancy could potentially be attributed to the fact that the order in which genes are arranged within

a polycistronic system can impact their expression levels. This phenomenon of position-dependent gene expression results in lower expression of the downstream gene compared to the upstream gene, leading to unequal protein production (Kawai *et al.*, 2006, 2009; Feichtinger *et al.*, 2014).

The robust delivery of genes and stable gene expression without the disadvantages of viral-vector systems, such as the propensity for carcinogenesis, immunogenicity, the limited delivery mass of genetic material, and broad tropism, are of great benefit (Rose, Kucharski and Uludağ, 2012; Skipper *et al.*, 2013; Ghosh *et al.*, 2020). However, it remains essential to improve the delivery of BMP constructs to target cells and tissues to fully realize the clinical potential of Sleeping Beauty technology in the field of bone regeneration (Ivics and Izsvák, 2015; Hudecek *et al.*, 2017).

In summary, the Sleeping Beauty transposon transposase system offers excellent properties to navigate the hurdles for efficient gene delivery (Ivics, Li and Mátés, 2009; Holstein *et al.*, 2018), without targeting the coding regions or the upstream proximity of the gene like retro- or lentiviruses. It inserts the GOI randomly, with a higher probability of integration into the large, non-transcriptional region of the genome (Hudecek *et al.*, 2017). This system demonstrates effectiveness in introducing BMPs as a therapeutic strategy in hMSCs to increase their osteogenic potential.

5.4. Signaling mechanism of recombinant BMPs: A comparative analysis of homodimeric and heterodimeric BMPs

BMPs, as members of the TGF-β superfamily, utilize the type I and type II TGF-β receptors to initiate both the canonical (SMAD) and non-canonical (MAPK/ERK) cell signal pathways (Von Bubnoff and Cho, 2001; Yue and Mulder, 2001; Lai and Cheng, 2002; Xiao *et al.*, 2002). Distinct BMPs reveal a specific affinity for these receptors. BMP-2 and BMP-4 work preferably on type I receptors, whereas BMP-6 and BMP-7 on type II receptors (Miyazono, Kamiya and Morikawa, 2010). One of the theories explaining the increased biological activity of heterodimeric BMPs can be attributed to their affinity for binding to both receptors due to their heterodimeric structure. Therefore, the collective activation of TGF-β receptors, a stable ligand-receptor complex, and the enhanced signaling results in the upregulation of BMP signaling pathways (Aono and Hazama M., 1995; Zhao *et al.*, 2005; Isaacs *et al.*,

2010; Valera *et al.*, 2010; Morimoto *et al.*, 2015; Nickel and Mueller, 2019; Gipson *et al.*, 2020).

An effective investigation of BMP biological activity can be performed by using BMP reporter cells. These cells are transfected with a BRE from the Id-1 promoter, which is fused to a luciferase reporter gene, and are subsequently employed for a BMP rapid assay. Following the activation of the Id-1 promoter by BMPs, the expression of the luciferase reporter gene is induced. The relative luciferase units (RLU) are then measured using a luminometer (Zilberberg *et al.*, 2007). In contrast to the ELISA assay, this method only measures the biological activity of BMPs after they induce a reporter gene, but not the total concentration of BMPs present (Herrera and Inman, 2009).

Our study aimed to demonstrate that recombinant homodimeric BMP-6 and heterodimeric BMP-2/6 were biologically active and effectively induced the luciferase gene. The data suggests that the supernatants of SCP1-BMP2/6-GFPh could induce nearly four times stronger luciferase activity compared to the supernatants of SCP1-BMP6-GFP. One possible explanation for the lower luciferase activity in BMP-6 supernatants could be attributed to the lower amounts of BMP-6 (only 3.6 ng BMP-6 per 10^6 cells) in the cell supernatants compared to BMP-2/6 (31 ng BMP-2 and 300 ng BMP-6 per 10^6 cells). Also, it has been reported that HepG2BRA BMP-reporter cells do not react equally to varying concentrations of BMPs. For example, in experiments from Zilberberg et al. (2007) was shown that BMP-2 reached 1 RLU of luciferase activity in the cell lysates at a concentration of 1 nM and BMP-6 at 1.2 nM. BMP-2 was thus identified as one of the most potent stimulators (Zilberberg *et al.*, 2007). Therefore, this BMP reporter cell assay would probably still not be precise enough to compare the biological superiority of homo- and heterodimeric BMP activities. However, it can be assumed that BMP-6 and BMP-2/6 derived by the SB-transposon system in hMSCs, are biologically active and can effectively stimulate BRE when compared to the control SCP1-GFPh cells.

We also investigated whether there was a significant upregulation of BMP SMAD and non-SMAD pathways between BMP homo- and heterodimers. Western blot analysis of BMP overexpressing cells revealed an overall enhancement in phosphorylated p38, ERK, and SMAD proteins compared to the control. In addition, BMP-2 and BMP-2/7 induced the highest levels of phosphorylation in the BMP-SMAD signaling pathway, while BMP-4, BMP-7, and BMP-4/7 more potently activated non-SMAD signaling pathways such as ERK.

Previous research has reported that the BMP-4 protein induces the upregulation of the MAPK/ERK pathway. BMP-4 induces dose-dependent upregulation of the MEK-ERK 1/2 pathway during vasculogenesis (Zhou *et al.*, 2007; Hu *et al.*, 2017). Our WB findings are consistent with these observations, indicating that BMP-4 overexpression leads to the phosphorylation of ERK proteins. Furthermore, the overexpression of the heterodimeric BMP-2/7 has been demonstrated to markedly activate SMAD signaling, leading to robust SMAD phosphorylation, as previously described (Koh, Zhao and et.al, 2008). Importantly, our study shows that BMP-2/7 overexpression also upregulates Runx2, and there is evidence of similar expression trends of Runx2 mRNA in RT-PCR and SMAD in Western blot analysis. Our results are consistent with those previously described that the SMAD-Runx2 axis is critical for skeletal development (Yan *et al.*, 2018).

The results demonstrate that all hMSC lineages overexpressing BMPs showed significantly higher efficiency in both the BMP reporter cell assay and WB analysis of cell signaling pathways when compared to the control. However, the results of this experiment did not clearly confirm the dominance of heterodimeric BMPs over homodimers. Nevertheless, BMPs influence even more signaling pathways and interact with various signaling molecules, making it difficult to estimate the exact route by which heterodimeric BMPs increase the cell biological activity (Valera *et al.*, 2010; Gipson *et al.*, 2020).

5.5. Role of BMPs in hMSC differentiation and specification towards adipocyte lineages

The differentiation of mesenchymal progenitors into adipocytes is influenced by a number of cytokines, including BMPs. Peroxisome proliferator-activated receptor gamma (PPAR-γ), a transcriptional factor, is of critical importance for the differentiation of adipocytes, insulin sensitivity, and overall metabolism (Lefterova *et al.*, 2014). BMPs have pleiotropic effects, that extend beyond their osteogenic potential, and they can affect the induction of PPAR-γ and other cytokines that are involved in adipogenesis (James *et al.*, 2016). Adipogenic differentiation is closely associated with the BMPR-IA isoform of the BMP-receptor family (Chen *et al.*, 1998; Yamaguchi, Komori and Suda, 2000). The inhibition of BMPR-IA signaling suppresses PPAR-γ expression, suggesting that PPAR-γ may serve as a downstream signaling molecule of BMPs during the process of adipogenic differentiation (Wang *et al.*,

1993; Chen *et al.*, 1998; Yamaguchi, Komori and Suda, 2000; Schulz and Tseng, 2009; Carreira *et al.*, 2014).

In this study, we investigated the impact of recombinant BMP overexpression on adipogenesis in hMSCs. Our findings indicate that hMSCs overexpressing BMP-6 and BMP-2/6 accumulated significantly more lipid droplets compared to the control. Additionally, these cells exhibited the highest levels of PPAR-γ on day 14. Moreover, the overexpression of BMP-4, BMP-6, and BMP-2/6 led to the highest levels of Adipsin upregulation based on semi-quantitative RT-PCR analysis. Previous studies demonstrated that BMP-2 and BMP-4 can effectively promote white adipogenesis (Tseng *et al.*, 2008). BMP-2 is known to induce PPAR-γ expression in a dose-dependent manner, but high doses of BMP-2 lead to bone formation and antagonize adipogenesis through the BMP-2 Wnt regulator (Chen *et al.*, 1998; James *et al.*, 2016; Shen *et al.*, 2016). In a study conducted by Wang (1993), it was found that treatment of mouse MSCs with BMP-2 at 100 ng/ml yielded approximately twice as many fat colonies as those without BMP-2 (Wang *et al.*, 1993). In our quantitative analysis of lipid area, we demonstrated a significant increase in the accumulation of lipid droplets in SCP1-BMP2-GFPh cells compared to control.

In the literature, BMP-4 is known to induce a shift from brown to white adipogenesis, support cells' commitment to preadipocytes, promote lipid storage, and act as a suppressor of lipolysis (Tang, Otto and Lane, 2004; Elsen *et al.*, 2014; Modica *et al.*, 2016). In our experiments, BMP-4 showed prominent upregulation of Adipsin in RT-PCR and enhanced accumulation of stained lipid droplet area, but the data did not reach statistical significance when compared to the control.

The adipogenic potential of BMP-6 has been less extensively studied than that of BMP-2,-4, and -7. Previous studies by Schreiber (2017) have shown that BMP-6 signaling effectively upregulates the expression of PPAR-γ and, therefore, the GLUT4 transporter and several other genes involved in lipid metabolism (Schreiber *et al.*, 2017). In our experiments, the upregulation of BMP-6 expression led to overly enhanced white fat adipogenesis. Specifically, we observed that the BMP-2/6 heterodimer significantly enhanced lipid accumulation in hMSCs. As previously discussed, heterodimeric cells overexpressed 300 ng of BMP-6 per 10^6 cells, whereas homodimeric cells produced 3.6 ng BMP-6 per 10^6 cells. Additionally, SCP1-BMP2/6-GFPh produced BMP-2 at a lower concentration (31 ng per 10^6 cells). Therefore, BMP-6 may potentially positively influence white fat adipogenesis. However, BMP-6 in higher doses, accompanied by BMP-2 in heterodimers, might have induced

stronger downstream effects in maturing adipocytes and therefore has stronger adipogenic potential.

Furthermore, BMP-7 and BMP-2/7 showed the lowest adipogenic potential. The levels of PPAR-γ observed in these cell lines were also the lowest. It is already well known that BMP-7 promotes the formation of brown adipose tissue and does not influence the differentiation of white adipose tissue (Tseng *et al.*, 2008; Boon *et al.*, 2011; Elsen *et al.*, 2014). Therefore, systemic administration of BMP-7 has been demonstrated to increase energy expenditure, reduce fat accumulation, and may potentially reverse the effects of obesity (Townsend *et al.*, 2012). In our experiments, BMP-7 overexpressing cells demonstrated the weakest adipogenic potential, even when compared to the control cells.

In summary, the process of adipogenesis is complex and involves the interaction of hMSCs with various signaling molecules. Some BMPs, especially BMP-6 and BMP-2/6, have been shown to effectively enhance adipocyte formation and adipocyte marker upregulation (Wang *et al.*, 1993) in the presence of an adipocyte-promoting medium. This enhancement occurs through increased cell metabolism and overexpression of adipogenic transcription factors. With regard to bone tissue, BMP-7 and BMP-2/7 are particularly interesting, as they have stimulated osteogenic potential without promoting adipogenesis of stem cells.

Chapter 6

6. Conclusion and Outlook

Taken together, our study shows that hMSCs overexpressing BMPs exhibit enhanced osteogenic properties compared to the control. Notably, heterodimeric BMPs, including BMP-2/6, BMP-2/7, and BMP-4/7, resulted in even greater osteogenic potential. In contrast, adipogenesis showed an increase only in some BMP overexpressing cells compared to the control. Both luciferase cell reporter assays and Western blot analysis confirmed the biological activity of these BMPs, demonstrating stronger signaling and phosphorylation in BMP-overexpressing cells.

In general, the results of the study provide evidence of the feasibility of generating hMSC lineages that overexpress high-level biologically active BMPs through a non-viral Sleeping Beauty transposon system. Here we provide the initial evidence and steps for the potential utilization of SB-derived BMP overexpressing hMSCs, which have the potential to be employed in a broader clinical setting.

Cell-based gene therapy is a promising and emerging trend that could establish a new approach for unsolved bone defect burdens. hMSCs can be easily prepared from a donor and quickly and inexpensively converted with the SB-transposon system into osteogenic, BMP overexpressing cells. Future research should include the following procedure to verify our hypothesis in vivo:

1. Non-viral gene therapeutics encounter a major challenge as they move from the laboratory to the clinical settings, largely due to well-recognized limitations associated with the transfection process. While our experiments have demonstrated the effectiveness of electroporation in transfecting human mesenchymal stem cells (hMSCs) with SB transposon transposase plasmids, the method remains a source of stress and electrotoxicity for the cells. It is crucial to improve the feasibility and efficacy of transfection to ensure cell survival during non-viral gene delivery. Consequently, there is an urgent necessity to address this critical requirement.

2. While the SB transposon system offers numerous benefits, it requires several technological upgrades before being utilized in clinical settings. One significant limitation of this system is the lack of targeted integration into the genome and the uncontrolled number of inserted copies. As previously mentioned, the system integrates the gene of interest randomly, without targeting specific sites. Although the ratio of transposon-transposase plasmids could theoretically balance the number of integrated transgenic copies, it is still impossible to tightly regulate the exact number of integrated genes. Hence, precise control over the integration process is not achievable. Therefore, future medicine would greatly benefit from a system that allows for safe integration and controlled expression of genes.

3. One hypothesis suggests that heterodimeric bone morphogenetic proteins (BMPs) may exhibit superior biological properties compared to homodimers, due to the complex upregulation and binding characteristics of BMP receptors. Therefore, BMP overexpression should result in an autocrine upregulation of various BMP receptors. It would be intriguing to investigate the hypothesis of whether receptor upregulation is indeed the root of the biological superiority of heterodimers. Studying the expression patterns of different BMP receptors has the potential to yield valuable insights into this mechanism.

4. The ultimate goal of bone tissue engineering research is to successfully translate *in vitro* systems into clinical practice. It is therefore essential to test the results *in vivo* models. We optimized and conducted the *in vitro* generation of homo- and heterodimeric BMP constructs in hMSCs using a non-viral SB transposon system and characterized the BMP overexpressing cells, which showed superiority of heterodimeric BMPs over homodimers. The subsequent *in vivo* experiments are expected to produce similar or even more favorable outcomes in the repair of skeletal defects in animal models. It would be valuable to evaluate the outcomes using bone scans and *ex vivo* analysis with the aim of demonstrating the potential of heterodimeric BMP overexpressing hMSCs to enhance bone regeneration, compared to the control. This could represent a significant advancement in the treatment of challenging conditions and move us closer to the ultimate goal of clinical translation.

List of Figures

List of Tables

Bibliography

Adomshick, V., Pu, Y. and Veiga-Lopez, A. (2020) 'Automated lipid droplet quantification system for phenotypic analysis of adipocytes using CellProfiler', *Toxicology Mechanisms and Methods*, 0(0), pp. 1–10. doi: 10.1080/15376516.2020.1747124.

Ahern, J. O. K. *et al.* (2021) 'Non-viral delivery of CRISPR – Cas9 complexes for targeted gene editing via a polymer delivery system', *Gene Therapy*, (July), pp. 1–14. doi: 10.1038/s41434-021-00282-6.

Alhadlaq, A. and Mao, J. J. (2004) 'Mesenchymal Stem Cells: Isolation and Therapeutics', *Stem Cells and Development*, 13(4), pp. 436–448. doi: 10.1089/1547328041797552.

Allareddy, Veerasathpurush *et al.* (2012) 'Factors associated with hospitalization charges for cleft palate repairs and revisions', *Journal of Oral and Maxillofacial Surgery*, 70(8), pp. 1968–1977. doi: 10.1016/j.joms.2011.07.026.

Annamalaia, R. T. *et al.* (2019) 'Injectable osteogenic microtissues containing mesenchymal stromal cells conformally fill and repair critical-size defects', *Biomaterials*, 208(3), pp. 32–44. doi: 10.1016/j.biomaterials.2019.04.001.

Aono, A. and Hazama M., et al. (1995) 'Potent ectopic bone-inducing activity of bone morphogenetic protein-4/7 heterodimer', p. Biochemical and biophysical research communication.

Bahney, C. S. *et al.* (2019) 'Cellular biology of fracture healing', *Journal of Orthopaedic Research*, 37(1), pp. 35–50. doi: 10.1002/jor.24170.

Baskin, D. S. *et al.* (2003) 'A prospective, randomized, controlled cervical fusion study using recombinant human bone morphogenetic protein-2 with the CORNERSTONE-SR™ allograft ring and the ATLANTIS™ anterior cervical plate', *Spine*, 28(12), pp. 1219–1224. doi: 10.1097/00007632-200306150-00003.

Berendsen, A. D. and Olsen, B. R. (2015) 'Bone development', *Bone*, 80, pp. 14–18. doi: 10.1016/j.bone.2015.04.035. Bone.

Birmingham, E. *et al.* (2012) 'Osteogenic differentiation of mesenchymal stem cells is regulated by osteocyte and osteoblast cells in a simplified bone niche', *European Cells and Materials*, 23(353), pp. 13–27. doi: 10.22203/eCM.v023a02.

Böcker, W. *et al.* (2008) 'Introducing a single- cell- derived human mesenchymal stem cell line expressing hTERT after lentiviral gene transfer.pdf', *J. Cell. Mol. Med.*, 12(4), pp. 1347–1359. doi: 10.1111/j.1582-4934.2008.0299.x.

Böcker, W. *et al.* (2022) 'Correction to: Fractures in untreated patients with osteoporosis in Germany: an InGef healthcare insurance database analysis (Osteoporosis International, (2022), 33, 1, (77-86), 10.1007/s00198-021-06051-w)', *Osteoporosis International*, 33(1), p. 87. doi: 10.1007/s00198-021-06244-3.

Bodnar, A. G. *et al.* (1998) 'Extension of life-span by introduction of telomerase into normal human cells', *Science*, 279(5349), pp. 349–352. doi: 10.1126/science.279.5349.349.

Boerckel, J. D. *et al.* (2011) 'Effects of protein dose and delivery system on BMP-mediated bone regeneration', *Biomaterials*, 32(22), pp. 5241–5251. doi: 10.1016/j.biomaterials.2011.03.063.

Bohner, M. and Miron, R. J. (2019) 'A proposed mechanism for material-induced heterotopic ossification', *Materials Today*, 22(February), pp. 132–141. doi: 10.1016/j.mattod.2018.10.036.

Boon, M. R. *et al.* (2011) 'Bone morphogenetic protein 7: A broad-spectrum growth factor with multiple target therapeutic potency', *Cytokine and Growth Factor Reviews*, 22(4), pp. 221–229. doi: 10.1016/j.cytogfr.2011.08.001.

Bormann, M. *et al.* (2023) 'Changing patterns in the epidemiology of tibial plateau fractures: a 10-year review at a level-I trauma center', *European Journal of Trauma and Emergency Surgery*, 49(1), pp. 401–409. doi: 10.1007/s00068-022-02076-w.

Boskey, A. L. West, P. (2005) 'Comparison of mineral quality and quantity in iliac crest biopsies from high- and low-turnover osteoporosis: an FT-IR microspectroscopic investigation', *Osteoporos Int.*, 16(12), pp. 2031–2038. Available at: https://pubmed.ncbi.nlm.nih.gov/16088360/.

Boskey, A. L. (2013) 'Bone composition: relationship to bone fragility and antiosteoporotic drug effects', *BoneKEy Reports*, 2(July), pp. 1–11. doi:

10.1038/bonekey.2013.181.

Botchkarev, V. A. (2003) ‘Bone morphogenetic proteins and their antagonists in skin and hair follicle biology’, *Journal of Investigative Dermatology*, 120(1), pp. 36–47. doi: 10.1046/j.1523-1747.2003.12002.x.

Bouillon, R. (1992) ‘Diabetic bone disease. Low turnover osteoporosis related to decreased IGF-I production’, *Verhandelingen - Koninklijke Academie voor Geneeskunde van Belgie*, 54(4), pp. 365—91; discussion 391—2. Available at: http://europepmc.org/abstract/MED/1466160.

Bourque, G. *et al.* (2018) ‘Ten things you should know about transposable elements 06 Biological Sciences 0604 Genetics’, *Genome Biology*, 19(1), pp. 1–12. doi: 10.1186/s13059-018-1577-z.

Boyle, W. J., Simonet, W. S. and Lacey, D. L. (2003) ‘Boyle Ocl Review’, *Nature Publishing Group*, 423(May), pp. 337–342.

Bragdon, B. *et al.* (2011) ‘Bone Morphogenetic Proteins: A critical review’, *Cellular Signalling*, 23(4), pp. 609–620. doi: 10.1016/j.cellsig.2010.10.003.

Bruce, D. L. and Sapkota, G. P. (2012) ‘Phosphatases in SMAD regulation’, *FEBS Letters*, 586(14), pp. 1897–1905. doi: 10.1016/j.febslet.2012.02.001.

Von Bubnoff, A. and Cho, K. W. Y. (2001) ‘Intracellular BMP signaling regulation in vertebrates: Pathway or network?’, *Developmental Biology*, 239(1), pp. 1–14. doi: 10.1006/dbio.2001.0388.

Buckwalter, J. A. *et al.* (1996) ‘Bone biology. I: Structure, blood supply, cells, matrix, and mineralization.’, *Instructional course lectures*, 45, pp. 371–386.

Burge, R. *et al.* (2007) ‘Incidence and economic burden of osteoporosis-related fractures in the United States, 2005-2025’, *Journal of Bone and Mineral Research*, 22(3), pp. 465–475. doi: 10.1359/jbmr.061113.

Burkus, J. K. *et al.* (2002) ‘Clinical and radiographic outcomes of anterior lumbar interbody fusion using recombinant human bone morphogenetic protein-2’, *Spine*, 27(21), pp. 2396–2408. doi: 10.1097/00007632-200211010-00015.

Burkus, J. K. *et al.* (2003) ‘Is INFUSE Bone Graft superior to autograft bone? An integrated analysis of clinical trials using the LT-CAGE Lumbar Tapered Fusion

device', *Journal of Spinal Disorders and Techniques*, 16(2), pp. 113–122. doi: 10.1097/00024720-200304000-00001.

Butler, S. J. and Dodd, J. (2003) 'A role for BMP heterodimers in roof plate-mediated repulsion of commissural axons', *Neuron*, 38(3), pp. 389–401. doi: 10.1016/S0896-6273(03)00254-X.

Cai, J. *et al.* (2012) 'BMP signaling in vascular diseases', *FEBS Letters*, 586(14), pp. 1993–2002. doi: 10.1016/j.febslet.2012.04.030.

Calori, G. M. *et al.* (2007) 'Risk factors contributing to fracture non-unions', *Injury*, 38(SUPPL. 2), pp. 11–18. doi: 10.1016/S0020-1383(07)80004-0.

Campana, V. *et al.* (2014) 'Bone substitutes in orthopaedic surgery: from basic science to clinical practice', *Journal of Materials Science: Materials in Medicine*, 25(10), pp. 2445–2461. doi: 10.1007/s10856-014-5240-2.

Caplan, A. I. (2007) 'Adult Mesenchymal Stem Cells for Tissue Engineering Versus Regenerative Medicine', *Journal Cellular Physiology*, 211(3)(May), pp. 736–747. doi: 10.1002/JCP.

Carragee, E. J., Hurwitz, E. L. and Weiner, B. K. (2011) 'A critical review of recombinant human bone morphogenetic protein-2 trials in spinal surgery: Emerging safety concerns and lessons learned', *Spine Journal*, 11(6), pp. 471–491. doi: 10.1016/j.spinee.2011.04.023.

Carreira, A. C. *et al.* (2014) 'Bone Morphogenetic Proteins: Structure, biological function and therapeutic applications', *Archives of Biochemistry and Biophysics*, 561, pp. 64–73. doi: 10.1016/j.abb.2014.07.011.

Chalfie, M. *et al.* (1994) 'Green Fluorescent Protein as a Marker for Gene Expression', *Science*, 263(8002).

Chen, D. *et al.* (1998) 'Differential Roles for Bone Morphogenetic Protein (BMP) Receptor Type IB and IA in Differentiation and Specification of Mesenchymal Precursor Cells to Osteoblast and Adipocyte Lineages', *The Journal of Cell Biology*, 142(1), pp. 295–305.

Chen, D., Zhao, M. and Mundy, G. (2004) 'Bone Morphogenetic Proteins', *Growth Factors*, 22(4), pp. 1–7. doi: 10.1080/08977190412331279890.

Chen, G., Deng, C. and Li, Y. P. (2012) 'TGF-β and BMP signaling in osteoblast differentiation and bone formation', *International Journal of Biological Sciences*, 8(2), pp. 272–288. doi: 10.7150/ijbs.2929.

Chen, Xiang *et al.* (2015) 'Sustained high level transgene expression in mammalian cells mediated by the optimized piggyBac transposon system', *Genes and Diseases*, 2(1), pp. 96–105. doi: 10.1016/j.gendis.2014.12.001.

Cho, Hyun Ju, Cho, Hyun Jai and Kim, H. S. (2009) 'Osteopontin: A multifunctional protein at the crossroads of inflammation, atherosclerosis, and vascular calcification', *Current Atherosclerosis Reports*, 11(3), pp. 206–213. doi: 10.1007/s11883-009-0032-8.

Chubinskaya, S. *et al.* (2000) 'Human articular chondrocytes express osteogenic protein-1', *Journal of Histochemistry and Cytochemistry*, 48(2), pp. 239–250. doi: 10.1177/002215540004800209.

Clarke, B. (2008) 'Normal bone anatomy and physiology.', *Clinical journal of the American Society of Nephrology : CJASN*, 3 Suppl 3, pp. 131–139. doi: 10.2215/CJN.04151206.

Collon, K., Gallo, M. C. and Lieberman, J. R. (2021) 'Musculoskeletal tissue engineering: Regional gene therapy for bone repair', *Biomaterials*, 275(January), p. 120901. doi: 10.1016/j.biomaterials.2021.120901.

Derynck, R. and Zhang, Y. E. (2003) 'Smad-dependent and Smad-independent pathways in TGF-b family signalling', *Nature*, 425, pp. 577–584.

Dimitriou, R. *et al.* (2005) 'Current concepts of molecular aspects of bone healing', *Injury*, 36(12), pp. 1392–1404. doi: 10.1016/j.injury.2005.07.019.

Downey, P. A. and Siegel, M. I. (2006) 'Bone biology and the clinical implications for osteoporosis', *Physical Therapy*, 86(1), pp. 77–91. doi: 10.1093/ptj/86.1.77.

Drummen, G. P. C. *et al.* (2002) 'C11-BODIPY581/591, an oxidation-sensitive fluorescent lipid peroxidation probe: (Micro)spectroscopic characterization and validation of methodology', *Free Radical Biology and Medicine*, 33(4), pp. 473–490. doi: 10.1016/S0891-5849(02)00848-1.

Du, Y., Xiao, Q. and Yip, H. K. (2010) 'Regulation of retinal progenitor cell

differentiation by bone morphogenetic protein 4 is mediated by the smad/id cascade', *Investigative Ophthalmology and Visual Science*, 51(7), pp. 3764–3773. doi: 10.1167/iovs.09-4906.

Ducy, P. *et al.* (1997) 'Osf2/Cbfa1: A transcriptional activator of osteoblast differentiation', *Cell*, 89(5), pp. 747–754. doi: 10.1016/S0092-8674(00)80257-3.

Einhorn, T. A. (1996) 'Enhancement of fracture healing.', *Instructional course lectures*, 45, pp. 401–416. doi: 10.2106/00004623-199506000-00016.

Einhorn, T. A. and Gerstenfeld, L. C. (2015) 'Fracture healing: Mechanisms and interventions', *Nature Reviews Rheumatology*, 11(1), pp. 45–54. doi: 10.1038/nrrheum.2014.164.

Ellis, J. (2005) 'Silencing and variegation of gammaretrovirus and lentivirus vectors', *Human Gene Therapy*, 16(11), pp. 1241–1246. doi: 10.1089/hum.2005.16.1241.

Elsen, M. *et al.* (2014) 'BMP4 and BMP7 induce the white-to-brown transition of primary human adipose stem cells', *American Journal of Physiology - Cell Physiology*, 306(5), pp. 431–440. doi: 10.1152/ajpcell.00290.2013.

Favata, M. F. *et al.* (1998) 'Identification of a novel inhibitor of mitogen-activated protein kinase kinase', *Journal of Biological Chemistry*, 273(29), pp. 18623–18632. doi: 10.1074/jbc.273.29.18623.

Feichtinger, G. A. *et al.* (2014) 'Constitutive and inducible co-expression systems for non-viral osteoinductive gene therapy', *European Cells and Materials*, 27, pp. 166–184. doi: 10.22203/eCM.v027a13.

Finnegan, D. J. (2012) 'Retrotransposons', *Current Biology*, 22(11), pp. 432–437. doi: 10.1016/j.cub.2012.04.025.

Fong, D. *et al.* (2013) *Bone morphogenetic protein-9 activates Smad and ERK pathways and supports human osteoclast function and survival in vitro*, *Cellular Signalling*. Elsevier B.V. doi: 10.1016/j.cellsig.2012.12.003.

Franz-Odendaal, T. A., Hall, B. K. and Witten, P. E. (2006) 'Buried alive How osteoblasts become osteocytes'. Developmental Dynamics, pp. 235:176–190,.

Friedlaender, G. E. *et al.* (2001) 'Osteogenic protein-1 (bone morphogenetic protein-7) in the treatment of tibial nonunions: A prospective, randomized clinical trial

comparing rhOP-1 with fresh bone autograft', *Journal of Bone and Joint Surgery - Series A*, 83(SUPPL. 1 II), pp. 1–17.

Fu, R. *et al.* (2012) 'Effectiveness and Harms of Recombinant Human Bone Morphogenetic', *Annals of Internal Medicine*, 158(13), pp. 890–902.

Fu, X. *et al.* (2016) 'Improved osteogenesis and upregulated immunogenicity in human placenta-derived mesenchymal stem cells primed with osteogenic induction medium', *Stem Cell Research and Therapy*, 7(1), pp. 1–11. doi: 10.1186/s13287-016-0400-6.

Gannon, F. H. *et al.* (1997) 'Bone morphogenetic protein 2/4 in early fibromatous lesions of fibrodysplasia ossificans progressiva', *Human Pathology*, 28(3), pp. 339–343. doi: 10.1016/S0046-8177(97)90133-7.

Gantenbein, B. *et al.* (2020) *Non-viral Gene Delivery Methods for Bone and Joints*. doi: 10.3389/fbioe.2020.598466.

Geurts, A. M. *et al.* (2003) 'Gene transfer into genomes of human cells by the Sleeping Beauty transposon system', *Molecular Therapy*, 8(1), pp. 108–117. doi: 10.1016/S1525-0016(03)00099-6.

Ghodadra, N. and Singh, K. (2008) 'Recombinant human bone morphogenetic protein-2 in the treatment of bone fractures', *Biologics: Targets and Therapy*, 2(3), pp. 345–354. doi: 10.2147/btt.s3394.

Ghosh, S. *et al.* (2020) 'Viral Vector Systems for Gene Therapy : A Comprehensive Literature Review of Progress and Biosafety Challenges', 25(1), pp. 7–18. doi: 10.1177/1535676019899502.

Gipson, G. R. *et al.* (2020) 'Structural perspective of BMP ligands and signaling', *Bone*, pp. 1–31. doi: 10.1016/j.bone.2020.115549.

Govender, S. and et.al (2002) 'Recombinant Human Bone Morphogenetic Protein-2 for Treatment of Open Tibial Fractures', *THE JOURNAL OF BONE AND JOINT SURGERY, INCORPORATED*, 84-A(12), pp. 2123–2134.

Grabundzija, I. *et al.* (2010) 'Comparative analysis of transposable element vector systems in human cells', *Molecular Therapy*, 18(6), pp. 1200–1209. doi: 10.1038/mt.2010.47.

Granéli, C. *et al.* (2014) ‘Novel markers of osteogenic and adipogenic differentiation of human bone marrow stromal cells identified using a quantitative proteomics approach’, *Stem Cell Research*, 12(1), pp. 153–165. doi: 10.1016/j.scr.2013.09.009.

Gregory, C. A. *et al.* (2004) ‘An Alizarin red-based assay of mineralization by adherent cells in culture: Comparison with cetylpyridinium chloride extraction’, *Analytical Biochemistry*, 329(1), pp. 77–84. doi: 10.1016/j.ab.2004.02.002.

Gronthos, S. *et al.* (2000) ‘Postnatal human dental pulp stem cells (DPSCs) in vitro and in vivo’, *Proceedings of the National Academy of Sciences of the United States of America*, 97(25), pp. 13625–13630. doi: 10.1073/pnas.240309797.

Guo, J. and Wu, G. (2012) ‘The signaling and functions of heterodimeric bone morphogenetic proteins’, *Cytokine and Growth Factor Reviews*, 23(1–2), pp. 61–67. doi: 10.1016/j.cytogfr.2012.02.001.

Hamann, A., Nguyen, A. and Pannier, A. K. (2019) ‘Nucleic acid delivery to mesenchymal stem cells: A review of nonviral methods and applications’, *Journal of Biological Engineering*, 13(1), pp. 1–16. doi: 10.1186/s13036-019-0140-0.

Hamidouche, Z. *et al.* (2008) ‘FHL2 mediates dexamethasone- induced mesenchymal cell differentiation into osteoblasts by activating Wnt/β- catenin signaling- dependent Runx2 expression’, *The FASEB Journal*, 22(11), pp. 3813–3822. doi: 10.1096/fj.08-106302.

Harris, R. S. *et al.* (2011) *Former Editors University of California University of Edinburgh University of Chicago University of North Carolina University of Liverpool School of Medicine State University of New York at Stony Brook National Institute of National Institutes of Health D*.

Haubold, M. *et al.* (2010) ‘Bone morphogenetic protein 4 (BMP4) signaling in retinoblastoma cells’, *International Journal of Biological Sciences*, 6(7), pp. 700–715. doi: 10.7150/ijbs.6.700.

Hazama, M. *et al.* (1995) ‘Efficient expression of a heterodimer of bone morphogenetic protein subunits using a baculovirus expression system’, *Biochemical and Biophysical Research Communications*, pp. 859–866. doi: 10.1006/bbrc.1995.1578.

Hegarty, S. V., Sullivan, A. M. and O’Keeffe, G. W. (2017) ‘Endocytosis contributes to

BMP2-induced Smad signalling and neuronal growth', *Neuroscience Letters*, 643, pp. 32–37. doi: 10.1016/j.neulet.2017.02.013.

Henkel, J. *et al.* (2013) 'Bone Regeneration Based on Tissue Engineering Conceptions-A 21st Century Perspective', *Bone Research*, 1(3), pp. 216–248. doi: 10.4248/BR201303002.

Hernlund, E. *et al.* (2013) 'Osteoporosis in the European Union: Medical management, epidemiology and economic burden: A report prepared in collaboration with the International Osteoporosis Foundation (IOF) and the European Federation of Pharmaceutical Industry Associations (EFPIA)', *Archives of Osteoporosis*, 8(1–2). doi: 10.1007/s11657-013-0136-1.

Herrera, B. and Inman, G. J. (2009) 'A rapid and sensitive bioassay for the simultaneous measurement of multiple bone morphogenetic proteins. Identification and quantification of BMP4, BMP6 and BMP9 in bovine and human serum', *BMC Cell Biology*, 10, pp. 1–11. doi: 10.1186/1471-2121-10-20.

Hogan, B. L. M. (1996) 'Bone morphogenetic proteins: Multifunctional regulators of vertebrate development', *Genes and Development*, 10(13), pp. 1580–1594. doi: 10.1101/gad.10.13.1580.

Hollinger, J. and Wong, M. E. K. (1996) 'The integrated processes of hard tissue regeneration with special emphasis on fracture healing', *Oral Surgery, Oral Medicine, Oral Pathology, Oral Radiology, and Endodontics*, 82(6), pp. 594–606. doi: 10.1016/S1079-2104(96)80431-8.

Holstein, M. *et al.* (2018) 'Efficient Non-viral Gene Delivery into Human Hematopoietic Stem Cells by Minicircle Sleeping Beauty Transposon Vectors', *Molecular Therapy*, 26(4), pp. 1137–1153. doi: 10.1016/j.ymthe.2018.01.012.

Horbelt, D., Denkis, A. and Knaus, P. (2012) 'A portrait of Transforming Growth Factor β superfamily signalling: Background matters', *International Journal of Biochemistry and Cell Biology*, 44(3), pp. 469–474. doi: 10.1016/j.biocel.2011.12.013.

Hsu, C. Y., Chen, L. R. and Chen, K. H. (2020) 'Osteoporosis in patients with chronic kidney diseases: A systemic review', *International Journal of Molecular Sciences*, 21(18), pp. 1–24. doi: 10.3390/ijms21186846.

Hu, M. *et al.* (2017) ‘BMP signaling pathways affect differently migration and invasion of esophageal squamous cancer cells’, *International Journal of Oncology*, 50(1), pp. 193–202. doi: 10.3892/ijo.2016.3802.

Huang, X. *et al.* (2020) ‘Current Trends in Research on Bone Regeneration: A Bibliometric Analysis’, *BioMed Research International*, 2020. doi: 10.1155/2020/8787394.

Hudecek, M. *et al.* (2017) ‘Going non-viral: the Sleeping Beauty transposon system breaks on through to the clinical side’, *Critical Reviews in Biochemistry and Molecular Biology*, 52(4), pp. 355–380. doi: 10.1080/10409238.2017.1304354.

Hudecek, M. and Ivics, Z. (2018) ‘Non-viral therapeutic cell engineering with the Sleeping Beauty transposon system’, *Current Opinion in Genetics and Development*, 52, pp. 100–108. doi: 10.1016/j.gde.2018.06.003.

Hue H. Luu and et al. (2007) ‘Distinct Roles of Bone Morphogenetic Proteins in Osteogenic Differentiation of Mesenchymal Stem Cells Hue’, *Journal of Orthopaedic Research September*, 25(May), pp. 665–677. doi: 10.1002/jor.

Id Boufker, H. *et al.* (2010) ‘The Src inhibitor dasatinib accelerates the differentiation of human bone marrow-derived mesenchymal stromal cells into osteoblasts’, *BMC Cancer*, 10. doi: 10.1186/1471-2407-10-298.

Isaacs, M. J. *et al.* (2010) ‘Bone morphogenetic protein-2 and -6 heterodimer illustrates the nature of ligand-receptor assembly’, *Molecular Endocrinology*, 24(7), pp. 1469–1477. doi: 10.1210/me.2009-0496.

Israel, D. I. *et al.* (1996) ‘Heterodimeric bone morphogenetic proteins show enhanced activity in vitro and in vivo’, *Growth Factors*, 13(3–4), pp. 291–300. doi: 10.3109/08977199609003229.

Ivics, Z. and Izsvák, Z. (2011) ‘Nonviral gene delivery with the sleeping beauty transposon system’, *Human Gene Therapy*, 22(9), pp. 1043–1051. doi: 10.1089/hum.2011.143.

Ivics, Z. and Izsvák, Z. (2015) ‘Sleeping beauty transposition’, *Mobile DNA III*, pp. 851–872. doi: 10.1128/9781555819217.ch38.

Ivics, Z., Li, M. A. and Mátés, L. (2009) ‘Transposon-mediated Genome

Manipulations in Vertebrates', *Nat Methods.*, 23(6(6)), pp. 415–422. doi: 10.1038/nmeth.1332.

James, A. W. *et al.* (2016) 'A Review of the Clinical Side Effects of Bone Morphogenetic Protein-2', *Tissue Engineering - Part B: Reviews*, 22(4), pp. 284–297. doi: 10.1089/ten.teb.2015.0357.

Jang, W. G. *et al.* (2012) 'BMP2 protein regulates osteocalcin expression via Runx2-mediated Atf6 gene transcription', *Journal of Biological Chemistry*, 287(2), pp. 905–915. doi: 10.1074/jbc.M111.253187.

Johnson, G. L. and Lapadat, R. (2002) 'Mitogen-activated protein kinase pathways mediated by ERK, JNK, and p38 protein kinases', *Science*, 298(5600), pp. 1911–1912. doi: 10.1126/science.1072682.

Jones, A. L. and et.al (2006) 'Recombinant Human BMP-2 and Allograft Compared with Autogenous Bone Graft for Reconstruction of Diaphyseal Tibial Fractures with Cortical Defects', *Journal of Bone and Joint Surgery - Series A*, 88-A(7), pp. 1431–1441. doi: 10.2106/00004623-200607000-00002.

Jonk, L. J. C. *et al.* (1998) 'Identification and functional characterization of a smad binding element (SBE) in the JunB promoter that acts as a transforming growth factor-β, activin, and bone morphogenetic protein-inducible enhancer', *Journal of Biological Chemistry*, 273(33), pp. 21145–21152. doi: 10.1074/jbc.273.33.21145.

Kanakaris, N. K. *et al.* (2008) 'Application of BMP-7 to tibial non-unions: A 3-year multicenter experience', *Injury*, 39(SUPPL.2). doi: 10.1016/S0020-1383(08)70019-6.

Kaneko, H. *et al.* (2000) 'Direct stimulation of osteoclastic bone resorption by bone morphogenetic protein (BMP)-2 and expression of BMP receptors in mature osteoclasts', *Bone*, 27(4), pp. 479–486. doi: 10.1016/S8756-3282(00)00358-6.

Kang, Q. *et al.* (2004) 'Characterization of the distinct orthotopic bone-forming activity of 14 BMPs using recombinant adenovirus-mediated gene delivery', *Gene Therapy*, 11(17), pp. 1312–1320. doi: 10.1038/sj.gt.3302298.

Kawabata, M., Imamura, T. and Kohei, M. (1998) 'Signal Transduction by Bone Morphogenetic Proteins', *Cytokine + Growth Factor Reviews*, 9, pp. 49–61. doi: 10.1080/09700160108458991.

Kawai, M. *et al.* (2006) ‘Simultaneous gene transfer of bone morphogenetic protein (BMP) -2 and BMP-7 by in vivo electroporation induces rapid bone formation and BMP-4 expression’, *BMC Musculoskeletal Disorders*, 7, pp. 1–11. doi: 10.1186/1471-2474-7-62.

Kawai, M. *et al.* (2009) ‘Simple strategy for bone regeneration with a BMP-2/7 gene expression cassette vector.’, *Biochemical and Biophysical Research Communications*, 390(3), pp. 1012–1017. doi: 10.1016/j.bbrc.2009.10.099.

Kebriaei, P. *et al.* (2017) ‘Gene Therapy with the Sleeping Beauty Transposon System’, *Trends in Genetics*, 33(11), pp. 852–870. doi: 10.1016/j.tig.2017.08.008.

Khan, W. S. *et al.* (2012) ‘An osteoconductive, osteoinductive, and osteogenic tissue-engineered product for trauma and orthopaedic surgery: How far are we?’, *Stem Cells International*, 2012. doi: 10.1155/2012/236231.

Kim, H. S. *et al.* (2019) ‘BMP7 functions predominantly as a heterodimer with BMP2 or BMP4 during mammalian embryogenesis’, *eLife*, 8, pp. 1–22. doi: 10.7554/eLife.48872.

Kim, N. W. *et al.* (1994) ‘Specific Association of Human Telomerase Activity with Immortal Cells and Cancer Nam’, *Science*, 266(December 1994), pp. 2011–2015. Available at: http://science.sciencemag.org/.

Kim, Y. *et al.* (2018) ‘Evaluation of mesenchymal stem cell sheets overexpressing BMP-7 in canine critical-sized bone defects’, *International Journal of Molecular Sciences*, 19(7). doi: 10.3390/ijms19072073.

Kjaer, K. W. *et al.* (2006) ‘A mutation in the receptor binding site of GDF5 causes Mohr-Wriedt brachydactyly type A2’, *Journal of Medical Genetics*, 43(3), pp. 225–231. doi: 10.1136/jmg.2005.034058.

Kneser, U. *et al.* (2002) ‘Tissue engineering of bone’, *Min Invas Ther & Allied Technol*, 11(3), pp. 107–116.

Kneser, U. *et al.* (2006) ‘Tissue engineering of bone: The reconstructive surgeon’s point of view’, *Journal of Cellular and Molecular Medicine*, 10(1), pp. 7–19. doi: 10.1111/j.1582-4934.2006.tb00287.x.

Koh, J. T., Zhao, Z. and et.al (2008) ‘Combinatorial Gene Therapy with BMP2/7

Enhances Cranial Bone Regeneration', *J Dent Res.*, 23(87(9)), pp. 845–849. Available at: https://www.ncbi.nlm.nih.gov/pmc/articles/PMC3624763/pdf/nihms412728.pdf.

Kohan, E. *et al.* (2013) 'Customized Bilaminar Resorbable Mesh With BMP-2 PromotesCranial Bone Defect Healin', *Annals of Plastic Surgery*, 74 (5)(5), pp. 603–608. doi: 10.1097/SAP.0b013e3182a6363c.

Konttinen, Y. T. *et al.* (2005) 'The microenvironment around total hip replacement prostheses', *Clinical Orthopaedics and Related Research*, (430), pp. 28–38. doi: 10.1097/01.blo.0000150451.50452.da.

Koons, G. L., Diba, M. and Mikos, A. G. (2020) 'Materials design for bone-tissue engineering', *Nature Reviews Materials*, 5(8), pp. 584–603. doi: 10.1038/s41578-020-0204-2.

Kowarz, Eric, Löscher, D. and Marschalek, R. (2015) 'Optimized Sleeping Beauty transposons rapidly generate stable transgenic cell lines', *Biotechnology Journal*, 10(4), pp. 647–653. doi: 10.1002/biot.201400821.

Kowarz, E, Löscher, D. and Marschalek, R. (2015) 'Optimized Sleeping Beauty transposons rapidly generate stable transgenic cell lines', *Biotechnol Journal*, 10(4) 647-, pp. 1–32. doi: 10.1002/biot.201400821.

Kraunz, K. S. *et al.* (2005) 'Interaction between the bone morphogenetic proteins and Ras/MAP-kinase signalling pathways in lung cancer', *British Journal of Cancer*, 93(8), pp. 949–952. doi: 10.1038/sj.bjc.6602790.

Kraus, K. H. and Kirker-Head, C. (2006) 'Mesenchymal stem cells and bone regeneration', *Veterinary Surgery*, 35(3), pp. 232–242. doi: 10.1111/j.1532-950X.2006.00142.x.

Kumar, V. *et al.* (2017) 'Robbins Basic Pathology 10th ed.', *Elsevier - Health Sciences Division*.

Lacey, D. L. *et al.* (2012) 'Bench to bedside: Elucidation of the OPG-RANK-RANKL pathway and the development of denosumab', *Nature Reviews Drug Discovery*, 11(5), pp. 401–419. doi: 10.1038/nrd3705.

Lai, C. F. and Cheng, S. L. (2002) 'Signal transductions induced by bone

morphogenetic protein-2 and transforming growth factor-β in normal human osteoblastic cells', *Journal of Biological Chemistry*, 277(18), pp. 15514–15522. doi: 10.1074/jbc.M200794200.

Langenbach, F. and Handschel, J. (2013) 'Cell sources for bone regeneration: The good, the bad, and the ugly (But Promising)', *Stem Cell Research and Therapy*, 4 (117)(6), pp. 423–430. doi: 10.1089/ten.teb.2011.0199.

Lavery, K. *et al.* (2008) 'BMP-2/4 and BMP-6/7 differentially utilize cell surface receptors to induce osteoblastic differentiation of human bone marrow-derived mesenchymal stem cells', *Journal of Biological Chemistry*, 283(30), pp. 20948–20958. doi: 10.1074/jbc.M800850200.

Lee, K. *et al.* (2018) 'Roles of mitogen-activated protein kinases in osteoclast biology', *International Journal of Molecular Sciences*, 19(10). doi: 10.3390/ijms19103004.

Lee, M. H. *et al.* (2003) 'BMP-2-induced Runx2 Expression Is Mediated by Dlx5, and TGF-β1 Opposes the BMP-2-induced Osteoblast Differentiation by Suppression of Dlx5 Expression', *Journal of Biological Chemistry*, 278(36), pp. 34387–34394. doi: 10.1074/jbc.M211386200.

Lefterova, M. *et al.* (2014) 'PPARγ and the Global Map of Adipogenesis and Beyond', *Trends Endocrinol Metab.*, 25(6)(1), pp. 293–302. doi: doi:10.1016/j.tem.2014.04.001. PPARγ.

Leslie P.Gartner and James L. Hiatt (2018) *Cell Biology & Histology. 8th edition. Philadelphia, Wolters Kluwer, 2018, 448 p.*

'Let's talk about lipid nanoparticles' (2021) *Nature Reviews Materials*, 6(2), p. 99. doi: 10.1038/s41578-021-00281-4.

Liang, F. *et al.* (2017) 'Efficient Targeting and Activation of Antigen-Presenting Cells In Vivo after Modified mRNA Vaccine Administration in Rhesus Macaques', *Molecular Therapy*, 25(12), pp. 2635–2647. doi: 10.1016/j.ymthe.2017.08.006.

Liu, H. and Visner, G. A. (2007) 'Applications of Sleeping Beauty transposons for nonviral gene therapy', *IUBMB Life*, 59(6), pp. 374–379. doi: 10.1080/15216540701435722.

Liu, M. *et al.* (2017) ‘Adipose-Derived Mesenchymal Stem Cells from the Elderly Exhibit Decreased Migration and Differentiation Abilities with Senescent Properties’, *Cell Transplantation*, 26(9), pp. 1505–1519. doi: 10.1177/0963689717721221.

Logeart-Avramoglou, D. *et al.* (2005) ‘An assay for the determination of biologically active bone morphogenetic proteins using cells transfected with an inhibitor of differentiation promoter-luciferase construct’, *Analytical Biochemistry*, 349(1), pp. 78–86. doi: 10.1016/j.ab.2005.10.030.

Long, F. (2012) ‘Building strong bones: Molecular regulation of the osteoblast lineage’, *Nature Reviews Molecular Cell Biology*, 13(1), pp. 27–38. doi: 10.1038/nrm3254.

Loozen, L. D. *et al.* (2018) ‘Bone formation by heterodimers through non-viral gene delivery of BMP-2/6 and BMP-2/7’, *European Cells and Materials*, 35, pp. 195–208. doi: 10.22203/eCM.v035a14.

Luo, J. *et al.* (2005) ‘Gene Therapy for Bone Regeneration’, *Current Gene Therapy*, 5(2), pp. 167–179. doi: 10.2174/1566523053544218.

Luo, J., Sun, M. H. and et al (2005) ‘Gene Therapy for Bone Regeneration’, *Current Gene Therapy*, 5, pp. 167–179.

Marsell, R. and Einhorn, T. A. (2011) ‘THE BIOLOGY OF FRACTURE HEALING Richard’, *Injury*, 42(6), pp. 551–555. doi: 10.4314/njm.v19i3.60231.

Massagué, J. (1998) ‘TGF-β signal transduction’, *Annual Review of Biochemistry*, 67, pp. 753–791. doi: 10.1146/annurev.biochem.67.1.753.

Massagué, J., Seoane, J. and Wotton, D. (2005) ‘Smad transcription factors’, *Genes and Development*, 19(23), pp. 2783–2810. doi: 10.1101/gad.1350705.

Mátés, L. *et al.* (2009) ‘Molecular evolution of a novel hyperactive Sleeping Beauty transposase enables robust stable gene transfer in vertebrates’, *Nature Genetics*, 41(6), pp. 753–761. doi: 10.1038/ng.343.

McClintock, B. (1950) ‘The Origin and Behavior of Mutable Loci in Maize’, *Proceedings of the National Academy of Sciences of the United States of America*, 36(6), pp. 344–355. doi: 10.1073/pnas.36.6.344.

McKay, W. F. and et al (2007) ‘A comprehensive clinical review of recombinant

human bone morphogenetic protein-2 (INFUSE® Bone Graft)', *International Orthopaedics*, 31(6), pp. 729–734. doi: 10.1007/s00264-007-0418-6.

Miao, C. *et al.* (2019) 'BMP2/7 heterodimer enhances osteogenic differentiation of rat BMSCs via ERK signaling compared with respective homodimers', *Journal of Cellular Biochemistry*, 120(5), pp. 8754–8763. doi: 10.1002/jcb.28162.

Miyazono, K., Kamiya, Y. and Morikawa, M. (2010) 'Bone morphogenetic protein receptors and signal transduction', *Journal of Biochemistry*, 147(1), pp. 35–51. doi: 10.1093/jb/mvp148.

Modica, S. *et al.* (2016) 'Bmp4 Promotes a Brown to White-like Adipocyte Shift', *Cell Reports*, 16(8), pp. 2243–2258. doi: 10.1016/j.celrep.2016.07.048.

Morimoto, T. *et al.* (2015) 'The bone morphogenetic protein-2/7 heterodimer is a stronger inducer of bone regeneration than the individual homodimers in a rat spinal fusion model.', *The spine journal : official journal of the North American Spine Society*, 15(6), pp. 1379–1390. doi: 10.1016/j.spinee.2015.02.034.

Mouillesseaux, K. P. *et al.* (2016) 'Notch regulates BMP responsiveness and lateral branching in vessel networks via SMAD6', *Nature Communications*, 7, pp. 1–12. doi: 10.1038/ncomms13247.

Mueller, T. D. and Nickel, J. (2012) 'Promiscuity and specificity in BMP receptor activation', *FEBS Letters*, 586(14), pp. 1846–1859. doi: 10.1016/j.febslet.2012.02.043.

Murakami, T. *et al.* (2017) 'Isolation and characterization of lymphoid enhancer factor-1-positive deciduous dental pulp stem-like cells after transfection with a piggyBac vector containing LEF1 promoter-driven selection markers', *Archives of Oral Biology*, 81(April), pp. 110–120. doi: 10.1016/j.archoralbio.2017.04.033.

Narayanavari, S. A. *et al.* (2017) 'Sleeping Beauty transposition: from biology to applications', *Critical Reviews in Biochemistry and Molecular Biology*, 52(1), pp. 18–44. doi: 10.1080/10409238.2016.1237935.

Nawshad, A. *et al.* (2005) 'Transforming growth factor-β signaling during epithelial-mesenchymal transformation: Implications for embryogenesis and tumor metastasis', *Cells Tissues Organs*, 179(1–2), pp. 11–23. doi: 10.1159/000084505.

Nickel, J. and Mueller, T. D. (2019) ‘Specification of BMP signaling’, *Cells*, pp. 1–27. doi: 10.3390/cells8121579.

Olsen, B. R., Reginato, A. M. and Wang, W. (2000) ‘Bone Development’, *Annual Review of Cell and Developmental Biology*, 16(1), pp. 191–220. doi: 10.1146/annurev.cellbio.16.1.191.

Pardi, N. and et.al (2015) ‘Expression kinetics of nucleoside-modified mRNA delivered in lipid nanoparticles to mice by various routes’, *Journal of controlled release : official journal of the Controlled Release Society*, 217, pp. 345–351. doi: 10.1016/j.jconrel.2015.08.007.Expression.

Pelled, G. *et al.* (2016) ‘BMP6-engineered MSCs induce vertebral bone repair in a pig model: A pilot study’, *Stem Cells International*, 2016. doi: 10.1155/2016/6530624.

Peng, H. *et al.* (2002) ‘Synergistic enhancement of bone formation and healing by stem cell–expressed VEGF and bone morphogenetic protein-4’, *Journal of Clinical Investigation*, 110(6), pp. 751–759. doi: 10.1172/jci200215153.

Phimphilai, M. *et al.* (2006) ‘BMP signaling is required for RUNX2-dependent induction of the osteoblast phenotype’, *Journal of Bone and Mineral Research*, 21(4), pp. 637–646. doi: 10.1359/jbmr.060109.

Pittenger, M. F. *et al.* (1999) ‘Multilineage potential of adult human mesenchymal stem cells’, *Science*, 284(5411), pp. 143–147. doi: 10.1126/science.284.5411.143.

Plasterk, R. H. A., Izsvák, Z. and Ivics, Z. (1999) ‘Resident aliens the Tc1/mariner superfamily of transposable elements’, *Trends in Genetics*, 15(8), pp. 326–332. doi: 10.1016/S0168-9525(99)01777-1.

Polack, F. P. *et al.* (2020) ‘Safety and Efficacy of the BNT162b2 mRNA Covid-19 Vaccine’, *New England Journal of Medicine*, 383(27), pp. 2603–2615. doi: 10.1056/nejmoa2034577.

Potier, E. *et al.* (2007) ‘Hypoxia affects mesenchymal stromal cell osteogenic differentiation and angiogenic factor expression’, *Bone*, 40(4), pp. 1078–1087. doi: 10.1016/j.bone.2006.11.024.

Rahman, M. S. *et al.* (2015) ‘TGF-β/BMP signaling and other molecular events: Regulation of osteoblastogenesis and bone formation’, *Bone Research*, 3(November

2014). doi: 10.1038/boneres.2015.5.

Rather, H. A. *et al.* (2019) ‘Dual functional approaches for osteogenesis coupled angiogenesis in bone tissue engineering’, *Materials Science and Engineering C*, 103(May), p. 109761. doi: 10.1016/j.msec.2019.109761.

Reddi, A. H. (1992) ‘Regulation of cartilage and bone differentiation by bone morphogenetic proteins’, *Current Opinion in Cell Biology*, 4, pp. 850–855.

Reddi, A. H. (1998) ‘Role of morphogenetic proteins in skeletal tissue engineering and regeneration’, *Nature Biotechnology volume*, 16, pp. 247–252. doi: https://doi.org/10.1038/nbt0398-247.

Rose, L. C., Kucharski, C. and Uludağ, H. (2012) ‘Protein expression following non-viral delivery of plasmid DNA coding for basic FGF and BMP-2 in a rat ectopic model’, *Biomaterials*, 33(11), pp. 3363–3374. doi: 10.1016/j.biomaterials.2012.01.031.

Rothhammer, T. *et al.* (2005) ‘Bone morphogenic proteins are overexpressed in malignant melanoma and promote cell invasion and migration’, *Cancer Research*, 65(2), pp. 448–456.

Rupp, M. *et al.* (2021) ‘Bone transplantation or biomaterials?’, *Unfallchirurg*, 124(2), pp. 146–152. doi: 10.1007/s00113-020-00861-z.

Salgado, A. J., Coutinho, O. P. and Reis, R. L. (2004) ‘Bone tissue engineering: State of the art and future trends’, *Macromolecular Bioscience*, 4(8), pp. 743–765. doi: 10.1002/mabi.200400026.

Salhotra, A. *et al.* (2020) *Mechanisms of bone development and repair*, *Nature Reviews Molecular Cell Biology*. doi: 10.1038/s41580-020-00279-w.

Samee, M. *et al.* (2008) ‘Bone morphogenetic protein-2 (BMP-2) and vascular endothelial growth factor (VEGF) transfection to human periosteal cells enhances osteoblast differentiation and bone formation’, *Journal of Pharmacological Sciences*, 108(1), pp. 18–31. doi: 10.1254/jphs.08036FP.

Sanchez-Duffhues, G. *et al.* (2020) ‘Bone morphogenetic protein receptors: Structure, function and targeting by selective small molecule kinase inhibitors’, *Bone*, 138(June). doi: 10.1016/j.bone.2020.115472.

Sapkota, G. *et al.* (2007) ‘Balancing BMP Signaling through Integrated Inputs into the Smad1 Linker’, *Molecular Cell*, 25(3), pp. 441–454. doi: 10.1016/j.molcel.2007.01.006.

Schemitsch, E. H. (2017) ‘Size Matters: Defining Critical in Bone Defect Size!’, *Journal of Orthopaedic Trauma*, 31(10), pp. S20–S22. doi: 10.1097/BOT.0000000000000978.

Schmidt, A. H. (2021) ‘Autologous bone graft: Is it still the gold standard?’, *Injury*, 52, pp. S18–S22. doi: 10.1016/j.injury.2021.01.043.

Schreiber, I. *et al.* (2017) ‘BMPs as new insulin sensitizers: Enhanced glucose uptake in mature 3T3-L1 adipocytes via PPARγ and GLUT4 upregulation’, *Scientific Reports*, 7(1), pp. 1–13. doi: 10.1038/s41598-017-17595-5.

Schulz, T. J. and Tseng, Y.-H. (2009) ‘Emerging Role of Bone Morphogenetic Proteins in Adipogenesis and Energy Metabolism’, *Cytokine Growth Factor Rev.*, 20(5–6), pp. 523–531. doi: doi:10.1016/j.cytogfr.2009.10.019.

Sell, S. (2013) *Stem cells handbook: Second edition*, *Stem Cells Handbook: Second Edition*. doi: 10.1007/978-1-4614-7696-2.

Shekaran, A. and García, A. J. (2011) ‘Extracellular matrix-mimetic adhesive biomaterials for bone repair’, *J Biomed Mater Res A.*, 96(1), pp. 261–272. doi: 10.1002/jbm.a.32979.Extracellular.

Shen, J. *et al.* (2016) ‘Novel wnt regulator NEL-like molecule-1 antagonizes adipogenesis and augments osteogenesis induced by bone morphogenetic protein 2’, *American Journal of Pathology*, 186(2), pp. 419–434. doi: 10.1016/j.ajpath.2015.10.011.

Shen, L., Glowacki, J. and Zhou, S. (2011) ‘Inhibition of Adipocytogenesis by Canonical WNT Signaling in Human Mesenchymal Stem Cells’, *Experimental Cell Research*, 317 (13), pp. 1796–1803. doi: doi:10.1016/j.yexcr.2011.05.018. Inhibition.

Shimasaki, S. *et al.* (2004) ‘The Bone Morphogenetic Protein System in Mammalian Reproduction’, *Endocrine Reviews*, 25(1), pp. 72–101. doi: 10.1210/er.2003-0007.

Simmonds, Mark C. and et al. (2013) ‘Safety and Effectiveness of Recombinant Human Bone Morphogenetic Protein-2 for Spinal Fusion’, *Annals of Internal*

Medicine, 158(12), p. 877. doi: 10.7326/0003-4819-158-12-201306180-00005.

Singh, S. K., Abbas, W. A. and Tobin, D. J. (2012) 'Bone morphogenetic proteins differentially regulate pigmentation in human skin cells', *Journal of Cell Science*, 125(18), pp. 4306–4319. doi: 10.1242/jcs.102038.

Skipper, K. A. *et al.* (2013) 'DNA transposon-based gene vehicles - Scenes from an evolutionary drive', *Journal of Biomedical Science*, 20(1), pp. 1–23. doi: 10.1186/1423-0127-20-92.

Smith, A. D. and Trempe, J. P. (2000) 'Luminometric quantitation of Photinus pyralis firefly luciferase and Escherichia coli β-galactosidase in blood-contaminated organ lysates', *Analytical Biochemistry*, 286(1), pp. 164–172. doi: 10.1006/abio.2000.4797.

Smith, A., Hocking, A. and Isik, F. (2004) 'Study of Telomere Length Reveals Rapid Aging of Human Marrow Stromal Cells following In Vitro Expansion', *Stem Cells*, 22, pp. 675–782.

Song, K. *et al.* (2010) 'Identification of a key residue mediating bone morphogenetic protein (BMP)-6 resistance to noggin inhibition allows for engineered BMPs with superior agonist activity', *Journal of Biological Chemistry*, 285(16), pp. 12169–12180. doi: 10.1074/jbc.M109.087197.

Spangenburg, E. E. *et al.* (2011) 'Use of BODIPY (493/503) to visualize intramuscular lipid droplets in skeletal muscle', *Journal of Biomedicine and Biotechnology*, 2011(May 2014). doi: 10.1155/2011/598358.

Su, S. *et al.* (2018) 'Immune Checkpoint Inhibition Overcomes ADCP-Induced Immunosuppression by Macrophages', *Cell*, 175(2), pp. 442-457.e23. doi: 10.1016/j.cell.2018.09.007.

Sun, P. *et al.* (2012) 'BMP2/7 heterodimer is a stronger inducer of bone regeneration in peri-implant bone defects model than BMP2 or BMP7 homodimer', *Dental Materials Journal*, 31(2), pp. 239–248. doi: 10.4012/dmj.2011-191.

Tang, Q. Q., Otto, T. C. and Lane, M. D. (2004) 'Commitment of C3H10T1/2 pluripotent stem cells to the adipocyte lineage', *Proceedings of the National Academy of Sciences of the United States of America*, 101(26), pp. 9607–9611. doi: 10.1073/pnas.0403100101.

Tang, Z. *et al.* (2018) 'The material and biological characteristics of osteoinductive calcium phosphate ceramics', *Regenerative Biomaterials*, 5(1), pp. 43–59. doi: 10.1093/rb/rbx024.

Theoleyre, S. *et al.* (2004) 'The molecular triad OPG/RANK/RANKL: Involvement in the orchestration of pathophysiological bone remodeling', *Cytokine and Growth Factor Reviews*, 15(6), pp. 457–475. doi: 10.1016/j.cytogfr.2004.06.004.

Townsend, K. L. *et al.* (2012) 'Bone morphogenetic protein 7 (BMP7) reverses obesity and regulates appetite through a central mTOR pathway', *FASEB Journal*, 26(5), pp. 2187–2196. doi: 10.1096/fj.11-199067.

Tseng, Y. H. *et al.* (2008) 'New role of bone morphogenetic protein 7 in brown adipogenesis and energy expenditure', *Nature*, 454(7207), pp. 1000–1004. doi: 10.1038/nature07221.

Tsutsumi, S. *et al.* (2001) 'Retention of multilineage differentiation potential of mesenchymal cells during proliferation in response to FGF', *Biochemical and Biophysical Research Communications*, 288(2), pp. 413–419. doi: 10.1006/bbrc.2001.5777.

Twine, N. A. *et al.* (2016) 'Transcription factor ZNF25 is associated with osteoblast differentiation of human skeletal stem cells', *BMC Genomics*, 17(1), pp. 1–15. doi: 10.1186/s12864-016-3214-0.

Urist, M. R. and McLean, F. C. (1965) 'Bone formation by autoinduction', *Science*, 150 (3698), pp. 893–899. doi: 10.1126/science.150.3698.893.

Valera, E. *et al.* (2010) 'BMP-2/6 heterodimer is more effective than BMP-2 or BMP-6 homodimers as inductor of differentiation of human embryonic stem cells', *PLoS ONE*, 5(6). doi: 10.1371/journal.pone.0011167.

Vigdal, T. J. *et al.* (2002) 'Common physical properties of DNA affecting target site selection of Sleeping Beauty and other Tc1/mariner transposable elements', *Journal of Molecular Biology*, 323(3), pp. 441–452. doi: 10.1016/S0022-2836(02)00991-9.

Wang, E. A. *et al.* (1990) 'Recombinant human bone morphogenetic protein induces bone formation', *Proceedings of the National Academy of Sciences of the United States of America*, 87(6), pp. 2220–2224. doi: 10.1073/pnas.87.6.2220.

Wang, E. A. *et al.* (1993) 'Bone morphogenetic protein-2 causes commitment and differentiation in c3hl0t1/2 and 3t3 cells', *Growth Factors*, 9(1), pp. 57–71. doi: 10.3109/08977199308991582.

Wang, H. *et al.* (2017) 'BMP6 Regulates Proliferation and Apoptosis of Human Sertoli Cells Via Smad2/3 and Cyclin D1 Pathway and DACH1 and TFAP2A Activation', *Scientific Reports*, 7(April), pp. 1–14. doi: 10.1038/srep45298.

Wang, R. N. *et al.* (2014) 'Bone Morphogenetic Protein (BMP) signaling in development and human diseases', *Genes and Diseases*, 1(1), pp. 87–105. doi: 10.1016/j.gendis.2014.07.005.

White, A. P. *et al.* (2007) 'Clinical applications of BMP-7/OP-1 in fractures, nonunions and spinal fusion', *International Orthopaedics*, 31(6), pp. 735–741. doi: 10.1007/s00264-007-0422-x.

Wicker, T. *et al.* (2007) 'A unified classification system for eukaryotic transposable elements', *Nature Reviews Genetics*, 8(12), pp. 973–982. doi: 10.1038/nrg2165.

Winkler, D. G. *et al.* (2003) 'Osteocyte control of bone formation via sclerostin, a novel BMP antagonist', *EMBO Journal*, 22(23), pp. 6267–6276. doi: 10.1093/emboj/cdg599.

Wozney, J. M. *et al.* (1989) 'Novel regulators of bone formation: Molecular clones and activities', *Obstetrical and Gynecological Survey*, 44(5), pp. 387–388. doi: 10.1097/00006254-198905000-00028.

Wu, M., Chen, G. and Li, Y. P. (2016) 'TGF-β and BMP signaling in osteoblast, skeletal development, and bone formation, homeostasis and disease', *Bone Research*, 4(December 2015). doi: 10.1038/boneres.2016.9.

Wu, M. and Yuan, F. (2011) 'Membrane binding of plasmid DNA and endocytic pathways are involved in electrotransfection of mammalian cells', *PLoS ONE*, 6(6). doi: 10.1371/journal.pone.0020923.

Xiao, G. *et al.* (2002) 'Bone Morphogenetic Proteins, Extracellular Matrix, and Mitogen-Activated Protein Kinase Signaling Pathways Are Required for Osteoblast-Specific Gene Expression and Differentiation in MC3T3-E1 Cells', *Journal of Bone and Mineral Research*, 17(1), pp. 101–110. doi: 10.1359/jbmr.2002.17.1.101.

Yamaguchi, A., Komori, T. and Suda, T. (2000) ‘Regulation of osteoblast differentiation mediated by bone morphogenetic proteins, hedgehogs, and Cbfa1’, *Endocrine Reviews*, 21(4), pp. 393–411. doi: 10.1210/edrv.21.4.0403.

Yamaguchi, M. (2009) ‘RANK／RANKL／OPG during orthodontic tooth movement’, *Orthod Craniofac Res*, 12, pp. 113–119.

Yan, J. *et al.* (2018) ‘Smad4 deficiency impairs chondrocyte hypertrophy via the Runx2 transcription factor in mouse skeletal development’, *Journal of Biological Chemistry*, 293(24), pp. 9162–9175. doi: 10.1074/jbc.RA118.001825.

Yang, S. *et al.* (2003) ‘In vitro and in vivo synergistic interactions between the Runx2/Cbfa1 transcription factor and bone morphogenetic protein-2 in stimulating osteoblast differentiation’, *Journal of Bone and Mineral Research*, 18(4), pp. 705–715. doi: 10.1359/jbmr.2003.18.4.705.

Yin, H. *et al.* (2014) ‘Non-viral vectors for gene-based therapy’, *Nature Publishing Group*, 15(8), pp. 541–555. doi: 10.1038/nrg3763.

Yoo, J. U. and Johnstone, B. (1998) ‘The role of osteochondral progenitor cells in fracture repair’, *Clinical Orthopaedics and Related Research*, (355 SUPPL.), pp. 73–81. doi: 10.1097/00003086-199810001-00009.

Yue, J. and Mulder, K. M. (2001) ‘Transforming growth factor-β signal transduction in epithelial cells’, *Pharmacology and Therapeutics*, 91(1), pp. 1–34. doi: 10.1016/S0163-7258(01)00143-7.

Zhao, M. *et al.* (2002) ‘Bone morphogenetic protein receptor signaling is necessary for normal murine postnatal bone formation’, *Journal of Cell Biology*, 157(6), pp. 1049–1060. doi: 10.1083/jcb.200109012.

Zhao, M. *et al.* (2005) ‘Combinatorial gene therapy for bone regeneration: Cooperative interactions between adenovirus vectors expressing bone morphogenetic proteins 2, 4, and 7’, *Journal of Cellular Biochemistry*, 95(1), pp. 1–16. doi: 10.1002/jcb.20411.

Zhou, N. *et al.* (2016) ‘BMP2 induces chondrogenic differentiation, osteogenic differentiation and endochondral ossification in stem cells’, *Cell and Tissue Research*, 366(1), pp. 101–111. doi: 10.1007/s00441-016-2403-0.

Zhou, Q. *et al.* (2007) ‘ERK signaling is a central regulator for BMP-4 dependent capillary sprouting’, *Cardiovascular Research*, 76(3), pp. 390–399. doi: 10.1016/j.cardiores.2007.08.003.

Zhu, H., Kavsak, P. and Abdollah, S. (1999) ‘A SMAD ubiquitin ligase targets the BMP pathway and affects embryonic pattern formation’, *Nature*, 400(August), pp. 687–693.

Zhu, W. *et al.* (2004) ‘Combined bone morphogenetic protein-2 and -7 gene transfer enhances osteoblastic differentiation and spine fusion in a rodent model’, *Journal of Bone and Mineral Research*, 19(12), pp. 2021–2032. doi: 10.1359/JBMR.040821.

Zhu, W. *et al.* (2006) ‘Noggin regulation of BMP 2/7 heterodimer activity in vitro’, *Bone*, 39(1), pp. 61–71. doi: 10.1016/j.bone.2005.12.018.Noggin.

Zhuang, Wenzhuo *et al.* (2015) ‘Upregulation of lncRNA MEG3 promotes osteogenic differentiation of mesenchymal stem cells from multiple myeloma patients by targeting BMP4 transcription’, *Stem Cells*, 33(6), pp. 1985–1997. doi: 10.1002/stem.1989.

Zilberberg, L. *et al.* (2007) ‘A rapid and sensitive bioassay to measure bone morphogenetic protein activity’, *BMC Cell Biology*, 8, pp. 1–10. doi: 10.1186/1471-2121-8-41.

List of Abbreviations

ALP	Alkaline phosphatase
ANOVA	Analysis of variance
AZS	Alizarin red staining
BMP	Bone morphogenetic protein
BMPR	BMP receptor
Bp	Base pair
BRE	BMP response element
BSA	Bovine serum albumin
BSP	Bone sialoprotein
cDNA	Complementary DNA
COL1α1	Collagen type 1 alpha 1
Co-SMAD	Common-mediator SMAD
DAPI	4′,6-diamidino-2-phenylindole
DR	Direct repeats
dH_2O	Distilled water
DMEM	Gibco Dulbecco's Modified Eagle Medium
DMSO	Dimethyl sulfoxide
DNase	Deoxyribonuclease
dNTP	Deoxynucleoside triphosphates
E. coli	Escherichia Coli
ECM	Extracellular matrix
ELISA	Enzyme-linked Immunosorbent Assay

ERK	Extracellular signal regulated kinase
EtBr	Ethidium bromide
FACS	Fluorescence activated cell sorting
FBS	Fetal bovine serum
GAPDH	Glyceraldehyde-3-phosphate dehydrogenase
GFP	Green fluorescent protein
GFPh	GFP-high
GOI	Gene of interest
hMSC	Human mesenchymal stem cells
hTERT	Telomerase reverse transcriptase
IBMX	3-isobutyl-1-methylxanthine
ITR	Inverted terminal repeats
IPTG	Isopropyl-beta-D-thiogalactopyranoside
kDa	Kilodalton
JNK	c-Jun-N-terminal Kinase
Lac-operon	Lactose operon
LB-Medium	Lysogeny broth medium
MAPK	Mitogen activated protein kinase
MCS	Multiple cloning sites
mRNA	Messenger RNA
OCN	Osteocalcin
OD	Optical density
OPN	Osteopontin
OSX	Osterix
P2A	Protein 2A

PBS	Phosphate buffered saline
PCR	Polymerase chain reaction
PDGF	Platelet-derived growth factor
PFA	Paraformaldehyde
PPAR-γ	Peroxisome proliferator-activated receptor gamma
PPE	Appropriate personal protective equipment
RANKL	Receptor Activator of NF-κB Ligand
rh-BMP	Recombinant bone morphogenic protein
RNase	Ribonuclease
Rpm	Revolutions per minute
R-SMADs	Receptor regulated SMADs
RT-PCR	Reverse transcription PCR
Runx2	Runt-related transcription factor 2
SB	Sleeping Beauty
SCP1	Single cell picked clone 1
SCP1-GFPh	SCP1-GFP-high
SD	Standard deviation
SDS	Sodium dodecyl sulfate
TBST	Tris-buffered saline with Tween 20
TGFβ	Transforming growth factor beta
TNFα	Tumor necrosis factor alpha
TRIS	(Hydroxymethyl)-aminomethan hydrochloride
VEGF	Vascular endothelial growth factor
X-Gal	5-Brom-4-chlor-3-indoxyl-β-D-galactoside

Appendix

1. Plasmid chart of pENTR223.1-HBMP6.

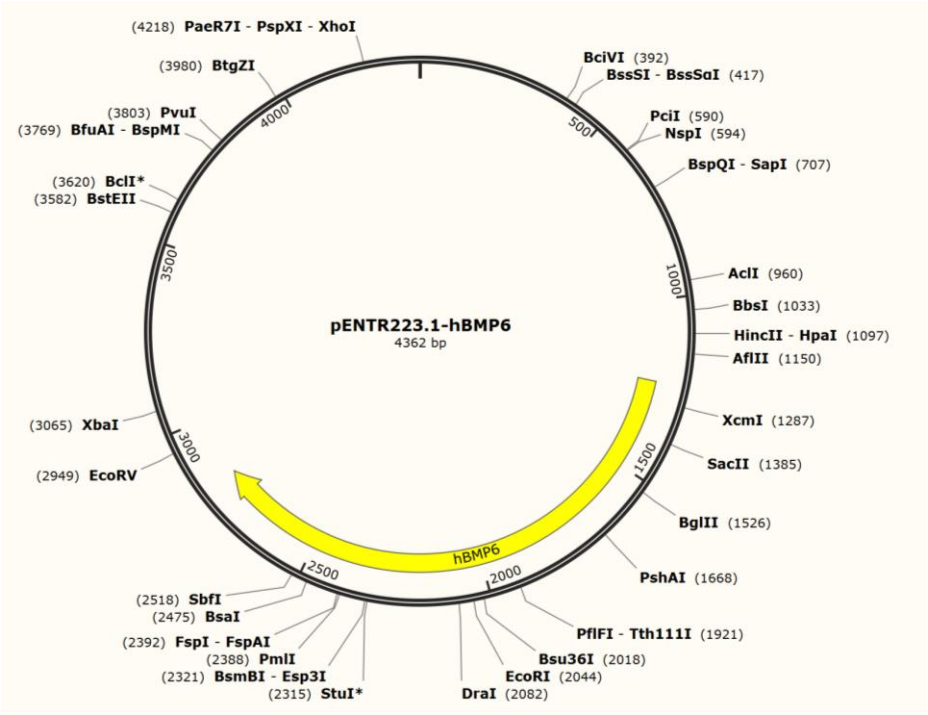

2. Plasmid chart of pSBbi-GP (Kowarz et al., 2015).

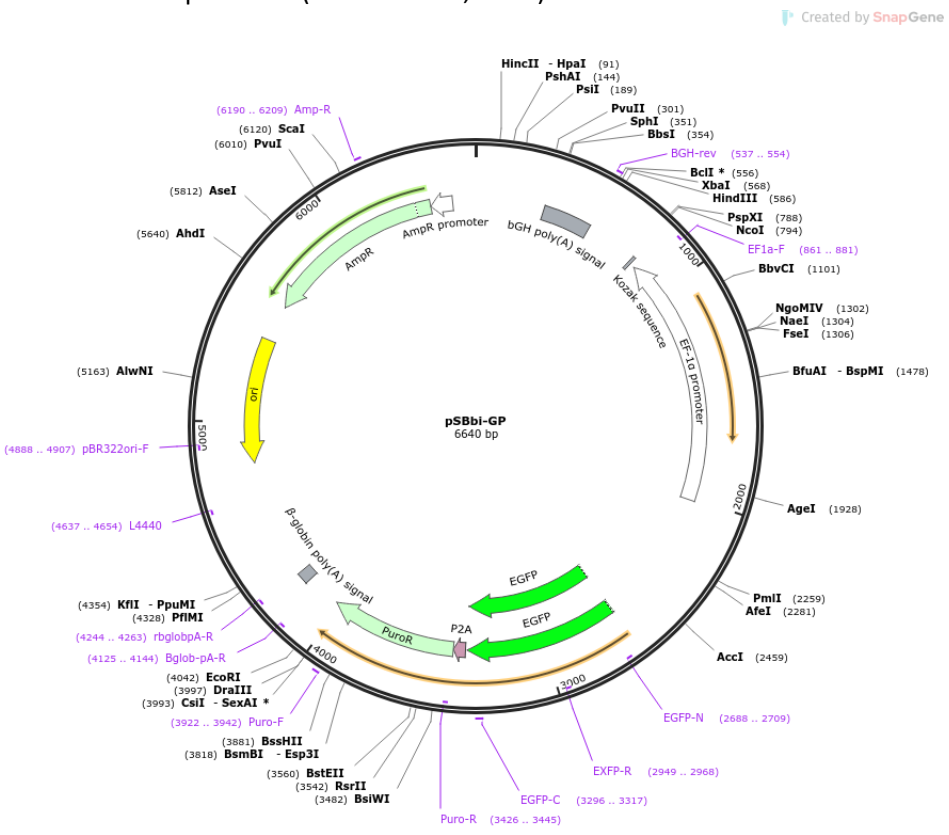

Acknowledgement

Lastly, I wish to sincerely express my gratitude to all the individuals whose contributions, in various ways, were instrumental in the successful completion of this thesis.

In particular, I am deeply thankful to my doctoral advisor, Prof. Dr. med. Wolfgang Böcker, for granting me the opportunity to explore such a fascinating and impactful topic, as well as for his invaluable professional guidance and unwavering support throughout this journey.

My warmest and most sincere thanks go to Dr. rer. nat. Veronika Schönitzer for her supervision and enduring support. I am grateful that we were able to navigate the challenges and bring this work to a successful conclusion together.

I would also like to extend my heartfelt thanks to Dr. rer. nat. Maximilian Saller and Martina Burggraf for their invaluable and decisive support, as well as their exceptional willingness to assist.

Additionally, I am deeply appreciative of Priv.-Doz. Dr. rer. nat. Attila Aszódi, Dr. rer. nat. Sebastian Reiprich, Dr. rer. nat. Paolo Albertoni, Zsuzsanna Farkas, and Heidrun Grondinger for warmly welcoming me from the very first day. Their assistance, professionalism, and the collaborative and inspiring work environment they created have been indispensable.

Lastly, I am profoundly grateful to my family and friends for their support and encouragement throughout this journey.

Affidavit

Bendeliani, Nina

Surname, first name

I hereby declare, that the submitted thesis entitled:

Characterization of Non-Virally Delivered BMP Overexpressing Human Mesenchymal Stem Cells

is my own work. I have only used the sources indicated and have not made unauthorised use of services of a third party. Where the work of others has been quoted or reproduced, the source is always given.

I further declare that the dissertation presented here has not been submitted in the same or similar form to any other institution for the purpose of obtaining an academic degree.

Munich, 13.11.2025

Place, Date

N. Bendeliani

Signature doctoral candidate

LMU LUDWIG-MAXIMILIANS-UNIVERSITÄT MÜNCHEN

Dekanat Medizinische Fakultät
Promotionsbüro

Confirmation of congruency between printed and electronic version of the doctoral thesis

Bendeliani, Nina

Surname, first name

I hereby declare that the electronic version of the submitted thesis, entitled:

Characterization of Non-Virally Delivered BMP Overexpressing Human Mesenchymal Stem Cells is congruent with the printed version both in content and format.

Munich, 13.11.2025

Place, Date

N. Bendeliani

Signature doctoral candidate

Congruency of submitted versions

Date: 13.11.2025